PRELIMINARY DESIGN STUDY OF A CENTRIFUGAL JET ENGINE WITH A SUPERSONIC PROPELLER

Arthur D. Struble

DUDLEY KNOX LIBRARY
NAVAL POSTGRADUATE SCHOOL
MONTEREY, CALIFORNIA 93943-5002

8854

Letter on spine: Struble

1951

Thesis
S856

Letter on cover:

PRELIMINARY DESIGN STUDY OF
A CENTRIFUGAL JET ENGINE WITH
A SUPERSONIC PROPELLER

Arthur D. Struble

PRELIMINARY DESIGN STUDY OF A CEN

WITH A SUPERSONIC PR

Thesis by

LCdr. Arthur D. Struble

In Partial Fulfillment of the Requirements

for the Degree of

Aeronautical Engineer

California Institute of Technology

Pasadena, California

1951

PRELIMINARY DESIGN STUDY OF A CENTRIFUGAL JET ENGINE WITH A SUPERSONIC PROPELLER

Thesis by

LCdr. Arthur D. Struble, U.S.N.

In Partial Fulfillment of the Requirements

for the Degree of

Aeronautical Engineer

California Institute of Technology

Pasadena, California

1951

Thesis
S876

ACKNOWLEDGMENTS

The author wishes to express his appreciation to Professor H. J. Stewart for his constant help and criticism during the course of the work. Sincere thanks are also due to Miss Shirley Woodbury for her assistance in the preparation of the manuscript and to Mrs. Betty Wood for her assistance in the preparation of the figures.

SUMMARY

A theoretical analysis was made of an aircraft propulsion system incorporating a centrifugal jet engine and a supersonic propeller. The primary aim was to increase the economy of a jet configurated engine. The design for a supersonic propeller was included, since it was necessary to use a propeller, in order to create maximum thrust for the installation.

The engine unit consists of a rotating disc with an internal combustion flow channel using essentially the ram-jet cycle, and the design configuration embodied only three basic moving parts for the entire propulsion plant. The performance of the engine was treated as an aerodynamic and thermodynamic problem. Computations were made on the internal flow system covering the effects of all variables. Then, using these results, specific engines were analyzed introducing all pertinent losses. In general, the numerical calculations showed theoretically that this type of engine would have slightly better economy than a reciprocating engine and was far superior to a turbojet at an aircraft speed range down to low subsonic values.

The analysis for the supersonic propeller indicated that the author's design approach, which includes three dimensional effects, could theoretically produce completely supersonic blades with efficiencies above 80%. Computations were made on a 10' diameter propeller which would produce 7,500 pounds of thrust with an efficiency of 83.5% at an aircraft speed of Mach number 1. This power absorption could easily be doubled, while at cruising powers efficiencies ranged up to 86%.

TABLE OF CONTENTS

PART	TITLE	PAGE
I.	Introduction	1
II.	General Description and Operation	5
	A. Disc Spinner	5
	B. The Rotating Disc	5
	C. Gear Train	7
	D. Engine's Stationary Casing	7
III.	Internal Flow Analysis	9
IV.	Disc Design	29
	A. Internal Face Friction Drag	30
	B. Internal End Friction Drag	33
	C. Exposed Face Friction Drag	34
	D. Disc Seals	35
	E. Bearing Losses	36
V.	Specific Engines	37
VI.	Propeller Blade Characteristics	44
VII.	Specific Supersonic Propeller	50
VIII.	Evaluation	58
	References	59
	Appendix A	63
	Appendix B	67
	Figures	68

LIST OF FIGURES

FIG. NO.	TITLE	PAGE
1	Ratio of Nozzle Area to Burner Area	68
2	Net Thrust Per Unit Engine Frontal Area vs. Flight Speed and Altitude	69
3	Net Thrust Specific Fuel Consumption vs. Flight Speed and Altitude	70
4	Net Thrust Per Unit Engine Frontal Area vs. Flight Speed at Seal Level	71
5	Net Thrust Specific Fuel Consumption vs. Flight Speed at Sea Level	71
6	Airplane Powered by a Jet-Operated Propeller	72
7	Isentropic Gas Law Relations Between Reservoir and any Point (Graphs Drawn for Air)	73
8	Centrifugal Jet Engine With Supersonic Propeller	74
9	Isometric Flow Diagram	75
10	Schematic Station Diagram	75
11	Sample Flow Characteristics at Each Station	76
12	Specific Volum Cu. Ft./Lb. Thermodynamic Cycle	76
13	Instantaneous Values of the Ratio of Specific Heats	77
14	Values of the Ratio of Specific Heats Averaged Between O and T	77
15	Variation of Gas Constant With Fuel-Air Ratio	78
16	Fuel-Air Ratio Values of Combustion Efficiency	78
17	S.F.C. vs. Disc Mach No. (Sea Level)	79
18	S.F.C. vs. Combustion Chamber Inlet Velocity	79
19	S.F.C. vs. Aircraft Speed	80
20	S.F.C. vs. Altitude	80

LIST OF FIGURES (Continued)

FIG. NO.	TITLE	PAGE
21	S.F.C. vs. Fuel/Air Ratio	81
22	Temperature vs. Fuel/Air Ratio	81
23	Thrust/Unit Combustion Chamber Area vs. μ	82
24	Area Ratios vs. Fuel Air Ratio	82
25	Thrust and Economy vs. Fuel Air Ratio for a Ram-Jet Operating at M = 1.5 (Sea Level)	83
26	Thrust/A_4 vs. Disc Mach No. (Sea Level)	84
27	Thrust/A_4 vs. Aircraft Speed	85
28	Thrust/A_4 vs. Combustion Chamber Inlet Velocity	86
29	Thrust/A_4 vs. Altitude	86
30	C_f vs. Mach Number	87
31	Coefficient of Friction vs. Sliding Velocity	88
32	Thrust/Unit Exit Area vs. Disc Mach Number	89
33	Mass Flow/Unit Combustion Chamber Area	89
34	Formula Determination for $(F_{P_o}/A_7)_{gross}$ & (m/A_7)	90
35	S.F.C. vs. Aircraft Speed and Altitude for a Turbo-Jet	91
36	S.F.C. vs. M_D and η_s	92
37	S.F.C. vs. Aircraft Speed with A_7 as Parameter	92
38	T.H.P. vs. Va and A_7	93
39	T.H.P. vs. M_D and η_s	93
40	Profile Lift-Drag Ratios vs. Mach Number and τ	94
41	Lift/Drag Ratios vs. k and M	95
42	Lift/Drag Ratio vs. k and Thickness Ratio	96

LIST OF FIGURES (Continued)

FIG. NO.	TITLE	PAGE
43	Lift/Drag Ratio vs. k and M	96
44	Lift/Drag Ratios vs. k at M = 1.1	97
45	Lift/Drag Ratios vs. k at M = 1.6	97
46	Lift/Drag Ratios vs. k at M = 2.0	98
47	Lift/Drag Ratios vs. k for $\tau = 2\%$ and $a = 0.2$	98
48	Supersonic Propeller Plan Forms for Leading Edge k = 0.5	99
49	Propeller Efficiency vs. Propeller Advance Angle	100
50	Propeller Efficiency vs. Parameter J	100
51	Plan Form for a Supersonic Propeller (untwisted)	101
52	Section vs. Radius and Propeller Speed	102
53	Section vs. Radius and Aircraft Speed	102
54	Propeller Loading vs. Radius	103
55	Economy Comparison for Various Type Engines	104
56	Propeller Efficiency vs. V/nD Envelope Efficiency Curves for Various Flight Speeds	105

I. INTRODUCTION

The theoretical analysis made in this study was an effort to reduce the specific fuel consumption of a jet configurated engine in an installation in which the speed of the aircraft was low. If possible, it was desired to gain the simplicity of a ram-jet type unit and not suffer its drawbacks of poor economy at low speeds. Power production for a minimum "package" was only of secondary importance and was not given any consideration in cases where it conflicted with the economy aspects. Thus, the primary aim of this thesis was directed toward the reduction of the specific fuel consumption and still obtain the advantages of the constant flow ram-jet cycle.

First, consider what results have been produced along this line. Fig. 1 taken from Ref. 1 is the result of a preliminary study made on a propeller powered by gas jets issuing from the blade tips. In this case, the Mach number of the propeller tip was limited to 0.85 with an aircraft speed of 100 mph. The minimum values of thrust specific fuel consumption are in the neighborhood of 3 lbs./T.H.P.-Hr. which is unsatisfactory from an economy standpoint. Next, refer to Figs. 2 and 3 taken from Ref. 2; these represent the power and the specific fuel consumption obtainable in a ram-jet installation. It is noticed that the specific fuel consumptions are considerably lower (2.4 lbs./lbs.-Hr.) than they were in the former case, and that the thrust per unit combustion chamber area is much higher. However, the aircraft speed range for these better values centers on 2,200 mph, a value hardly conceivable at the present state of the art. From a different source (Ref. 3), Figs. 4 and

5 are presented for the ram-jet. Here, the specific fuel consumption is expressed in lbs./T.H.P.-Hr. It is seen that a Mach number of 2 must be reached in order to compete with the reciprocating engine whose thrust specific fuel consumption is 0.61 lbs./T.H.P.-Hr. at sea level. The thrust for this case is expressed in thrust per unit combustion chamber area and reaches a maximum of 3,750 lbs./ft.^{2} at a Mach number of 3 or 2,280 mph. Thus, it would seem desirable to obtain the optimum values indicated in these figures in an installation such as that shown in Fig. 6.

To gain good thermodynamic efficiency, it is known that high compression ratios should be used. If the isentropic gas laws shown graphically in Fig. 7 of this paper are studied, the rapid increase in pressure rise as the Mach number is increased is clearly evident. If the pressure curve in the Mach number range of 2 to 3 is considered, compression ratios in the neighborhood of 20 might be gained. It would seem expedient therefore, to attempt in some manner to use this feature to gain better thermodynamic efficiency. It follows that with larger thermodynamic efficiencies better economy would result.

As previously indicated, the ram-jet unit has a compression high enough for a good efficiency at supersonic velocities and a large mass flow of air per unit frontal area which gives high power output. However, both of these advantages fall off at lower speeds. It was desired to obtain this good efficiency at low subsonic speeds. By using an internal combustion system incorporated in a rotating disc, it was found that satisfactory compression could be gained by centrifugal

force; and that if the disc speed were allowed to reach high enough values, very satisfactory economy and power outputs were gained. In the present paper, performance computations were made covering the speed range up to a disc Mach number of 2.4. The ram-jet cycle, used herein, shall be referred to henceforth as a "centrifugal jet" engine, because the ram was small in comparison to the compression produced through centrifugal force.

The centrifugal jet engine performance is treated as an aerodynamic and thermodynamic problem. The performance is given in terms of areas, velocities, and temperatures involved in the design of such a unit. The various parameters that effect the economy and the power output, as well as the above listed physical properties, were allowed to range over pertinent values in the computations to show the separate effect of each. Examples of specific designs are included to show the overall performance rating of the power plant compared with present day types of engines that produce comparable power.

The system is essentially a separate power plant and a separate supersonic propeller. In order to create maximum thrust, the power plant must use a propeller; although, the engine itself produces a sizeable percentage of the thrust depending on the speed of the airplane. Since the installation must use a propeller to operate at optimum conditions, it was felt that an analysis of a supersonic propeller design was necessary to see what could be accomplished in this direction. Present day subsonic propellers are satisfactory on aircraft whose maximum speed approaches 500 mph. With the enclosed

design of a supersonic propeller, the propeller's useful range can theoretically be increased to speeds approaching 1,000 mph. The importance of a design which will increase the speed range of the propeller cannot be over emphasized, since at present, there is a crying need in higher speed aircraft for a satisfactory power converter (B.H.P. to T.H.P.), so that various jet type engines may be utilized. By the proper combination of engine and propeller, it would seem that more efficient installations could be designed, thereby increasing the range of present day aircraft particularly of jet powered aircraft and helicopters.

There are numerous major problems to be encountered in the successful design and operation of an engine as herein described. Many of the problems which will be enumerated later are only partially investigated or are beyond the scope of this paper. It is to be realized that this paper is preliminary and serves only as a basis for further investigations, and that the enclosed information is the culmination of numerous designs considered. After each investigation the most desirable features of each were retained to produce the most effective end result. With the material already presented as a background and the authors views creating the problem, the following design is presented as one answer.

II. GENERAL DESCRIPTION AND OPERATION

The power plant configuration and included supersonic propeller of the proposed centrifugal jet engine, is shown on Fig. 8. With reference to the diagram, it will be seen that the system is made up basically of only three moving parts. These consist of the nose spinner with attached propeller, the centrifugal jet rotating disc, and the necessary gear train coupling. The rotating disc is mounted on the engine's stationary structure. The latter is in turn mounted directly to the aircraft. On Fig. 8, the nose spinner is shown hatched, the outline of the disc is shown solid, and the engine's stationary casing is shown double hatched.

A detailed description and function of each of the major components is as follows:

A. Disc Spinner

The disc spinner serves to mount the propeller with its necessary mechanical mechanisms. Through the nose of the spinner, free air is conducted to the intake of the rotating disc. The spinner also serves as a shield for the disc. Its bearings turn on a journal mounted on the outside of the disc intake. The spinner receives its propulsive power from the gear train shown.

B. The Rotating Disc

Intake ram air is fed into the center of the rotating disc. It is there directed to the periphery of the rotating disc through channels in such a manner that the air ducts do not interfere with the gear train. The dimensions of the channel are so constructed that the

velocity at the outer most radius is low, of such magnitude as to be suitable for burning in a constant flow type combustion chamber. The combustion chamber runs the length of the disc in an offset direction to that of rotation by some specific angle, "O", which is determined by later included analysis.

An isometric flow diagram is shown in Fig. 9. The air is compressed by centrifugal force in its travel from the root of the disc to its outer circumference. The fuel is injected when it reaches the periphery at the entrace to the combustion chamber. The fuel air mixture is then burned in the combustion chamber, passed through a suitable nozzle, and ejected into free air. The cycle of flow is continuous and extremely simple. The configuration may be altered slightly to permit induction of ram air from the rear of the rotating disc as well as from the forward end.

The disc is mounted on bearings of the engine's stationary structure and its shaft carries a gear suitable for operating the necessary auxiliaries, such as, a fuel pump, vacuum pump, lubrication pump, generator, magnetes, etc. The disc-spinner and disc-casing clearances are designed small to elimate, as much as possible, the pumping action of the air which arises from the relative motion between the afore mentioned parts and the centrifugal pressure gradient that is setup. Air seals are located at the two clearances occurring at the position of the jet exit. These seals serve to maintain a difference in pressure between the free air and the clearance spaces. By this device, the clearance spaces are evacuated thereby reducing the air friction

drag and resulting loss in horsepower.

C. Gear Train

One possible configuration of a gear train appears on the diagram (Fig. 8). This unit serves to transmit the horsepower of the rotating disc via the nose spinner to the propeller. Since the nose spinner and rotating disc are operating at different rpms, it must be realized that a configuration in which the propeller is mounted directly on the rotating disc, thus eliminating the nose spinner, is quite possible; but, because of the various factors involved, this would not be particularly efficient except in very special cases.

D. Engine's Stationary Casing

This structure serves as a mounting pad for the bearings of the rotating disc and as a housing for the auxiliaries. It, in turn, is mounted to the aircraft primary structure.

The system of Fig. 8, would appear to have the following advantages:

1. No engine torque is applied to the aircraft except for the jet slip stream.
2. Lighter weight/unit power occurs as compared with a reciprocating engine.
3. Small frontal area is achieved with a streamlined shape.
4. Small volume for the entire engine results.
5. The lubrication problems are simple, probably incorporating a closed system.
6. Low vibrating loads are expected with vibration due only to intermittent burning and alternating aerodynamic loads.

3. The configuration is simple with a small number of moving parts.

Disadvantages to the system would be, primarily:

1. The stress problem would be very critical due to large centrifugal loads created by high rotational speeds and the existance of high temperature gradients.
2. With high rotational speeds, the balance problem would be major specifically to counteract ice formation and engine malfunction.
3. Poor acceleration characteristics, inherent in jet configurations, would probably be found.

Detailed analysis of the system as far as advantages and disadvantages are concerned will be more throughly discussed in later sections as the various problems are analyzed.

III. INTERNAL FLOW ANALYSIS

The flow pattern through the engine is shown in Figs. 9 and 10. The analysis is so arranged that the various characteristics have been found for each of the seven stations shown in Fig. 10. To reduce the amount of calculations involved, the section from Station 2 to 3 was eliminated for this will be primarily a function of the individual design and may not necessarily be involved in any specific configuration. The actions of compression and diffuser action have been combined in the process between Stations 3 and 4. Combustion in a constant area chamber will include momentum pressure and combustion chamber friction losses between Stations 4 and 5. At Station 5 it is assumed that burning has been completed. The combustion gases are then expanded in a nozzle through Stations 6 and 7.

Station 6 is the throat of the nozzle where Mach number 1 occurs; this, of course, will in most cases be under expanding if the nozzle is cut off there. Station 7 is for a full expanding nozzle down to free air pressure. For most of the conditions involved in the design, the area at Station 7 approximates that of Station 5 so that a full expanding nozzle can easily be incorporated. Because of the configuration, even if these two areas were not particularly compatible, they could be used without any great loss in the design. This is not the case with the ram-jet engine, in which it is desired to maintain the exit area commensurate with the combustion chamber or inlet area.

For good specific fuel consumption it is quite evident that the disc must be allowed to rotate at as high an rpm as the stress analysis

will allow. The general dimensions of the engine must be such that the inlet areas to the disc are small in relation to the plan form disc area so that full utilization of centrifugal force compression may be gained. On the other hand, too large a disc will incorporate large disc friction losses, and considerably enlarge the frontal area of the overall engine. The latter would in turn increase engine volume and engine weight per horsepower developed. Thus, it would seem that a happy medium for the dimensions of the engine should be arrived at after consideration of the factors involved and of the results most desired.

The variation in gas temperature, velocity, and pressure as it flows through the engine is shown in Fig. 11 for two representative cases. The changes in each may be followed from station to station to understand the general flow picture. The cycle represented on a P.V. diagram for one of the cases is shown on Fig. 12. It appears that the cycle closely parallels those used in common jet practice.

The following analysis is now treated as a aerodynamic and thermodynamic problem; and as such, requires certain constants to be assumed to make the power plant computation possible. The constants chosen were gained either from empirical charts or from other sources that have been well established in actual practice. The constants used are as follows:

1. The friction coefficient of drag is .0030 in the entrance pipe. This value can be obtained only in a smooth polished pipe.

2. The subsonic diffuser has an efficiency of 90%.

3. The centrifugal compression is at an efficiency of 95%. This value, although high as compared with values of normal centrifugal compressors, is deemed possible by the fact that the flow velocity is low, that the flow contour is smooth with no sharp breaks, and that the flow itself contacts no broken surfaces or sharp discontinuities as are involved in the normal centrifugal compressor between the rotating blade exit and the diffuser. Neither of these three factors are involved in this configuration. If the product of the diffuser efficiency and the compression efficiency is determined for the assumed values, it is seen that the overall efficiency is on the order of 85%; this is certainly entirely obtainable in the light of modern design.

4. The lower heating value of the fuel is 19,000 British thermal units per pound.

5. The instantaneous values of the ratios of the specific heats γ and for $\bar{\gamma}$ corresponding to the average value between 0° F and the temperature in question, is given in Figs. 13 and 14 for air and for the products of combustion. Arguments are temperature and fuel air ratio.

6. The variation of the gas constant with fuel air ratio is shown on Fig. 15.

7. Fig. 16 gives combustion efficiency versus air fuel ratio.

8. Since the fuel is added at the entrance of the combustion chamber, momentum is required to bring it up to the combustion chamber velocity. The loss is charged as a momentum pressure loss.
9. The friction pressure loss in the combustion chamber is taken as 50% of the average of the initial and final dynamic pressures in the combustion chamber.
10. The heat loss through the combustion chamber walls is treated as a reduction in combustion efficiency.
11. The exhaust nozzle is assumed to have a velocity coefficient of .98 when operating at design pressure ratio or as an under expanding nozzle.
12. Standard density altitude tables were used for the determination of the initial free air conditions. Partial reproduction of this table is given in Appendix B.

Before proceeding with the analysis, it was also necessary to limit certain of the variables because of physical reasons. Maximum combustion chamber temperatures above 3,000 degrees F were considered impractical. If at any time, Mach number 1 was reached in the internal flow, except at the nozzle throat, it was assumed that chocking occurred and further examination was abandoned. In all computations the physical dimensions of areas along the channel flow were assumed to be compatible with the continuity relationships. Therefore, the power plant operation, so far as considered herein, has been with specific design operating conditions; each case would involve different fixed areas so as to

produce optimum conditions. For a system with fixed dimensions and specific operating conditions there exists only one mass flow to be "on design". Thus with an analysis for a particular air fuel ratio, specific inlet conditions and fixed nozzle dimensions, the flow for a different fuel air ratio will not correspond to the former analysis, but to one with its own dimensions. For a system with the same dimensions and a different air fuel ratio, computations must be based on flow controlled by the nozzle whose dimensions have been determined by the previous conditions. Consequently, the computations made are valid for only the conditions assumed since the dimensions of the system will change in each new case.

The variables chosen as parameters are as follows:

1. Altitude: This determines the free air temperature, pressure, and density.
2. Aircraft Speed: The aircraft speed will determine the inlet velocity. In the case where the aircraft speed is supersonic, it is assumed that a normal shock occurs prior to the inlet entrance and the corresponding changes in pressure, temperature, and density are calculated according to normal shock theory.
3. Disc Rotational Velocity: As indicated earlier this should be as high as possible to obtain good results and will be determined more or less in any actual design by the stress considerations involved.
4. Combustion Chamber Inlet Velocity: This velocity must necessarily be low in order to obtain satisfactory

combustion; thus, it is a function in any actual design of the combustion chamber characteristics and the type of fuel and ignition system used. A range of representive values has been used.

5. The Fuel Air Ratio: This value is concerned in both the specific fuel consumption and the power per unit area developed. Since the maximum combustion chamber temperature is a function of the fuel air ratio, it is seen that if the combustion chamber temperature is to be limited to a particular maximum value, then there is a maximum value of the fuel air ratio that can be used. Also, since combustion can be supported only at some lower value of the fuel air ratio, its minimum is determined in any specific design. By the artifice of burning the fuel in only a portion of the air flow thereby increasing the local air fuel ratio and following this process by proper mixing of the burned products and remaining air, an equilibrium temperature for the total volume is reached, and lower values of fuel air ratio can be realized. Thus, the minimum value of the fuel air ratio is also a function of design.

The latter three parameters are within the control of the designer, the most important being the disc rotational velocity.

The actual method of computation is now considered. Using the various parameters, the flow is solved for the characteristics at each of the seven stations shown on Fig. 10, starting with free air and going

through the engine in the flow direction. A list of symbols is included in Appendix A. All numbered subscripts refer to the station as per Fig. 10. The computational procedure parallels that of Ref. 3.

Station 1: Free air conditions are taken from the Standard Altitude Table in Appendix B.

Station 2: Free Air Conditions Following a Normal Shock. Normal shock theory relationships, represented graphically in Ref. 27, are used.

Station 3: Flow Through a Straight Pipe (constant area inlet channel). The flow may be solved graphically using the two charts given on page 142, Ref. 11, which give the friction losses in round or rectangular ducts. The pressure change is presented in inches of Hg./ft. vs velocity with parameters of size in round or rectangular ducts. It may also be calculated by means of the approximation that the friction pressure drop is proportional to the product of the friction factor, length-diameter ratio of the pipe, and the mean dynamic pressure.

$$\Delta p_f = 4C_D \times \frac{\ell_{2,3}}{d_2} \times \frac{q_2 + q_3}{2}$$

where

$$q = \frac{\rho V^2}{2}.$$

The laws of energy, momentum, and mass then yield a solution for V_3

$$V_3 = \frac{b_3 - \sqrt{b_3^2 - 4c_3}}{2}$$

where

$$b_3 = \frac{2\,\bar{\gamma}_3}{\bar{\gamma}_3\left(1 + 2C_D\,\frac{\ell}{D}\right) + 1}\left[\frac{P_2}{\rho_2 V_2} + \left(1 - C_D\,\frac{\ell}{D}\right) V_2\right]$$

$$c_3 = \frac{2\,\bar{\gamma}_3}{\bar{\gamma}_3\left(1 + 2C_D\,\frac{\ell}{D}\right) + 1}\left[\frac{2\,\bar{\gamma}_2}{\bar{\gamma}_2 - 1}\,\frac{P_2}{\rho_2} + V_2^2\right].$$

When $4c_3$ is equal to b_3^2, the velocity at Station 3 equals the speed of sound, and shocking occurs; a value of $4c_3$ larger than b_3^2 signifies that an impossible flow situation has been assumed; a shorter entrance pipe is one remedy. Using the continuity relation:

$$\rho_3 = \frac{\rho_2 V_2}{V_3}.$$

Using the equation of momentum:

$$p_3 = p_2 - \rho_2 V_2 (V_3 - V_2) - \Delta P_f.$$

Using the general gas law:

$$T_3 = \frac{p_3}{\rho_3\, g\, Ra}.$$

Station 4: Centrifugal Compression. Since the inlet combustion chamber velocity V_4 is one of the variables and is specifically chosen for any specific design, then it is evident that diffuser action must occur between Stations 3 and 4. Also, the Mach number of the disc periphery is chosen and this determines the extent of compression work added to

the fluid. These two actions will be considered separately and then combined to produce formulas relating the flow from 3 to 4.

Using the compressible form of the Bernoulli equation

$$\frac{2}{\gamma_4 - 1} a_4^2 = \frac{2}{\gamma_3 - 1} a_3^2 + V_3^2 + V_D^2$$

and the isentropic gas laws (Fig. 7)

$$\frac{a_3^2}{a_4^2} = \frac{1 + \frac{\gamma_4 - 1}{2} M_4^2}{1 + \frac{\gamma_3 - 1}{2}(M_3^2 + M_D^2)} = \frac{T_3}{T_4} = \left(\frac{P_3}{(P_4)_{C.F.}}\right)^{\frac{n-1}{n}}$$

where $(P_4)_{C.F.}$ is the pressure at 4 if only centrifugal force is considered. The equation is rewritten,

$$\frac{(P_4)_{C.F.}}{P_3} = \left[\frac{1 + \frac{\gamma_3 - 1}{2}(M_3^2 + M_D^2)}{1 + \frac{\gamma_4 - 1}{2} M_4^2}\right]^{\frac{n}{n-1}}$$

Since the flow is with friction and if η_c is defined as the efficiency of compression for centrifugal process only then,

$$\eta_c = \frac{\frac{n-1}{n}}{\frac{\gamma - 1}{\gamma}} \quad \text{or} \quad \frac{n}{n-1} = \frac{\gamma \eta_c}{\gamma - 1}$$

according to Ref. 15, page 39. Thus,

$$\frac{(P_4)_{C.F.}}{P_3} = \left[\frac{1 + \frac{\gamma_3 - 1}{2}(M_3^2 + M_D^2)}{1 + \frac{\gamma_4 - 1}{2} M_4^2}\right]^{\frac{\gamma_{3,4}\,\eta_c}{\gamma_{3,4} - 1}}$$

and

$$(P_4)_{C.F.} - P_3 = \Delta P_{C.F.} = P_3 \left[\frac{1 + \frac{\gamma_3 - 1}{2}(M_3^2 + M_D^2)}{1 + \frac{\gamma_4 - 1}{2} M_4^2} \right]^{\frac{\gamma_{3,4}\ \eta_c}{\gamma_{3,4} - 1}} - P_3 .$$

Next considering the diffuser process between 3 and 4, η_d is the diffuser efficiency whose equation expresses the total pressure recovery as a percentage of the reduction in dynamic pressure:

$$\eta_d = 1 - \frac{H_3 - H_4'}{q_{c_3} - q_{c_4}}$$

where

$$q_c = H - P \qquad \text{(compressible dynamic pressure)}$$

and

$$H_4' = H_4 - \Delta P_{C.F.} \qquad \text{(total head less the change in centrifugal force)}$$

$$H_3 = P_3 \left(1 + \frac{\gamma_3 - 1}{2} M_3^2\right)^{\frac{\gamma_3}{\gamma_3 - 1}}$$

from the isentropic gas law. By definition,

$$q_{c_3} = H_3 - P_3 .$$

Since the velocity at Station 4 will always have low subsonic values (less than 350 ft./sec.), then

$$q_{c_4} = q_4$$

$$H_4 = P_4 + q_{c_4} = P_4 + \frac{\rho_4 V_4^2}{2}$$

then

$$\eta_d = 1 - \frac{H_3 - P_4 - \frac{\rho_4 V_4^2}{2} + \Delta P_{C.F.}}{H_3 - P_3 - \frac{\rho_4 V_4^2}{2}}$$

finally

$$P_4 = \eta_d P_3 \left[1 + \frac{\gamma_3 - 1}{2} M_3^2\right]^{\frac{\gamma_3}{\gamma_3 - 1}} - \eta_d \frac{\rho_4 V_4^2}{2}$$

$$+ P_3 \left[\frac{1 + \frac{\gamma_3 - 1}{2}(M_3^2 + M_D^2)}{1 + \frac{\gamma_4 - 1}{2} M_4^2}\right]^{\frac{\gamma_{3,4}\eta_a}{\gamma_{3,4} - 1}}$$

Next it is known that the work added to the fluid per unit mass as it flows from Station 3 to 4 is $C_p \Delta T$ or u^2 for compressible fluids (page 601, Ref. 15); the energy equation then can be written:

$$\frac{2\bar{\gamma}_4}{\bar{\gamma}_4 - 1} \frac{P_4}{\rho_4} + V_4^2 = \frac{2\bar{\gamma}_3}{\bar{\gamma}_3 - 1} \frac{P_3}{\rho_3} + V_3^2 + V_D^2 .$$

Substituting P_4 into this equation and solving, ρ_4 is obtained:

$$\rho_4 = \frac{r}{s + t}$$

where

$$r = P_3 \left\{ \left[\frac{1 + \frac{\gamma_3 - 1}{2}(M_3^2 + M_D^2)}{1 + \frac{\gamma_4 - 1}{2} M_4^2} \right]^{\frac{\gamma_{3,4}\ \eta_c}{\gamma_{3,4} - 1}} + \eta_d \left[1 + \frac{\gamma_3 - 1}{2} M_3^2 \right]^{\frac{\gamma_3}{\gamma_3 - 1}} - \eta_d \right\}$$

$$s = \frac{\eta_d V_4^2}{2}$$

$$t = \left(\frac{\bar{\gamma}_4 - 1}{2\bar{\gamma}_4}\right) \left(\frac{2\bar{\gamma}_3}{\bar{\gamma}_3 - 1} \frac{P_3}{\rho_3} + V_3^2 + V_D^2 - V_4^2\right)$$

$$P_4 = t\rho_4$$

$$T_4 = \frac{P_4}{\rho_4\ g\ R_a} \qquad \text{(Eq. of State)}$$

$$A_3 = \frac{\rho_4 V_4}{\rho_3 V_3} \quad \text{where } A_4 = 1 \quad \text{(Continuity)}.$$

Station 5: Constant Unit Area Combustion Chamber. By continuity

$$m = \rho_5 V_5 = \rho_4 V_4 + \frac{W_f}{g}$$

$$\rho_5 = \rho_4 \frac{V_4}{V_5} \left(\frac{W_a + W_f}{W_a}\right).$$

Using momentum

$$P_5 + (\rho_4 V_4 + \frac{W_f}{g}) + C(\frac{q_4 + q_5}{2}) - P_4 - \rho_4 V_4^2 = 0$$

where $C(\frac{q_4 + q_5}{2})$ is the combustion chamber friction pressure loss. Then

$$P_5 = P_4 + \rho_4 V_4^2 (1 - \frac{C}{4}) - \rho_4 V_4 V_5 (1 + \frac{C}{4})(\frac{W_a + W_f}{W_a}).$$

Using energy

$$\left[(\frac{\bar{\gamma}_5}{\bar{\gamma}_5 - 1}) \frac{P_5}{g\rho_5} + \frac{V_5^2}{2g}\right] (W_a + W_f) =$$

$$\left[(\frac{\bar{\gamma}_4}{\bar{\gamma}_4 - 1}) \frac{P_4}{g\rho_4} + \frac{V_4^2}{2g}\right] (W_a + W_f) + J(H.V.)\eta_b W_f$$

where η_b is the burning efficiency. Substituting the equations for ρ_5 and P_5 into the latter equation:

$$V_5 = \frac{b_5 + \sqrt{b_5^2 - 4C_5}}{2}.$$

Where

$$b_5 = \frac{2\bar{\gamma}_5}{\bar{\gamma}_5(1 + \frac{C}{2}) + 1} \quad (\frac{W_a}{W_a + W_f}) \quad \left[\frac{P_4}{\rho_4 V_4} + V_4 (1 - \frac{C}{4})\right].$$

$$c_5 = \frac{\bar{\gamma}_5 - 1}{\bar{\gamma}_5\left(1 + \frac{c}{2}\right) + 1}\left[\frac{2\bar{\gamma}_4}{\bar{\gamma}_4 - 1}\frac{P_4}{\rho_4} + V_4^2 + \frac{5 \times 10^4 \text{ H.V. } \eta_b}{(W_a + W_f)/W_f}\right]$$

As before, b_5^2 must be greater than $4c_5$ so that chocking will not occur.

$$T_5 = \frac{P_5}{\rho_5 g R_c}$$

Station 6: Conditions at the Nozzle Throat

$$P_6 = P_5\left[\frac{2}{\gamma_5 + 1} + \frac{\gamma_5 - 1}{\gamma_5(\gamma_5 + 1)}\frac{\rho_5 V_5^2}{P_5}\right]^{\frac{\gamma_5}{\gamma_5 - 1}}$$

$$T_6 = T_5\left[\frac{2}{\gamma_5 - 1} + \frac{\gamma_5 - 1}{\gamma_5(\gamma_5 + 1)}\frac{\rho_5 V_5^2}{P_5}\right]$$

where γ_5 is used for simplicity in both equations instead of the average.

$$\rho_6 = \frac{P_6}{gR_cT_6}$$

$$V_6 = \sqrt{\gamma_6 gR_cT_6}$$

where γ_6 is instantaneous for the products of combustion.

$$A_6 = \frac{\rho_5 V_5}{\rho_6 V_6}$$

Station 7: Flow Out the Nozzle Exit (conditions fully expanded to the free air pressure P_1). The temperature at Station 7 is first guessed and the instantaneous value of γ for the average between Stations 5 and 7 is used. Then the process is repeated if the error in the guess was greater than 25°.

$$T_7 = T_5 \left[\left(\frac{P_1}{P_5}\right)\right]^{\frac{\gamma_{5,7} - 1}{\gamma_{5,7}}}$$

$$V_7 = C_v \sqrt{2gR_e\left(\frac{\bar{\gamma}_5 T_5}{\bar{\gamma}_5 - 1} - \frac{\bar{\gamma}_7 T_7}{\bar{\gamma}_7 - 1}\right) + V_5^2}$$

where C_v is a velocity coefficient allowing for friction in the nozzle.

$$\rho_7 = \frac{P_7}{gR_e T_7}$$

$$A_7 = \frac{\rho_5 V_5}{\rho_7 V_7}.$$

The expression for thrust consists of three terms: The first gives the thrust from the acceleration of the air mass, the second gives the thrust from the acceleration of the fuel mass, and the third becomes effective if the exhaust pressure is above atmospheric. The thrust per unit combustion chamber area then is

$$\frac{F}{A_4} = \rho_4 V_4 (V_x) + \rho_4 V_4 \left(\frac{W_f}{W_a}\right) V_x + (P_x - P_1)\frac{A_x}{A_4}$$

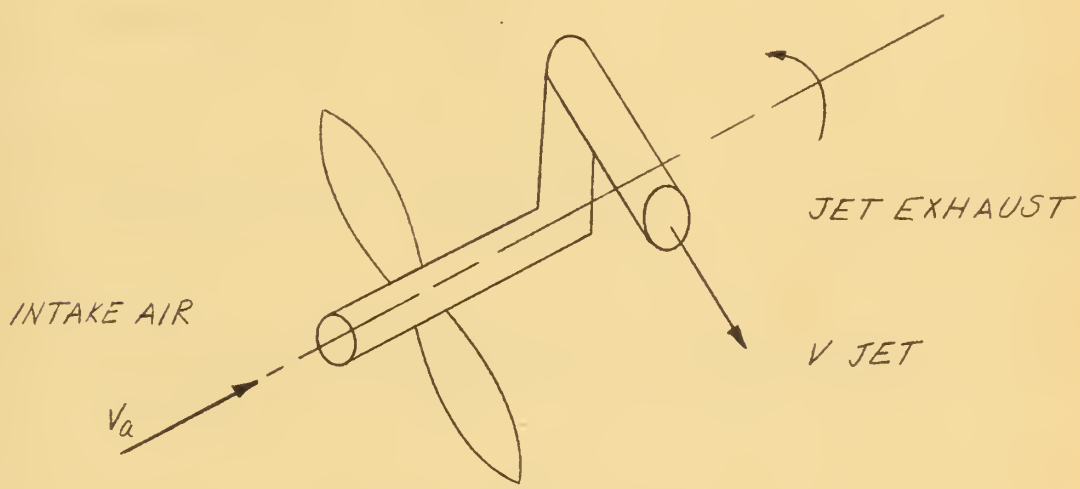
or

$$\left(\frac{F}{A_4}\right)_6 = \rho_4 V_4 V_6 (1+\mu) + (P_6 - P_1)\frac{A_6}{A_4}$$

and

$$\left(\frac{F}{A_4}\right)_7 = \rho_4 V_4 V_7 (1+\mu) .$$

The loss in thrust due to the intake air is charged as an engine loss. It must be supplied by the propeller if the situation is idealized as in the sketch, since the intake air is brought to rest in



the axial direction. Later the gas is accelerated from zero velocity to V_{jet} in the circumferential direction. The expression for (F/A_4) previously referred to will be a gross value since it does not include thrust needed to supply work for spinner intake or centrifugal compression. Thus $\left(\frac{F_{P_0}}{A_4}\right)_{gross}$ will be for a full expanding nozzle, $\left(\frac{F_t}{A_4}\right)_{gross}$ will be for

a sonic throat exit, and $(\frac{F_{P_o}}{A_4})_{\text{net}}$ will be for a full expanding nozzle with included losses in an idealized arrangement as shown where the jet exit is circumferential, perpendicular to the longitudinal axis. $(\frac{F_{P_o}}{A_4})_{\text{net}}$ is computed as follows:

$$\frac{\text{Inlet H.P. loss}}{A_4} = \frac{(m/A_4)V_a^2}{\eta_z\ 500} \quad \text{where } \eta_z \text{ is the efficiency of}$$

conversion B.H.P. to T.H.P.

$$\frac{\text{Compression H.P.}}{A_4} = \frac{(m/A_4)V_D^2}{550}$$

$$\frac{\text{Gross Jet H.P.}}{A_4} = \frac{(F_{P_o}/A_4)_{\text{gross}}\ V_D}{550}$$

$$\frac{\text{Net Jet H.P.}}{A_4} = \frac{(F_{P_o}/A_4)_{\text{gross}}\ V_D}{550} = \frac{(F_{P_o}/A_4)_{\text{gross}}\ V_D}{550}$$

$$- (\frac{m}{A_4})\ \frac{1}{550}\ (\frac{V_a^2}{\eta_z} + V_D^2)$$

or

$$(F_{P_o}/A_4)_{\text{net}} = (\frac{F_{P_o}}{A_4})_{\text{gross}} - (\frac{m}{A_4})\ (\frac{V_a^2}{\eta_z V_D} + V_D)$$

The specific fuel consumption in lb. fuel/lb. thrust-Hr. was computed in accordance with the following formula:

$$S.F.C. = \frac{3600\, g\mu\, (m/A_4)}{(F/A_4)}$$

where (F/A_4) is the net or gross value as desired.

The net values of S.F.C. and thrust were included in the computations so as to give a basis of comparison with other jet cycles. It will be shown later that these values are conservative to what can be obtained by proper orientation of the jet exit angle for any specific set of design conditions.

The results of the computations are represented graphically on Figs. 17 through 28. The conditions of, (a) sea level, (b) $M_D = 2.0$, (c) $V_a = 300$ ft./sec., (d) $V_4 = 280$ ft./sec., and (e) $\mu = .020$, were chosen as a basis and then all variables were fanned out from these values as appropriate. Figs. 17 through 21 give S.F.C., both gross and net, for the five variables. It should be noted that in general the net S.F.C. at low aircraft speeds and moderate disc Mach numbers is considerably below that of the ram-jet operating at its optimum speed of about 2,200 mph, (Fig. 3). The rapid rise of (S.F.C.) net as the aircraft speed is increased towards M = 1 is due to the influence of the intake loss which is a function of V_a^2. It is seen that the major effect on S.F.C. is the fuel-air ratio followed by the disc Mach number. Altitude has a normal effect as in other jet cycles, but S.F.C. seems to be practically unsensitive to combustion chamber inlet velocity.

Fig. 22 shows cycle temperature variations with μ. It is seen that for the basic condition if the maximum temperature of 3,000° F is not to be exceeded, then the fuel-air ratio would have to be limited to an upper limit in the neighborhood of .05. It should also be called to the attention of the reader that in most of the conditions for which the variables were allowed to range, the stochometric value of .067 could not be attained since chocking would occur in the combustion chamber. In many of the runs μ was limited to 1/2 stochometric as an upper value (μ = .033) because of chocking or the 3,000° F limitation.

The curves of Figs. 21 through 24 have the air-fuel ratio as one argument. Consequently, the results must be tempered by the discussion already made on the effect of a change in fuel-air ratio with a system of fixed dimensions. By comparison of Figs. 21 and 23, it is seen that a greater effect is obtained on the specific fuel consumption than on the thrust per unit combustion chamber area by a change in fuel-air ratio. Fig. 24 gives the relative sizes of the nozzle throat exit areas in comparison to the combustion chamber areas. Fig. 25 is included to show the comparison with the ram-jet. The different Mach number operation in each case should be taken into consideration.

Figs. 26 through 29 give the results of the thrust curves versus the five variables. The rapid rise in thrust per unit combustion chamber area for an increase in the disc Mach number is readily evident on Fig. 26. As with specific fuel consumption, the effects of combustion chamber inlet velocity and of altitude are the same. Referring to Fig. 27, it should be noted that the net thrust curve seems to be fairly constant at the lower velocities but drops off at higher velocities;

this result is again due to the increased loss of the intake ram as higher values of speed are used.

The factors in any particular design would be determined more or less by the parameter trends indicated on the various plots. Thus, although the flow is not particularly sensitive to combustion chamber inlet velocity, both specific fuel consumption and thrust are enhanced by the higher values; it would seem desirable then, to use as high a value as possible to gain better values of specific fuel consumption and thrust. Since altitude is beyond the control of the designer, the altitude trends produce no design criterion except for the desires of certain results at a specific altitude. In regard to the aircraft speed which is also beyond the control of the designer, it would seem that better results could be expected at the lower velocities. The function of the fuel air ratio is such as to require as low a value for cruising conditions and as high a value where thrust conditions are paramount. All of the afore mentioned trends seem to fit into the pattern of other standard jet propulsion systems except for the variation involved in aircraft speed. By comparison to the results of other types already given in the form of graphs on Figs. 1, 2, 3, 4, 5, and 25, it would seem that in general, superior values of the specific fuel consumption and thrust per unit combustion chamber are achieved in the centrifugal jet cycle.

IV. DISC DESIGN

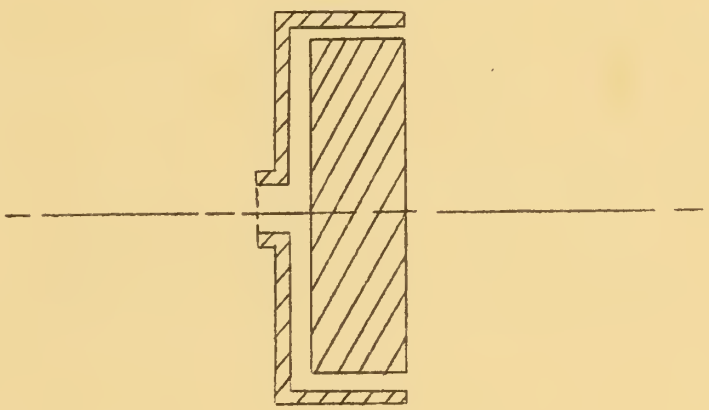
The general arrangement of the disc has been described in Section III and appears in solid color on Fig. 8. The flow channel is clearly depicted on Fig. 9. To secure minimum frontal area and engine compactness, the disc diameter should be as small as possible commensurate with good internal flow conditions. Small disc size will result in lower disc losses, lower weight per horsepower, and a smaller power "package". Since the disc stress is proportional to V_D^2, changing the size (disc radius) will not affect the maximum stress condition if V_D is maintained constant.

The disc must accommodate the necessary fuel, ignition, and lubrication components. This appears to be no problem since adequate, accessible space is provided. Provision for driving the auxiliaries is made by incorporation of an accessary gear drive on the end of the disc shaft; the drive turns within the stationary casing where ample room is available for housing the necessary units.

In computing the losses sustained by the rotating disc the following were considered: (1) internal face friction drag, (2) internal end friction drag, (3) external face friction drag, (4) disc seals, and (5) disc bearing. It should be noted that losses in the flow channel were accounted for in the internal flow analysis of the previous section. Also, the losses incurred by the gear train are figured along with the propeller loss. Their sum appears as an efficiency, η_z, of conversion from brake horsepower to thrust horsepower and is charged to the propeller-spinner section and not to the engine itself. This is done

since it was felt that the gear train and propeller will vary considerably with the specific installation and as such, should be kept integral. Also, the percentage of the power output transmitted to the propeller is a function of aircraft speed as is the efficiency of the propeller η_p. This will be shown later in the next section. Actually the bearing loss as computed, is of such a magnitude that it probably could include a large portion of the gear train loss.

The detailed method of computing each of the losses will now be considered. Each is figured as a horsepower loss. Necessary assumptions made are discussed as presented. The disc will be assumed to have the following shape for computational purposes.

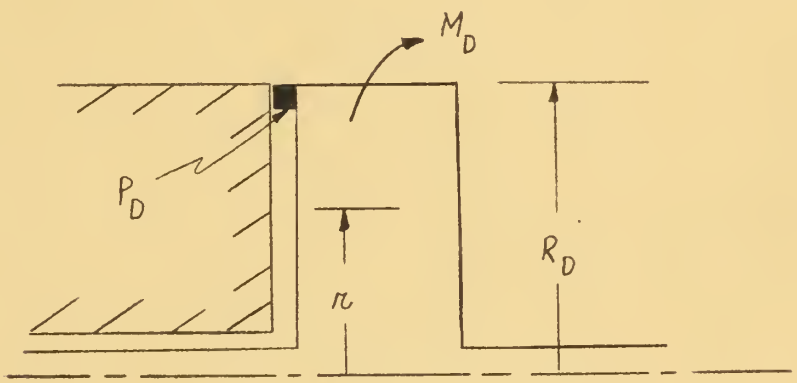


A. Internal Face Friction Drag

In the design it was proposed to evacuate the clearance spaces in order to reduce the skin friction drag. This can be done since in theory drag is directly proportional to the pressure. This desire would necessitate incorporation of seals. According to the calculations,

the sum of the seal losses and reduced pressure drag losses is considerably less than theat which would be experienced by allowing free air pressure and no seals. Using a reduction ratio of 1/20, the seal and face losses amount to approximately 2-1/2% for a 2,000 T.H.P. engine. If no seals were used this loss would increase to a prohibitive value. The face and seal loss is a function of the engine size; it decreases in percentage for the larger engines. As an example, it drops to the order of 1% for a 10,000 T.H.P. unit.

The incorporation of seals would also tend to reduce the pumping action in the clearance void by isolating it from the free air.



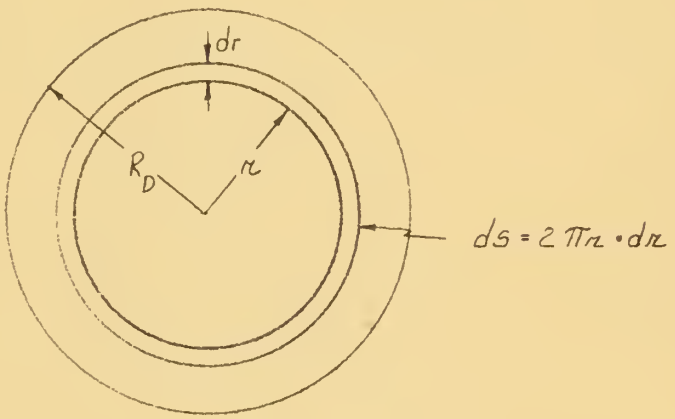
If the equilibrium condition is considered: $dP = \rho dr \cdot \frac{V^2}{r}$ and use is made of the gas law $\rho = \frac{P}{RT}$ and speed of sound $a = \sqrt{\gamma RT}$; then it is found

$$P = P_D e^{\frac{\gamma}{2} M_D^2 \left(\frac{r^2}{R^2} - 1\right)}$$

This indicates the existance of a pressure gradient decreasing exponentially toward the center of the disc. The effect of the decrease in pressure is somewhat offset by the fact that the major portion of the disc area is operating at pressures approaching P_D. The pressure gradient effect will not be considered in the computations because of its complications and the arbitrary choice of pressure reduction ratio. Using the formula

$$D = C_f \frac{\gamma P M^2}{2} S \quad \text{where} \quad M = \frac{r}{R} M_D$$

the moment due to the skin friction may be computed:



$$M_o/\text{side} = \int_o^{R_D} C_f \frac{\gamma P (\frac{r}{R} M_D)^2}{2} 2\pi r dr \cdot r$$

$$= \frac{C_f \gamma P M_D^2 \pi R_D^3}{5} .$$

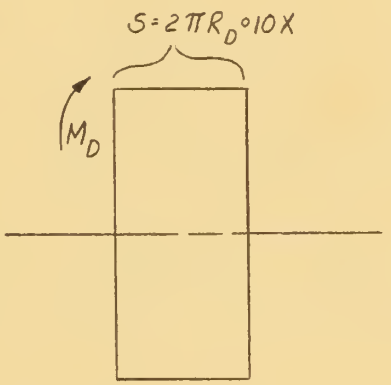
Comparison of results found by methods contained in Ref. 36 with those obtained by this approach, indicate that more conservative values are

realized from the latter. Thus, this formula will be used because of its simplicity. If "e" is the pressure reduction ratio and P is for free air then the pressure acting on the face is eP. Then the H.P. for two sides is:

$$H.P._{2\ sides} = \frac{2}{5}\,\frac{C_f \gamma_e P M_D^{\,3} \pi R_D^{\,2} a}{550}.$$

B. Internal End Friction Drag

If "x" is the radial width of the jet exit, then it will be said that the disc width is 10x. This can be justified since in current practice the combustion chamber length is of the order of 7 to 8 times its width and the nozzle length 2 to 3 times its width. In like manner the H.P. is computed:

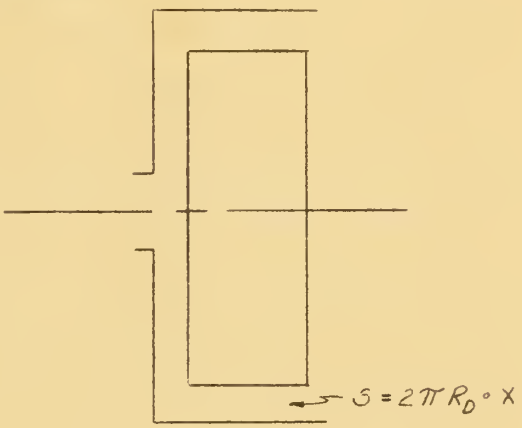


$$H.P. = \left(C_f \frac{\gamma_e P M_D^{\,2}}{2}\, 2\pi R_D 10x\right) \frac{V_D}{550}$$

$$= \frac{C_f \gamma_e P M_D^{\,3} \pi R_D\, a\, 10x}{550}.$$

C. Exposed Face Friction Drag

In the smaller engines it will often be the case that only a portion of the annular jet exit ring will be occupied by exit area. This is due to the geometry and the requirement that the jet exit width must be of sufficient magnitude so that the channel has practical ratios of area to perimeter. It was arbitrarily decided to charge off the entire exposed ring area as a loss in every case to somewhat compensate for other non-included losses at this point. It is assumed that x is small in comparison to R_D.



$$\therefore \text{H.P.} = \left(C_f \frac{\gamma P M_D^2}{2} 2\pi R_D x\right) \frac{V_D}{550}$$

$$= \frac{C_f \gamma P M_D^3 \pi R_D a x}{550}$$

The three losses just computed can be combined as follows assuming an $e = \frac{1}{20}$:

$$\therefore \text{H.P.}_{\text{skin friction}} = a M_D^3 (C_f \gamma_0 P)\left[\frac{R_D x}{5.83} + \frac{R_D^2}{437}\right].$$

The value of C_f in the above equation may be taken from the curve of Fig. 30 which was pieced together from Ref. 10. An average value of .0032 was assumed; this will be conservative since the major part of the disc areas operate at the higher Mach numbers.

D. Disc Seals

To find a value for the coefficient of kinetic friction at high sliding velocities, Fig. 31 taken from Ref. 34, was used. Because the relative motion between the stationary casing and the rotating disc would be in the neighborhood of $M_L = 2$ or 2,230 ft./sec., values of the coefficient were required at considerably higher velocities than those shown in Ref. 34. Consequently, the curve of Fig. 31 was arbitrarily extended in what was considered to be a conservative manner. This gave a coefficient of .08 at 20,000 ft./min. From Ref. 17, pages 4-44 is found the statement "----above 100 ft./min. the coefficient of friction varies approximately as the square root of the speed---". Using this approximation the curve could be extrapolated on out to the speeds in question; this method gave comparatively low losses.

In order to use a more conservative approach, the seal was considered to be made up of a series of rings fitted one inside the other, each with a velocity in respect to adjacent rings of 20,000 ft./min. or 33 ft./sec. The seal will then be comprised of $\frac{V_D}{333}$ separate rings. The coefficient of .08 will be assumed to be acting between each ring. The contact width of each ring will be assumed to be 1/10"; the rubbing surface area will then be $S = \frac{V_D}{333} \cdot \frac{1}{12 \times 10} \cdot 2 R_D$ sq. ft. The normal pressure that each ring exerts will be assumed to be one pound per square

inch. The total normal force on the sliding surfaces is $F_n = 144S$. The drag force then is $F_D = .08(144S)$ per seal. The complete closure for the disc will be assumed to be four seals, two for each side at the jet exit. The resulting loss in horsepower is:

$$\frac{H.P.}{4 \text{ ring seal}} = .1328 \cdot 10^{-4} R_D V_D^2 .$$

The effect of lower relative velocity than V_D between the disc and spinner is neglected.

E. Bearing Losses

Bearing losses were computed according to the methods outlined in Ref. 16 for assumed dimensions. These dimensions were governed by current practice according to the engine horsepower. If the engine size was expressed in terms of the jet gross horsepower, it was concluded that a conservative estimate of the bearing loss was 3% of the jet horsepower.

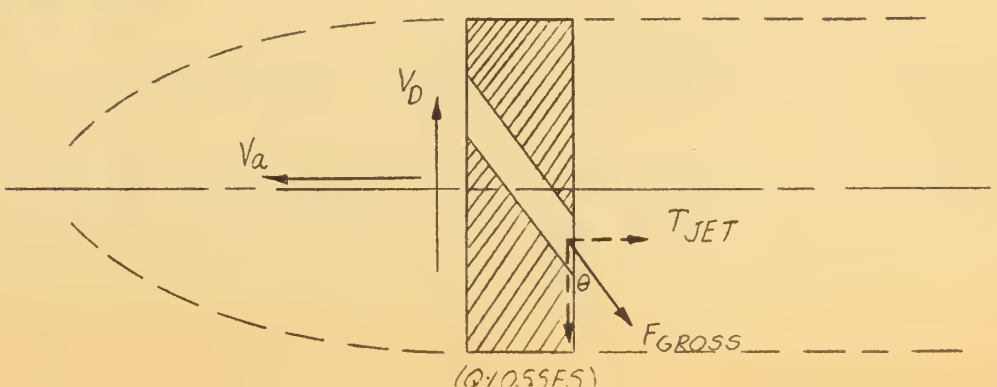
$$H.P. = .03 \frac{(F/A_7)_{gross} A_7}{550} \cdot \left(\frac{V_D}{\cos \theta}\right) .$$

V. SPECIFIC ENGINES

In this section the performance of several complete engines will be covered. In order to solve for all losses, specific dimensions must be assumed; this is done in such a manner as to be the most efficient within the limits of practicality. Since the installation is to produce thrust as economically as possible, this problem will now be investigated. The first phase is to calculate the thrust produced; or for our computational procedure, the T.H.P. for a particular set of conditions.

For the determination of T.H.P. an η_z is assumed; this efficiency factor relates the conversion of the disc B.H.P. to the T.H.P. furnished by the propeller. It is expressed by T.H.P. = η_z B.H.P. The reduction in conversion from B.H.P. to T.H.P. therefore includes gear train, propeller, and spinner losses. It is considered that gear train and spinner losses will be fairly small. Propeller efficiencies have been well established over the subsonic aircraft speed range; η_p in the neighborhood of .93 up to a Mach number of 0.6 are referred to in Ref. 39. Thus, it would seem that a value of 0.9 for η_z was perhaps about the upper limit. Computations have been included with η_z = 0.7, 0.8, and 0.9.

By reference to the below sketch a formula for the T.H.P. may now be derived.



The quantities (Q-Losses) and T_{jet} are the components of the jet gross thrust in the circumferential and axial directions, respectively. The force (Q-Losses) must produce the horsepower to drive the propeller and account for the disc losses, pumping power, and intake ram loss. "Q" represents that portion driving the propeller and "Losses" the combined losses. Q.H.P. and L.H.P. are the propeller and disc loss horsepowers, respectively.

$$\text{T.H.P.} = \eta_z \text{Q.H.P.} + \frac{T_{jet}\, V_a}{550} - \text{Intake Ram H.P.}$$

but

$$\frac{F \cos \theta\, V_D}{550} = \text{Q.H.P.} + \text{L.H.P.} + \text{Pumping H.P.}$$

or

$$\text{Q.H.P.} = \frac{F \cos \theta\, V_D}{550} - \text{L.H.P.} - \text{Pumping H.P.}$$

Then

$$\text{T.H.P.} = \eta_z \frac{F \cos \theta\, V_D}{550} + \frac{F \sin \theta\, V_a}{550} - \eta_z \text{ L.H.P.}$$

$$- \eta_z \text{ Pumping H.P.} - \text{Intake Ram H.P.}$$

The above equation is now rewritten in tabular form:

T.H.P. = Summation of the quantities (A) through (G).

(A) (propeller-losses) $+ \eta_z \cdot \frac{(F/A_7)A_7}{550} \cdot \cos \theta \cdot V_D$

(B) (jet thrust) $+ \cdot \frac{(F/A_7)A_7}{550} \cdot \sin \theta \cdot V_a$

(C) (pumping) $$-\eta_z \cdot \frac{(m/A_7)A_7}{550} \cdot V_D^2$$

(D) (intake ram) $$- \cdot \frac{(m/A_7)A_7}{550} \cdot V_a^2$$

(E) (disc skin friction) $$-\eta_z \cdot \frac{C_f \rho P}{a^2}\left[\frac{R_D^2}{438} + \frac{xR_D}{5.83}\right] \cdot V_D$$

(F) (disc seals) $$-\eta_z \cdot 13.28 \cdot 10^{-6} R_D \cdot V_D^2$$

(G) (disc bearing) $$-\eta_z \cdot \frac{(F/A_7)A_7}{18320} \cdot \sec\theta \cdot V_D$$

Now, it is desired that the maximum return of T.H.P. be gained; consequently, the T.H.P. equation will be maximized in regard to θ.

$$\frac{\partial \text{ T.H.P.}}{\partial \theta} = \frac{\eta_z V_D (F/A_7)A_7}{550} \cdot (\sin\theta) + \frac{V_a (F/A_7)A_7}{550} \cos\theta$$

$$- \frac{\eta_z V_D (F/A_7)A_7}{18320} \sec\theta \tan\theta$$

$$0 = -\eta_z V_D \sin\theta - \frac{V_D}{33.3} \frac{\sin\theta}{\cos^2\theta} + V_a \cos\theta$$

$$\sin\theta\, \eta_z V_D \left(1 + \frac{1}{33.3\cos^2\theta}\right) = V_a \cos\theta$$

$$\tan\theta = \frac{V_a}{\eta_z V_D}\left[\frac{1}{1 + \frac{1}{33.3\cos^2\theta}}\right]$$

Next, limit θ_{min} to 20° which is reasonable if any jet egress is to result without alternation of the design. It is of interest to note that the limiting θ to 20°, where actually if θ should be in the neighborhood of 10° for optimum conditions (low subsonic speeds and fairly high velocity), results in a T.H.P. loss of only about 1.3%. Choosing values of V_a and V_D conductive to large θ's, it is found that 40° corresponds approximately to V_a = 1200'/sec. (M = 1.07 at sea level), V_D = 1800'/sec. (M = 1.61) and η_z = 0.8. For θ between 20° and 40° the term in the parenthesis will vary between 0.966 and 0.952. A value of 0.96 will be assumed as an average. In this way a simple formula is evolved for θ.

$$\tan \theta = \frac{.96\ V_a}{\eta_z V_D}$$

By use of the above formula, θ no longer appears as a variable in the T.H.P. equation. T.H.P. is then a function of the following variables: V_D, R_D, x, and A_7. The disc velocity V_D will be limited by stress considerations. The jet exit area A_7 is a function of the power required of the engine since it determines F for any particular V_D. R_D and x in turn depend primarily on A_7. By these considerations the maximum output may be realized.

To compute T.H.P. the values of (F/A_7), (m/A_7), A_7, V_D, η_z, x, and R_D are needed. (F/A_7) and (m/A_7) are given vs M_D on Figs. 32 and 33, respectively. They were computed from the internal flow analysis. For ease of computation and obtaining optimum conditions in any actual design, the formula for these two curves was found. The method and

results are shown on Fig. 34. The formulas are valid for an M_D greater than 1.5 and less than 2.1.

A_7 is estimated according to the thrust that the engine must produce at a particular V_a. The values of x and R_D were next estimated from the value of A_7 chosen; consideration of the inlet area and engine size governed practical values of R_D, while θ and A_7 gave an explicit value of x. The jet exit width, x, was limited to a minimum value of 0.6 inches. The following table gives the values used.

A_7 sq. ft.	R_D ft.	x ft.
0.2	1.0	0.05
0.6	1.125	0.085
1.0	1.25	0.1273

The disc velocity and conversion efficiency were allowed to range over representative values. To gain an idea into the relative magnitude of the components of T.H.P., the values computed for the "basic" condition (defined in the Internal Flow Section) for an engine producing 4,100 pounds of thrust at an aircraft speed of 300 fps. are listed below:

V_a = 300 fps.

Altitude = sea level

M_D = 2.0

A_7 = 0.2

$\eta_z = 0.9$

$\theta = 8.2^\circ$

(A)	(propeller-losses) H.P.	+ 7,330
(B)	direct jet H.P.	+ 157
(C)	pumping H.P.	- 4,860
(D)	intake ram H.P.	- 98
(E)	disc skin friction H.P.	- 41
(F)	disc seal H.P.	- 59
(G)	disc bearing H.P.	- 225
	Final T.H.P.	+ 2,240

This corresponds to an economy S.F.C. of 0.628 lbs./T.H.P. Hr. or 0.343 lbs./lbs. Hr.; economy S.F.C. is defined as $\frac{\text{lbs. fuel}}{\text{Thrust H.P. Hr.}}$ to differentiate it from the jet S.F.C. The former figure may be compared with 0.612 for a good reciprocating engine at sea level ($0.55 \frac{\text{lbs.}}{\text{B.H.P. Hr.}}$) and the latter to 0.99 for the turbojet engine. The turbojet S.F.C. was taken from Fig. 35 which is a graph of Ref. 2.

Turning now to Figs. 36 and 37, the results of the computations are seen. S.F.C. seems to vary almost linearly with M_D particularly at the higher conversion efficiencies. The change in S.F.C. with aircraft speed reaches a minimum at about 700 fps. or 477 mph. The variation with V_a with an assumed $\eta_z = 0.9$ is such as to give very satisfactory values over the range of speeds up to 900 fps. Attainment of an η_z approaching 0.9 above 900 fps. is very doubtful.

Figures 38 and 39 give the T.H.P. characteristics.

For the sake of comparison and evaluation of the results, the following table is included using Fig. 37 for sea level conditions and an aircraft speed of 300 mph. The engine size corresponds to $A_7 = 0.6$ for the below comparison.

Engine Size	Centrifugal Jet Economy	Turbojet Economy
9,000 lbs. thrust	0.476 $\frac{\text{lbs.}}{\text{lbs. Hr.}}$	1.06 $\frac{\text{lbs.}}{\text{lbs. Hr.}}$

Engine Size	Centrifugal Jet Economy	Reciprocating Eng. Economy
7,200 T.H.P.	0.595 $\frac{\text{lbs.}}{\text{T.H.P. Hr.}}$	0.612 $\frac{\text{lbs.}}{\text{T.H.P. Hr.}}$

Thus, for the "basic condition", the superiority in economy for the proposed centrifugal jet engine design over both the reciprocating and turbojet engines is shown.

VI. PROPELLER BLADE CHARACTERISTICS

The next phase of study will involve the design approach for a supersonic propeller. This approach will be based on the standard strip theory analysis. Experience has shown that the theory is reliable, within satisfactory limits, for relatively conventional propellers. It will account for most of the variables in design and operation, but typical theory application neglects some factors, such as interaction between sections and boundary layer action in centrifugal fields.

First, in order to use the theory, it is necessary to have the propeller blade section characteristics. For the analysis contained herein, all airfoil characteristics will be presented in the form of (L/D) ratios. Figs. 40, showing (L/D) ratios vs Mach number for various thickness ratios, has been computed from the data presented in Ref. 39. The data for Mach numbers less than one were taken from test measurements while that for Mach numbers above M = 1 is attributed to calculations according to Busemann. The results are for infinite aspect ratio wings; thus, they are two dimensional curves. Using Ref. 29, the curve giving (L/D) ratios of 50 below M = 0.6 can be conservatively maintained up to thickness ratios of 21% where the Reynolds number is 3×10^6.

The poor (L/D) ratios for Mach numbers approaching M = 1 and above, is clearly evident. Since a high level of propeller performance demands good (L/D) ratios, it would naturally be expected that low strip efficiencies would be experienced for sections operating above M = 0.8. It now becomes clear that if a satisfactory supersonic propeller is to be developed, it is not going to be done with the supersonic curves of

Fig. 40.

The author proposes as an answer to the problem, to use an appropriate delta wing plan form which will produce higher (L/D) ratios. At the same time this method involves a finite aspect ratio and thus accounts for three dimensional effects along the supersonic span. Curves 41 through 47 show what can be theoretically accomplished in this direction. Ref. 30 was used to calculate the lift coefficient, the supersonic wave drag coefficient, and the correction for drag due to lift. All data presented is for double wedge profiles. Ref. 26 may be used to calculate equivalent information for biconvex or multislope airfoil sections. A general treatment of the subject matter is found in Ref. 28.

The (L/D) ratios were computed by the following method.

$$C_L = \left(\frac{dC_L}{d\alpha}\right) \alpha$$

$$C_D = C_{D_w} + C_{D_f} + C_{D_\alpha}$$

(wave drag) (skin friction) (drag due to lift)

$$C_{D_\alpha} = C_L \alpha \left(\frac{C_D}{\alpha C_L}\right) = \left(\frac{dC_L}{d\alpha}\right) \alpha^2 \left(\frac{C_D}{\alpha C_L}\right)$$

where $\left(\frac{C_D}{\alpha C_L}\right)$ is a correction term to the coefficient of drag due to lift. Using Fig. 30, $C_f = .003$ is assumed as a practical value; then $C_{D_f} = .006$ for both sides of the airfoil surface. Finally

$$\frac{C_L}{C_D} = \frac{\left(\frac{dC_L}{da}\right) a}{C_{D_w} + C_{D_f} + \left(\frac{dC_L}{da}\right) a^2 \left(\frac{C_D}{aC_L}\right)} .$$

Since the maximum (L/D) ratio is desired, the last formula will be maximized with respect to a.

$$\frac{d(C_L/C_D)}{da} = \frac{2a^2\left(\frac{dC_L}{da}\right)^2 \left(\frac{C_D}{aC_L}\right) - \left[C_{D_w}\left(\frac{dC_L}{da}\right) + C_{D_f}\left(\frac{dC_L}{da}\right) + a^2 \left(\frac{dC_L}{da}\right)^2 \left(\frac{C_D}{aC_L}\right)\right]}{C_D^2}$$

$$0 = a^2 \left(\frac{dC_L}{da}\right) \left(\frac{C_D}{aC_L}\right) - C_{D_w} - C_{D_f}$$

or

$$a = \sqrt{\frac{C_{D_w} + C_{D_f}}{\left(\frac{dC_L}{da}\right) \left(\frac{C_D}{aC_L}\right)}} \qquad \text{for (L/D) max.}$$

$$C_D = 2(C_{D_w} + C_{D_f}) \qquad \text{for (L/D) max.}$$

$$C_L = a\left(\frac{dC_L}{da}\right) = \sqrt{\left(\frac{dC_L}{da}\right) \frac{(C_{D_w} + C_{D_f})}{(C_D/aC_L)}} \qquad \text{for (L/D) max.}$$

then it follows that:

$$\left(\frac{L}{D}\right)_{max} = \frac{\sqrt{\frac{dC_L}{d\alpha}\,\frac{(C_{D_w} + C_{D_f})}{(C_D/\alpha C_L)}}}{2(C_{D_w} + C_{D_f})}$$

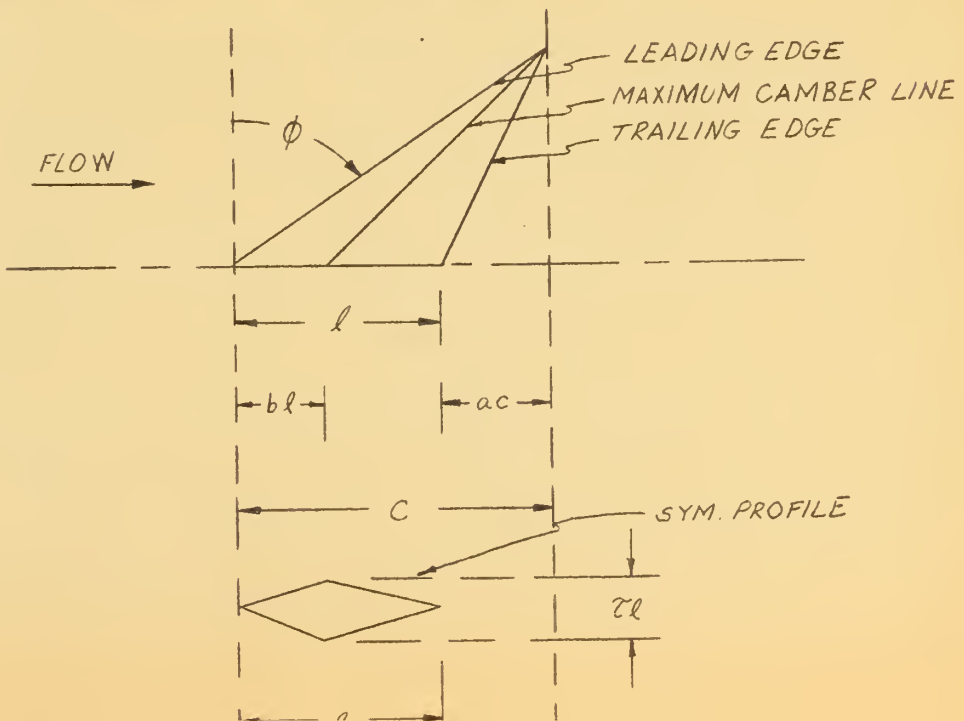
$$= \frac{1}{2}\sqrt{\frac{(dC_L/d\alpha)}{(C_D/\alpha C_L)(C_{D_w} + C_{D_f})}}$$

or

$$= \frac{1}{2(C_D/\alpha C_L)[\alpha]_{optimum}}.$$

To use the above formulas the values of C_{D_w}, $(dC_L/d\alpha)$, and $(C_D/\alpha C_L)$ are required. Their evaluation may be computed from graphs involving certain parameters which are now discussed.

The delta wing is assumed to be of a symmetrical double wedge profile and it takes the following plan form.



A study of the sketch will show that for any root chord "ℓ", the plan form is completely determined by the leading edge sweepback angle "ϕ", the constant "b" which determined the position of the maximum camber line, and the constant "a" which sweeps the trailing edge back if positive and forward if negative. The variables ϕ and stream Mach number M are combined in the parameter k where k is defined:

$$k = \frac{\sqrt{M^2 - 1}}{\tan \phi} .$$

By entry into the Figs. of Ref. 30, C_{D_w}, $(dC_L/d\alpha)$, and $(C_D/\alpha C_L)$ are given vs k with parameters a and b. For further detailed discussion of the computations, the reader is referred to the references given.

The results of the calculations are now considered. Unless otherwise stated a = 0 (no trailing edge sweep), b = 0.2 except for k greater or equal to 0.8 when b = 0.5, and correction for $C_D/\alpha C_L$) is included. Fig. 41 gives $(L/D)_{max.}$ vs k for a 1% section at Mach numbers from 1.1 to 2.5. The characteristic drop in the (L/D) ratio as Mach number increases is clearly shown. It should be noticed that the maximum values occur at the same k for any Mach number and any particular τ. These two trends have been substantiated by the author, for thickness ratios up through 6%. Fig 42 shows the change in the character of the curves as thickness ratio is increased for M = 1.1. The shift towards lower "k's" as the τ is increased is common to other Mach numbers since all curves of any one thickness ratio have the same general shape. For the lower τ's considerable choice of k is possible

for high (L/D) values but less latitude of choice and greater sweepback (lower "k's") is required at larger τ's. This trend is attributed to the much greater ratio of C_{D_w}/C_D at the larger thickness ratios.

If the (C_D/aC_L) correction is neglected, the curves of Fig. 43 result. It is seen that these curves allow, in general, higher "k's" while the maximum values of $(L/D)_{max.}$ are considerably reduced. Also, k for the maximum values for any particular thickness ratio is no longer constant. Comparison of corrected and uncorrected curves for several τ's is made in Fig. 44. The spread between each pair of curves becomes least at the higher k values.

Next the problem of trailing edge sweepback is considered in Figs. 45, 46, and 47. The first two are results at Mach numbers of 1.6 and 2.0, respectively. Both Figures evidence the marked improvement in (L/D) ratios with trailing edge sweepback; this improvement is accompanied by a shift to larger leading edge sweep (smaller "k's") for attainment of maximum ratios. The decrease in values with Mach number increase is not changed by incorporation of trailing edge sweepback. The final figure of this section shows this geometrical decrease.

Sufficient airfoil (L/D) data and trends have been presented in this section to allow design of a supersonic propeller. The author's design approach will next be demonstrated in the following section.

VII. SPECIFIC SUPERSONIC PROPELLER

The configuration of a supersonic propeller based on the data of the preceding section will depend primarily on "k" because it governs the maximum (L/D) ratio. If a propeller is operating at a particular rpm., then its sections will be operating at Mach numbers depending on the section radius. With the Mach number determined and a specific thickness ratio indicated, the most advantageous "k" can be decided upon by consulting curves of the type shown on Fig. 41. If the trailing edge sweepback is involved, then curves of the same nature shown in Fig. 47 should be used. With the choice of "k" made, the leading edge sweepback for the section is then computed from the formula $k = \frac{\sqrt{M^2 - 1}}{\tan \phi}$. The trailing edge sweep angle, if involved, may be computed by ordinary geometry.

If section Mach numbers are laid out on a radial line from the center of a propeller as in Fig. 48, and a k = 0.5 is assumed throughout, then the curve AC is found to be the leading edge. The dotted section AO is arbitrary but shows about the steepest practical curvature. The hatched circle in the center comprises the propeller spinner. The radial lines drawn intersecting the leading edge line AC at various points indicate the position of blade "cutoff" for a particular propeller tip Mach number. The dotted lines to some of the leading edge "cutoff" points indicate arbitrary trailing edges and thereby serve to show the relative scope of such a propeller. The tremendous increase in plan form area by a small increase in tip speed at the larger "cutoff" points should be noted. The area is essentially doubled by going

from a Mach number of 1.6 to 1.8.

With the general outline in mind for drawing a plan form, attention will now be turned toward creating a specific propeller. In order to do this a few of the more important problems will be mentioned which affect the design. It should be recognized that the optimum propeller, for any given aircraft speed and propeller tip Mach number, could easily be designed; but for practical cases this is not satisfactory. A propeller must be able to produce good performance over a range of speeds. This requirement has a large effect on the choice of "k" which will be evident if the situation is examined.

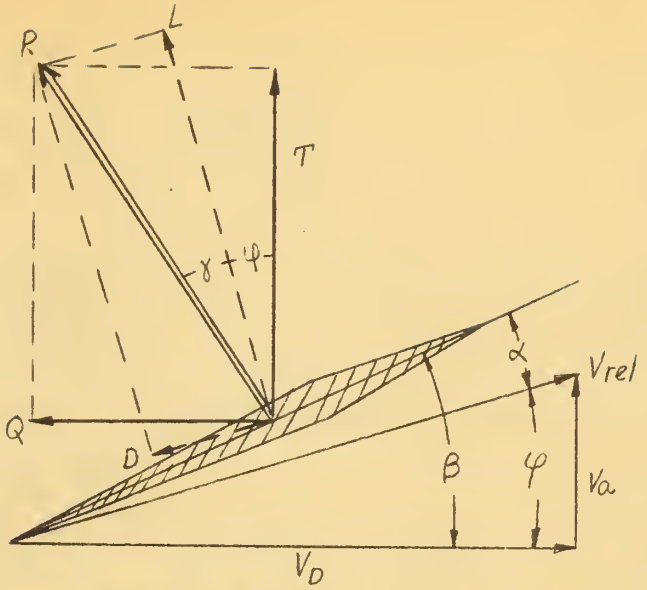
Once the leading edge is laid down, ϕ is a fixed value; then "k" is a function of the blade element Mach numbers. The latter is the vector sum of both the aircraft speed and the propeller velocity for the section. Thus, "k" will vary with a change in either one, which indicates that a range of "k" values will have to be considered if best results are to be obtained.

The leading edge is designed for the "k" corresponding to the highest relative Mach number at which good performance is required. This means choosing as high a "k" as possible which will produce high (L/D) ratios for the thickness ratio and Mach number in question. Then as the relative Mach number is reduced by a reduction in either aircraft speed or propeller rpm., the various sections will operate at lower "k" values. In this connection, the airfoil characteristics seem to indicate a spread of 0.4 to 0.5 for "k" where the curves are fairly flat; this should be the range used for design.

If trailing edge sweepback can be tolerated by the stress situation, it should be incorporated since it produces higher (L/D) ratios and has its "flat" range at lower "k's" as seen on Figs. 45 and 46. This has an advantage aside from the better performance in the fact that with lower "k's", larger sweep angles are dictated which allow considerable plan form area enlargement with no increase in propeller diameter.

In regard to thickness ratios, it should be clear by now that the thinner sections are far superior both in (L/D) ratios and in their "flat" range of "k's". It is proposed by the author to make the propeller blade very thin and flexible as compared to the present practice of making propellers as stiff as possible to reduce vibrational complications. With a very flexible blade, bending stresses would be reduced since the blade would assume a very small dihedral angle (on the order of 1°) dependent on the relation of the magnitude of the thrust and centrifugal force loads. Operation could be likened to fans currently produced that have cloth tape for blades.

Next, the calculation for performance will be considered. The measurement of propeller efficiency for a blade element is developed as follows:



$$\eta = \frac{\text{power output}}{\text{power input}} = \frac{TV_a}{QV_p} = \frac{V_a}{V_p}\,\frac{L\cos\varphi - D\sin\varphi}{L\sin\varphi + D\cos\varphi}$$

$$= \frac{V_a}{V_p}\,\frac{1 - \frac{D}{L}\tan\varphi}{\tan\varphi + \frac{D}{L}}$$

but

$$\frac{V_a}{V_p} = \tan\varphi \quad \text{and} \quad \frac{D}{L} = \tan\gamma$$

then

$$\eta = \frac{\tan\varphi}{\tan(\varphi + \gamma)}$$

This function is plotted in Fig. 48 which was taken from Ref. 11.

If

$$J = \frac{\pi V_a}{V_p} = \pi\tan\varphi$$

then

$$\eta = \frac{1 - \frac{D}{L}\left(\frac{J}{\pi}\right)}{1 + \frac{D}{L}\left(\frac{\pi}{J}\right)} .$$

This function is plotted in Fig. 49 and will be the graph used to determine section efficiencies. Maximizing the propeller efficiency equation with respect to shows that best theoretical efficiency is obtained when $\varphi = \left(\frac{\pi}{4} - \frac{\gamma}{2}\right)$.

To calculate the blade performance, individual radial increments are considered. Call ΔR the element width and $b\Delta R$ the element length; then $b\Delta\bar{R}^2$ will be the section area.

$$L = \frac{\rho M_{rel}^2}{2} (b\Delta\bar{R}^2) C_L$$

$$D = \frac{\rho M_{rel}^2}{2} (b\Delta\bar{R}^2) C_L \left(\frac{C_D}{C_L}\right)$$

$$= \frac{\rho M_{rel}^2}{2} (b\Delta\bar{R}^2) C_L \tan \gamma$$

$$T = L \cos\varphi - D \sin\varphi$$

$$Q = L \sin\varphi + D \cos\varphi$$

$$M = \frac{M_a}{\sin\varphi} \; ; \; V_a = M_a \cdot a \; ; \; V_P = \frac{M_a \cdot a}{\tan\varphi} .$$

Then, combining the above properly, the following formulas are obtained:

$$T.H.P. = \left(\frac{\rho M_a^3 a}{1100}\right) \Delta\bar{R}^2 \left[bC_L \left(\frac{1}{\tan\varphi \sin\varphi} - \frac{\tan\gamma}{\sin\varphi}\right)\right]$$

$$Q.H.P. = \left(\frac{\gamma P M_a^3 a}{1100}\right) \Delta \bar{R}^2 \left[bC_L \left(\frac{1}{\tan \varphi \sin \varphi} + \frac{\tan \gamma}{\tan^2 \varphi \sin \varphi} \right) \right].$$

The performance for the propeller shown on Fig. 51 is now given. In connection with the design and computations of this propeller, the following assumptions were made:

(1) A high speed condition of $M_a = 1.0$ and $M_p = 2.0$ was selected.

(2) For ease of computation, τ was assumed as 1% for all sections. Actually the thickness ratios would probably be increased slightly toward the root.

(3) A straight trailing edge was drawn for ease of computation.

(4) The spinner had a radius equal to 0.2 R.

(5) The section width increment, ΔR, was chosen as 0.1 R and all section characteristics were taken for the element median.

(6) The leading edge was designed with a k = 0.9 for all sections at a relative Mach corresponding to $M_a = 1.0$ and $M_p = 2.0$.

(7) The plan form was laid out in the untwisted condition.

(8) The (L/D) ratio for sections operating between M = 0.9 and M = 1.0 was assumed to be the same as the section operating just above M = 1.0. This seems to be conservative if Fig. 40 is consulted.

(9) The (L/D) ratio for sections operating below M = 0.9 was assumed to be 33.

(10) The (L/D) ratios for all supersonic sections were decreased by 10% to allow for rounding the edges. This change was

attributed entirely to a drag increase leaving the C_L unaltered.

In connection with the last assumption it is felt that by rounding the leading edge and keeping the angle of attack small, the correction $(\frac{C_D}{aC_L})$ could be attained. This correction amounts to a decrease of the drag due to lift. In practice, with a sharp leading edge the decrease does not occur due to separation at the leading edge. Angles of attack on the order of 2 to 3 degrees occur for the (L/D) ratios computed. In actual practice biconvex sections should probably be used because the leading edge angles would be twice as great. Also, they would perform better as subsonic sections since their profile have no sharp breaks as the double wedge does. The (L/D) ratios would not be affected appreciably by use of biconvex sections although the wave drag coefficient is increased 33% over that of the double wedge. This is due to the fact that the ratio of C_{D_w}/C_D is small for low τ's and a's occurring in this design. Ratios of wave drag to total drag are on the order of 0.05 or less.

Section efficiencies for a range of propeller speeds at $M_a = 1$ is given in Fig. 52, while Fig. 53 is for a range of aircraft speeds with $M_p = 1.1$. The higher values of η_p approaching 95% in the latter figure occur when that portion of the blade operates subsonically below M = 0.9. The T.H.P. and Q.H.P. loading curves along the propeller radius are given on Fig. 54 for the high speed condition. The overall efficiency for this condition was 83.5%. Overall propeller efficiencies at $M_a = 1$ for lower propeller speeds reached 86%. The total T.H.P. per

blade was 304.6 R^2 for a Q.H.P. = 365.3 R^2. It should be realized that the power absorbing qualities could easily be doubled since the operating C_L's are very low, ranging approximately between 0.1 and 0.2. Further investigation would have to determine first how much the (L/D) ratios would be damaged by increasing the C_L's; it is felt by the author that the drop would be small for reasonable increases of C_L.

These computations indicate the probable maximum efficiencies that could be attained by such a plan form. This is because the upper limit of the (L/D) ratios was used for the supersonic sections with τ = 1%. The thickness ratio of 1% might prove to be impractical particularly in smaller chord propeller where a τ of 1% would dictate almost impossible physical thicknesses. The use of larger thickness ratios would lower efficiencies somewhat, but as long as the (L/D) ratio was maintained at or above 10, efficiencies on the order of 80% could be realized. The lower curve of Fig. 49 clearly illustrates this. The propeller section characteristics showed that (L/D) ratios exceeding 10 were easily attainable at moderate Mach numbers for larger thickness ratios. According to common practice, the τ would normally decrease toward the propeller tip while the Mach number increases according to a linear law. These two changes over the blade span are compatible in their effects, tending to give a more or less constant (L/D) ratio. Consequently, it is felt that thickness ratios approaching those used in present day practice could be used and still give a supersonic propeller with an efficiency around 80%.

VIII. EVALUATION

For evaluation of the proposed power plant, two graphs are presented which compare the engine and propeller characteristics with the best of other current designs. The favorable position of the centrifugal jet engine in relation to the reciprocating and jet engines is shown in Fig. 55. The simplicity of the centrifugal jet in comparison to the three complex designs with which it seems to be competing in Fig. 55 should be taken into consideration. The data for the other engine types was taken from Ref. 3. In addition to performance, other considerations involved in evaluation of a power system includes cost and safety. Since neither experience nor analysis provides accurate information, the discussion will be left to the reader.

For the propeller, Fig. 56 indicates the efficiency which theoretically could be approached by the proposed design. It is seen that it is considerably superior to the best of todays laboratory designs. The current propeller performance was drawn from Ref. 39. If the radius of the propeller of Section VII is chosen equal to 5 feet, it will absorb 18,250 H.P. and produce 7,500 pounds of thrust at $M_a = 1$ with an efficiency of 83.5%. Compare this with the propeller for the DC-6 Airplane which handles 2,400 H.P. on a 13 ft. diameter with twice as many blades. The hub radius of 1 foot in this case is compatible with the proposed engine disc sizes.

Thus, it would seem that theoretically an efficient, simple, "small package" aircraft propulsion system has been evolved by the author's enclosed design.

REFERENCES

1. Sanders, J. C. and Sanders, N. D., "A Preliminary Study of a Propeller Powered by Gas Jets Issuing From the Blade Tips", N.A.C.A. Technical Note No. 1155, November 1946.

2. Cleveland Laboratory Staff, "Performance and Ranges of Application of Various Types of Aircraft Propulsion System", N.A.C.A. Technical Note No. 1349, August 1947.

3. Hill, Paul R., "Parameters Determining Performance of Supersonic Pilotless Airplanes Powered by Ram-Compression Power Plants", N.A.C.A. War Time Report L-755, June 1946.

4. Stewart, H. J., "The Lift of a Delta Wing at Supersonic Speeds", Quarterly of Applied Mathematics, Vol. IV, October 1946.

5. Harmon, Sidney M., "Theoretical Supersonic Wave Drag of Untapered Sweptback and Rectangular Wings at Zero Lift", N.A.C.A. Technical Note No. 1449, October 1947.

6. Puckett, Allen E., "Supersonic Wave Drag of Thin Airfoils", Journal of the Aeronautical Sciences, Vol. 13, No. 9, September 1946.

7. von Karman, Th., "Supersonic Aerodynamics - Principles and Applications", Journal of the Aeronautical Sciences, Vol. 4, No. 7, July 1947.

8. Evvard, John C., "Distribution of Wave Drag and Lift in the Vicinity of Wing Tips at Supersonic Speeds', N.A.C.A. Technical Note No. 1382, July 1947.

9. Jones, Robert T. and Margalos, Kenneth, "Flow Over a Splender Body of Revolution at Supersonic Velocities", N.A.C.A. Technical Note No. 1031, August 1947.

REFERENCES (Continued)

10. Keenan, Joseph H. and Newman, Ernest P., "Measurements of Friction Coefficients in a Pipe for Subsonic and Supersonic Flow of Air", N.A.C.A. War Time Report W-44, July 1943.

11. Young, Raymond A., "Helicopter Engineering", The Ronald Press Company, New York, 1949.

12. Nelson, Wilbur C., "Airplane Propeller Principles", John Wiley and Sons, Inc., 1944.

13. Ferri, Antonio, "Elements of Aerodynamics of Supersonic Flows", The MacMillan Company, New York, 1949.

14. Bailey, Neil P., "The Thermodynamics of Air at High Velocities", Journal of the Aeronautical Sciences, Vol. 11, No. 3, July 1944.

15. Staff, Guggenheim Aeronautical Laboratory, C.I.T., "Jet Propulsion", Air Technical Service Command, A.A.F. Publication, 1946.

16. Marks, Lionel S. (edited), "Mechanical Engineer's Handbook", McGraw and Hill Book Company, Inc.

17. Eshbach, Ovid W., "Handbook of Engineering Fundamentals", John Wiley and Sons, Inc.

18. Piening, Werner, "The Efficiency of Combustion Trubines with Constant Pressure Combustion", N.A.C.A. Technical Memorandum No. 975, April 1941.

19. Tetervin, Neal, "Approximate Formulas for the Computation of Turbulent Boundary Layer Momentum Thickness in Compressible Flows", N.A.C.A. War Time Report L-119, March 1946.

20. McLellan, Charles H. and Nichols, Mark R., "An Investigation of Diffuser Resistance Combinations in Duct Systems", N.A.C.A. War

REFERENCES (Continued)

Time Report L-329, February 1942.

21. Desmond, Gerald L. and Freitag, Robert F., "Working Charts for the Computations of Propeller Trhust Throughout the Take-Off Range", N.A.C.A. War Time Report W-100, July 1943.

22. ANC-5, "Strength of Aircraft Elements", December 1942, Revised Edition.

23. CAR-04, "Airplane Air Worthiness", November 1945.

24. Wood, K. D., "Airplane Design", September 1943, 7th Edition, 1947.

25. Hardenhalt-Kerr-Sasso, "Handbook of Mechanical Design", McGraw and Hill Book Company, Inc., 1942.

26. Deane, Beverly, "The Characteristics of Supersonic Wings Having Biconvex Sections", Meteor Report UAC-35.

27. Dailey, C. L. and Wood, F. C., "Computation Curves for Compressible Fluid Problems", John Wiley and Sons, 1949.

28. Bonney, E. Arthur, "Engineering Supersonic Aerodynamics", McGraw and Hill Book Company, Inc., 1950.

29. Abbott, I. H., Doenhoff, A. E. and Stivers, L. S., "Summary of Airfoil Data", N.A.C.A. Technical Report No. 824, 1945.

30. Puckett, A. E. and Stewart, H. J., "Aerodynamic Performance of Delta Wings at Supersonic Speeds", Journal of the Aeronautical Sciences, Vol. 14, No. 10, October 1947.

31. Manson, S. S., "Direct Method of Design and Stress Analysis of Rotating Discs with Temperature Gradient", N.A.C.A. Technical Report No. 952, 1950.

REFERENCES (Continued)

32. Titanium Metals Corporation of America, "Handbook on Titanium Metal", December 1950.

33. Roy Maurice, "Propulsion by Reaction", N.A.C.A. Technical Memorandum No. 571, June 1930.

34. Johnson, R. L., Swibert, M. A. and Bisson, E. E., "Friction at High Sliding Velocities", N.A.C.A. Technical Note No. 1442, October 1947.

35. Stodola, A., "Steam and Gas Turbines", McGraw and Hill Book Company, Vol. II, 1927, Nernst Turbine, p. 1220.

36. Goldstein, S., "On the Resistance to the Rotation of a Disc Immersed in a Fluid", Cambridge Philosophical Society, Vol. 31, Part 2, Reprint File No. 201.

37. Timoshenko, S., "Strength of Materials", 1940.

38. Timoshenko, S., "Theory of Elasticity", McGraw and Hill Book Company, 1934.

39. Rhines, R. B., "Design Refinements in Modern Propellers", Aeronautical Engineering Review, August 1950.

40. Doelhoff, F. L. V., "The Helicopter Pressure Jet", Aeronautical Engineering Review, September 1950.

41. Stone, I., "New Propellers for Turbine Power", Aviation Week, October 30, 1950.

42. Driggs, I. H., "Why We Still Need the Propeller", Aviation Week, October 23, 1950.

43. Mockley, W. O., "Jet Nozzles for Aircraft Gas Turbines", Aeronautical Engineering Review, October 1950.

APPENDIX A

LIST OF SYMBOLS

a speed of sound, fps; also constant for defining trailing edge sweepback.

A area in square feet.

b coefficient of x in quadratic equation; also constant for defining maximum camber position.

B.H.P. brake horsepower.

c coefficient of x^0 in quadratic equation.

C ratio of friction pressure loss in combustion chamber to average dynamic pressure.

C_D drag coefficient.

C_{D_f} skin friction drag coefficient.

C_{D_α} drag coefficient due to lift.

C_{D_w} supersonic wave drag coefficient.

C_L lift coefficient.

C_v nozzle velocity coefficient.

D diameter, lb.; drag, lb.

e ratio of clearance pressure to free air pressure.

f friction factor.

F jet thrust, lb.

F_{P_o} thrust for full expanding nozzle, lb.

F_t thrust for underexpanding throat nozzle, lb.

G acceleration of gravity (32.17 ft./sec.^{2}) at sea level.

H stagnation pressure, lb./sq. ft.

H.V. lower heating value of fuel, Btu./lb.

J mechanical equivalent of heat (778 ft. lb./Btu.)

LIST OF SYMBOLS (Continued)

k	parameter relating Mach number and leading edge sweepback angle.
l	airfoil root chord.
L	lift, lb.; also disc losses.
(L/D)	lift to drag ratio, also written (C_L/C_D).
L.H.P.	disc loss horsepower.
m	mass flow per second lb./sec.
M	Mach number.
M_D	disc periphery Mach number; $M_D = V_D/a_{\text{sea level}}$.
P	static pressure, lb./sq. ft.
P_f	friction pressure drop, lb./sq. ft.
$\Delta P_{C.F.}$	pressure rise due to centrifugal force, lb./sq. ft.
q	dynamic pressure, lb./sq. ft. $(\frac{1}{2}\rho v^2)$.
q_c	impact pressure, lb./sq. ft. (H - P).
Q	component of propeller resultant force in plane of rotation.
Q.H.P.	propeller brake horsepower.
r	constant term used in computations; also radius.
R_a	gas constant for air (53.3 ft. lb./(F^o)(lb.)).
R_c	gas constant for products of combustion, ft. lb./(F^o)(lb.)).
R_D	disc radius.
s	constant term used in computations.
S	area, sq. ft.
S.F.C.	specific fuel consumption, lb. fuel/lb. thrust-Hr., or lb. fuel/H.P.-Hr.
t	constant term used in computations.
T	temperature, ^oF abs.; also aircraft thrust.

LIST OF SYMBOLS (Continued)

T_{jet} direct jet thrust; lb.

T.H.P. thrust horsepower.

v specific volume cu. ft./lb.

V air or gas speed, fps.

V_a speed of airplane, fps.

V_D peripheral speed of rotating disc, fps.

W_a weight rate of air flow, lb./sec.

W_f weight rate of fuel flow, lb./sec.

x jet exit width, ft.

μ fuel-air ratio.

α airfoil section angle of attack.

ψ propeller angle of advance.

ϕ angle of leading edge sweepback.

β propeller blade angle

γ angle whose tangent is (L/D) ratio

θ jet exit offset angle measured from disc circumferential direction.

γ ratio of specific heat at constant pressure to specific heat at constant volume.

$\bar{\gamma}$ average value of γ between 0° F abs. and temperature T.

τ airfoil section thickness ratio

η_b combustion efficiency.

η_c centrifugal compression efficiency.

η_d subsonic diffuser efficiency.

η_p efficiency of propeller

η_z conversion efficiency, B.H.P. to T.H.P.

LIST OF SYMBOLS (Continued)

ρ mass density, slugs/cu. ft.

Subscripts denoting station along power-plant duct:

1 free stream

2 pipe entrance

3 end of cylindrical entrance pipe; entrance to diffuser

4 end of diffuser; entrance to combustion chamber.

5 end of combustion chamber; entrance to nozzle.

6 nozzle throat

7 end of nozzle.

APPENDIX B

STANDARD ALTITUDE TABLE

(Reproduced in Part)

Alt.	P	P/P_o	^oR	T/T_o	$'c$	ρ	ρ/ρ_o
0	2116.2	1	518.4	1	1115.6	.002378	1
5,000	1760.4	.8320	500.57	.9656	1096.3	.002049	.8616
10,000	1455.6	.6876	482.74	.9312	1076.2	.001756	.7384
20,000	972.5	.4594	447.08	.8624	1036.1	.001267	.5327
30,000	628.1	.2968	411.42	.7936	993.9	.000889	.3740
35,332	489.8	.2314	392.40	.7569	970.7	.000727	.3058

APPENDIX A

LIST OF SYMBOLS

a	speed of sound, fps; also constant for defining trailing edge sweepback.
A	area in square feet.
b	coefficient of x in quadratic equation; also constant for defining maximum camber position.
B.H.P.	brake horsepower.
c	coefficient of x^0 in quadratic equation.
C	ratio of friction pressure loss in combustion chamber to average dynamic pressure.
C_D	drag coefficient.
C_{D_f}	skin friction drag coefficient.
C_{D_α}	drag coefficient due to lift.
C_{D_w}	supersonic wave drag coefficient.
C_L	lift coefficient.
C_v	nozzle velocity coefficient.
D	diameter, lb.; drag, lb.
e	ratio of clearance pressure to free air pressure.
f	friction factor.
F	jet thrust, lb.
F_{P_o}	thrust for full expanding nozzle, lb.
F_t	thrust for underexpanding throat nozzle, lb.
g	acceleration of gravity (32.17 ft./sec.^{2}) at sea level.
H	stagnation pressure, lb./sq. ft.
H.V.	lower heating value of fuel, Btu./lb.
J	mechanical equivalent of heat (778 ft. lb./Btu.)

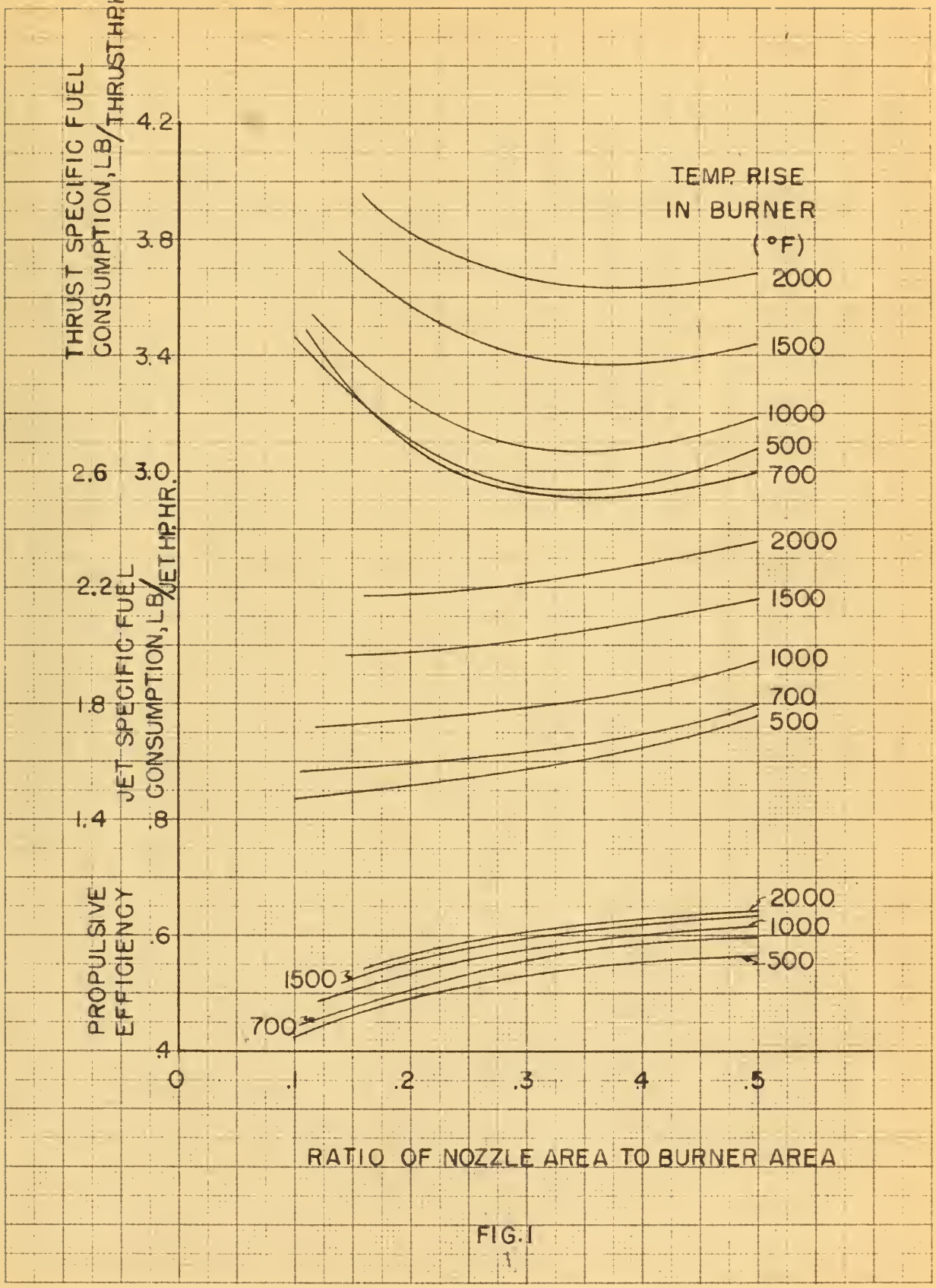
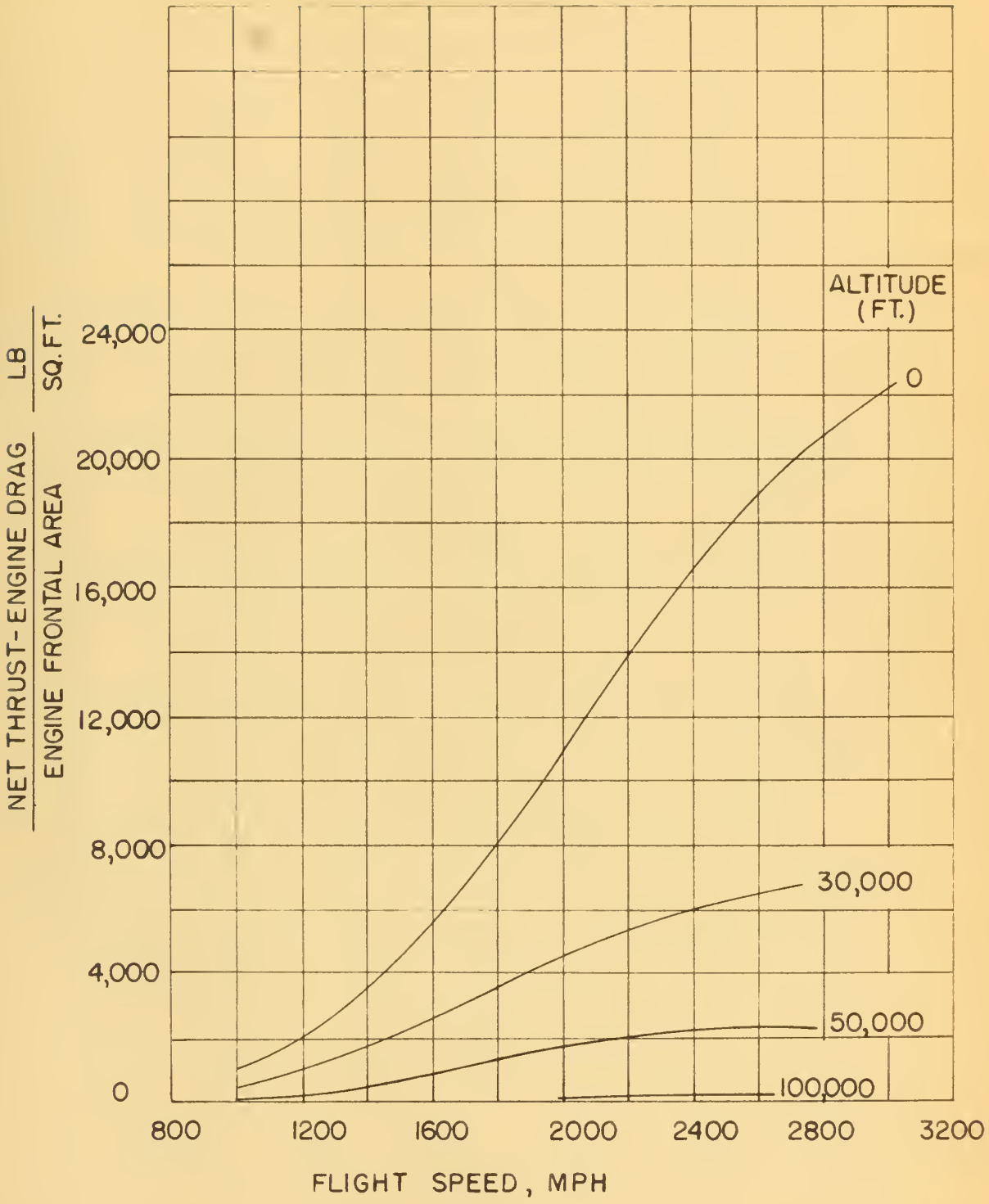
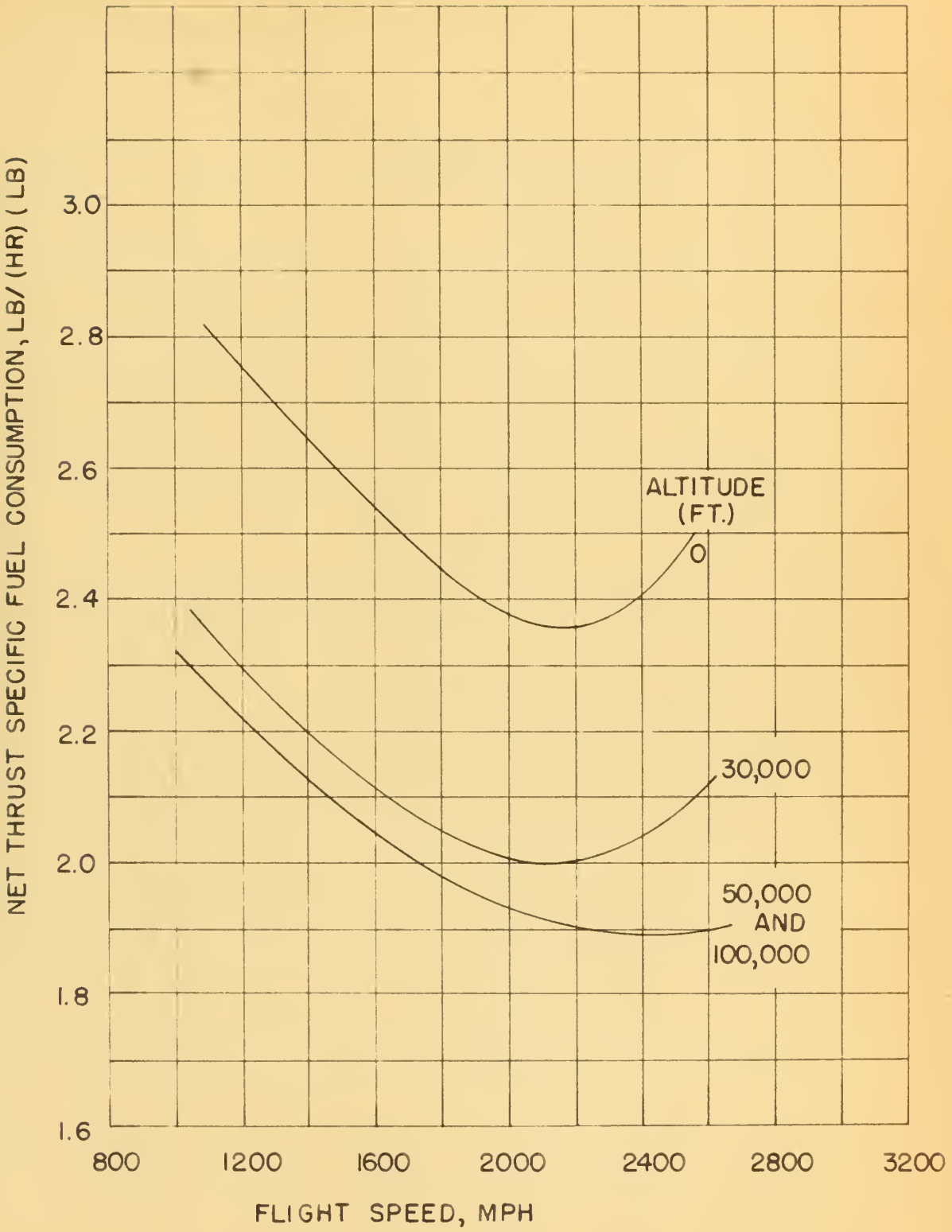

THRUST SPECIFIC FUEL CONSUMPTION, LB/THRUST HP. HR.
JET SPECIFIC FUEL CONSUMPTION, LB/JET HP. HR.
PROPULSIVE EFFICIENCY
4.2
3.8
3.4
3.0
2.6
2.2
1.8
1.4
.8
.6
.4
0
.1
.2
.3
.4
.5
TEMP. RISE IN BURNER (°F)
2000
1500
1000
500
700
2000
1500
1000
700
500
2000
1000
500
1500
700
RATIO OF NOZZLE AREA TO BURNER AREA

FIG. 1



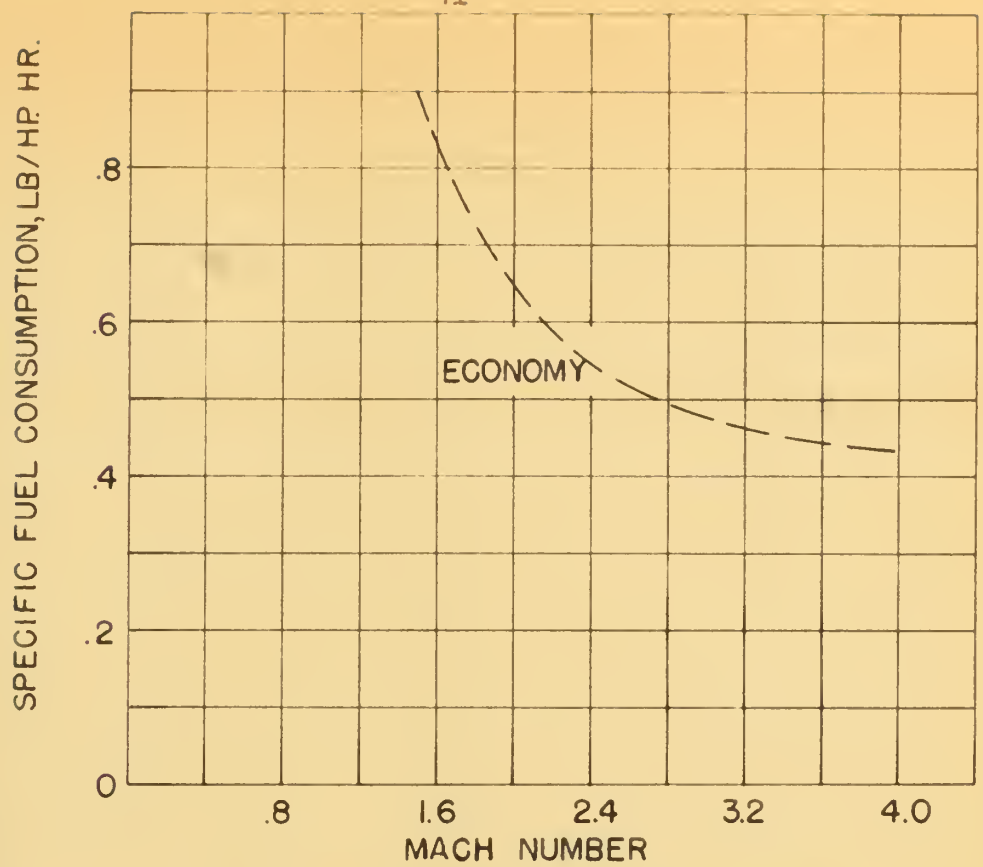
NET THRUST PER UNIT ENGINE FRONTAL AREA
VS. FLIGHT SPEED AND ALTITUDE

FIG. 2



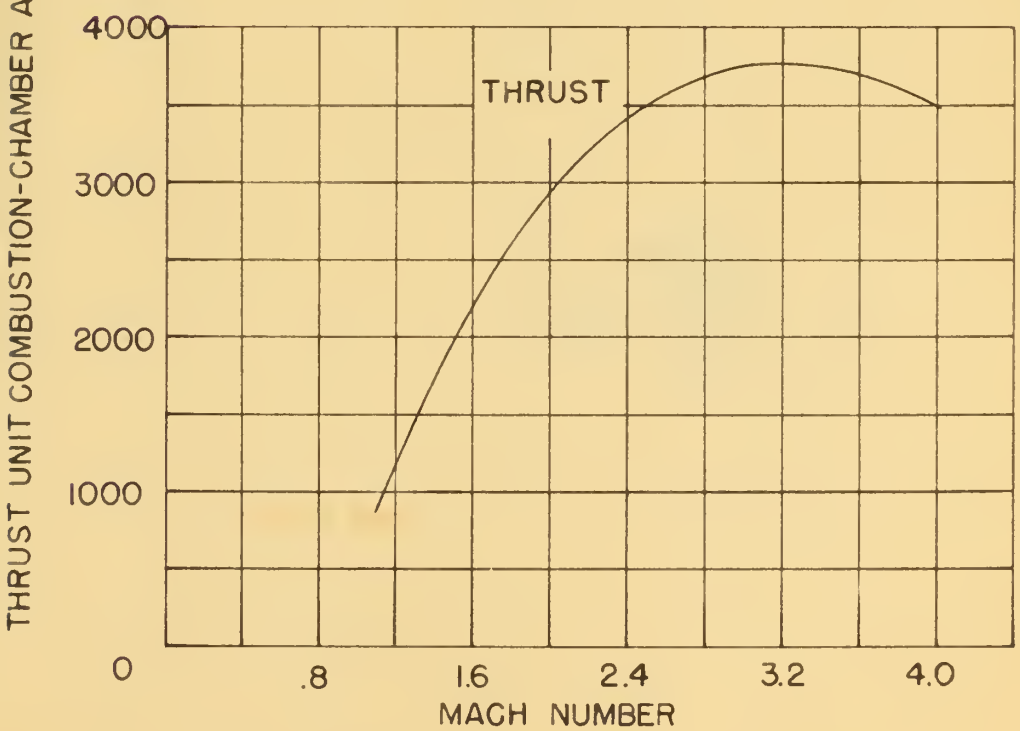
NET THRUST SPECIFIC FUEL CONSUMPTION
VS. FLIGHT SPEED AND ALTITUDE

FIG. 3



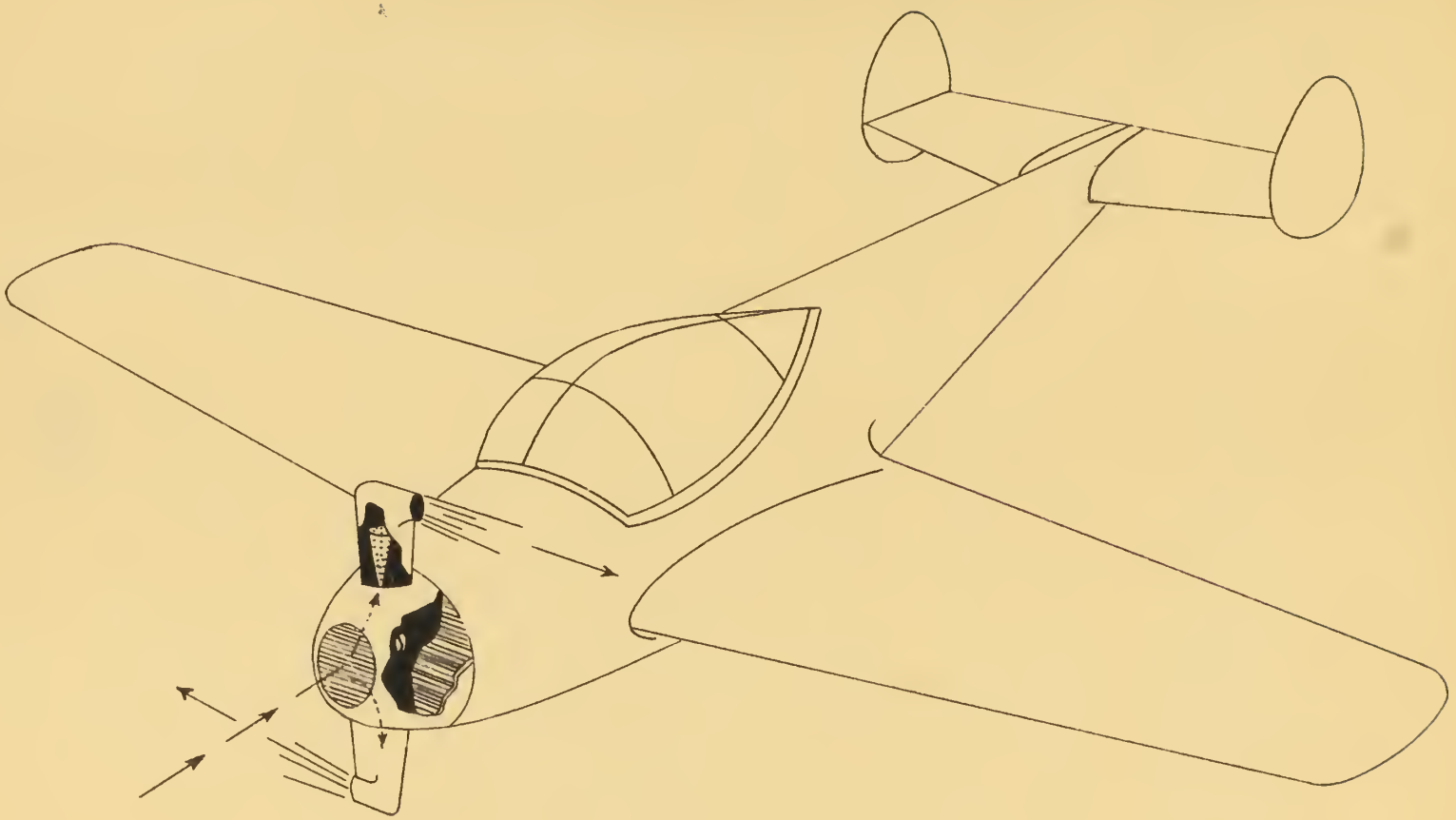
NET THRUST PER UNIT ENGINE FRONTAL AREA VS. FLIGHT SPEED AT SEA LEVEL

FIG. 4



NET THRUST SPECIFIC FUEL CONSUMPTION VS. FLIGHT SPEED AT SEA LEVEL

FIG. 5



AIRPLANE POWERED BY A JET-OPERATED PROPELLER

FIG. 6

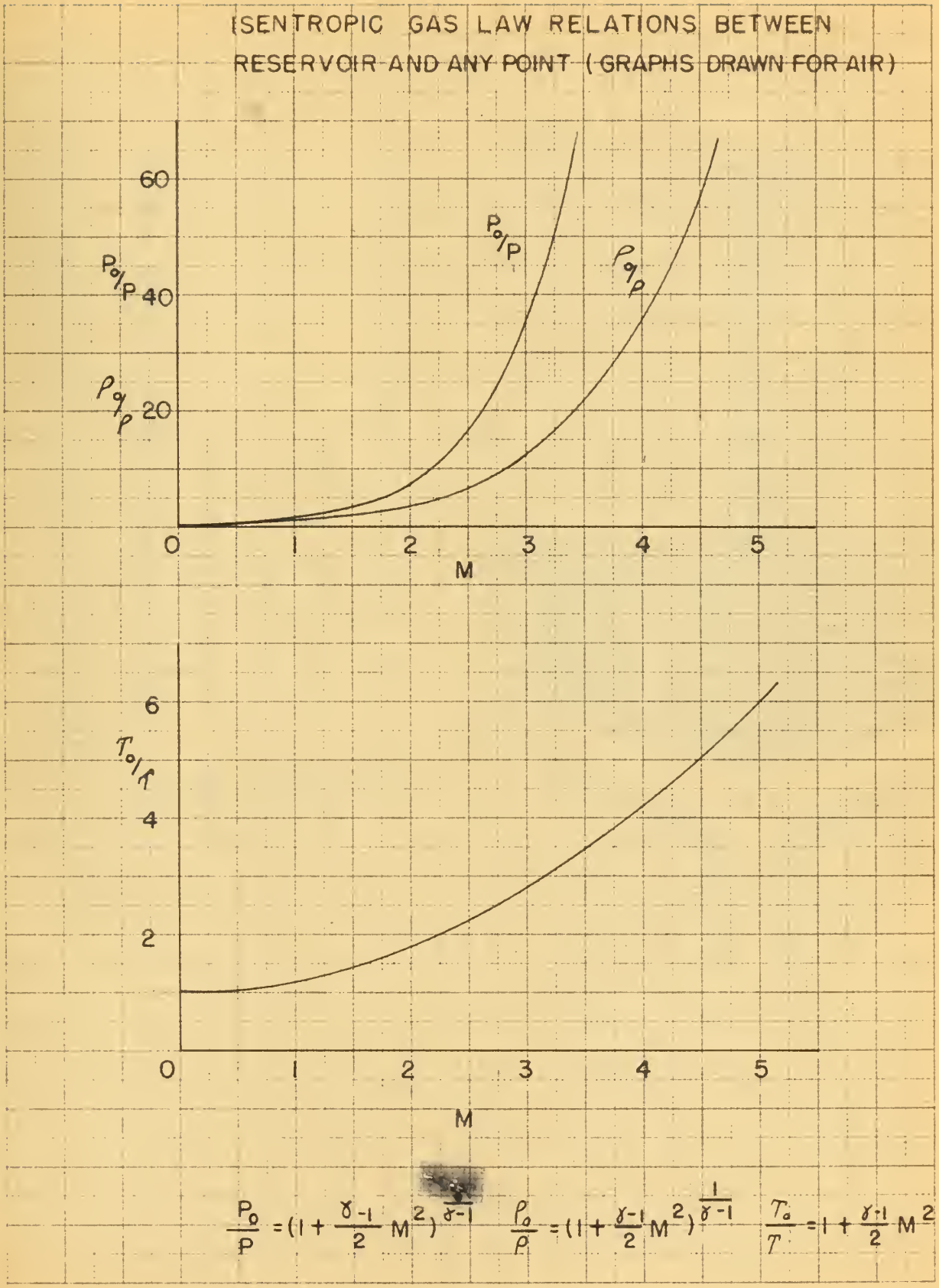

ISENTROPIC GAS LAW RELATIONS BETWEEN
RESERVOIR AND ANY POINT (GRAPHS DRAWN FOR AIR)
60
40
20
P_o/P
ρ_o/ρ
0
1
2
3
4
5
M
6
4
2
T_o/T
0
1
2
3
4
5
M
$\frac{P_o}{P} = (1 + \frac{\gamma-1}{2} M^2)^{\frac{\gamma}{\gamma-1}}$
$\frac{\rho_o}{\rho} = (1 + \frac{\gamma-1}{2} M^2)^{\frac{1}{\gamma-1}}$
$\frac{T_o}{T} = 1 + \frac{\gamma-1}{2} M^2$

FIG. 7

CENTRIFUGAL JET ENGINE WITH SUPERSONIC PROPELLER

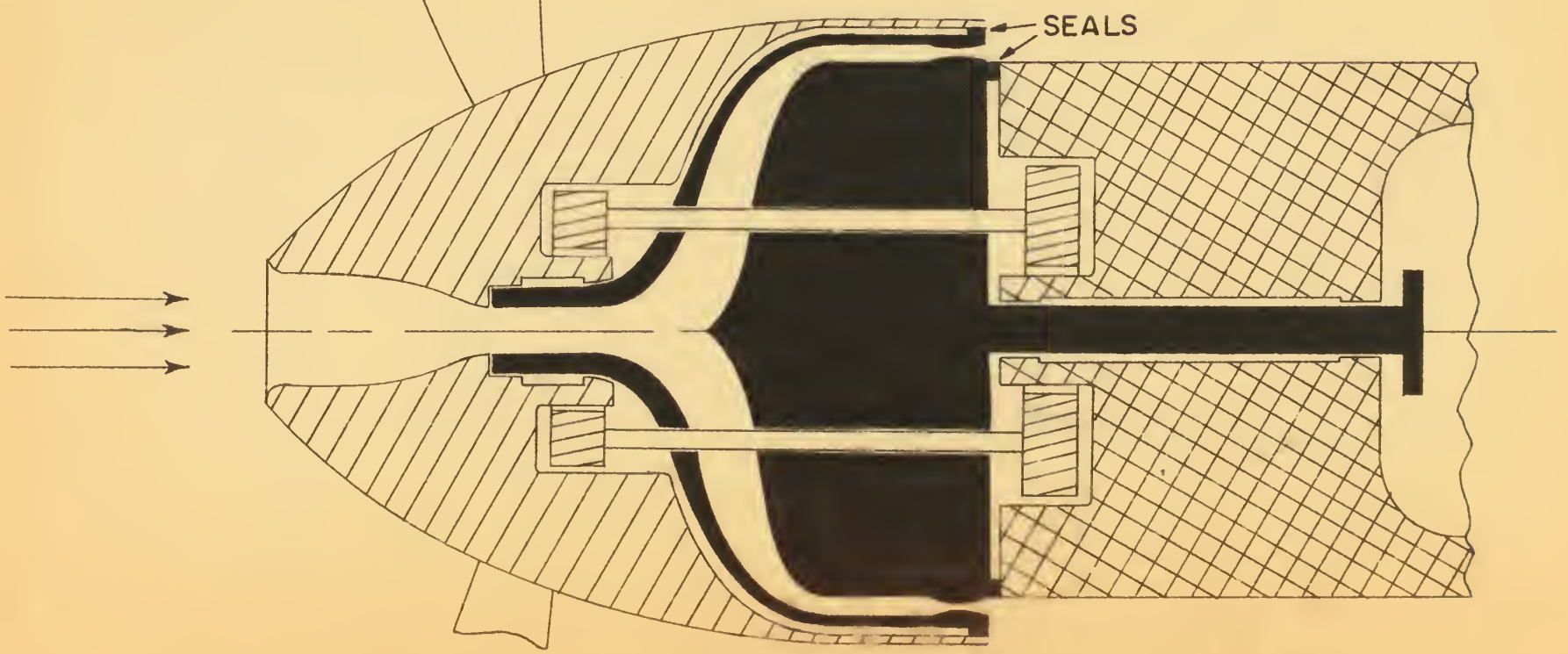
NOSE SPINNER WITH ATTACHED PROPELLER

ROTATING DISC

GEAR TRAIN

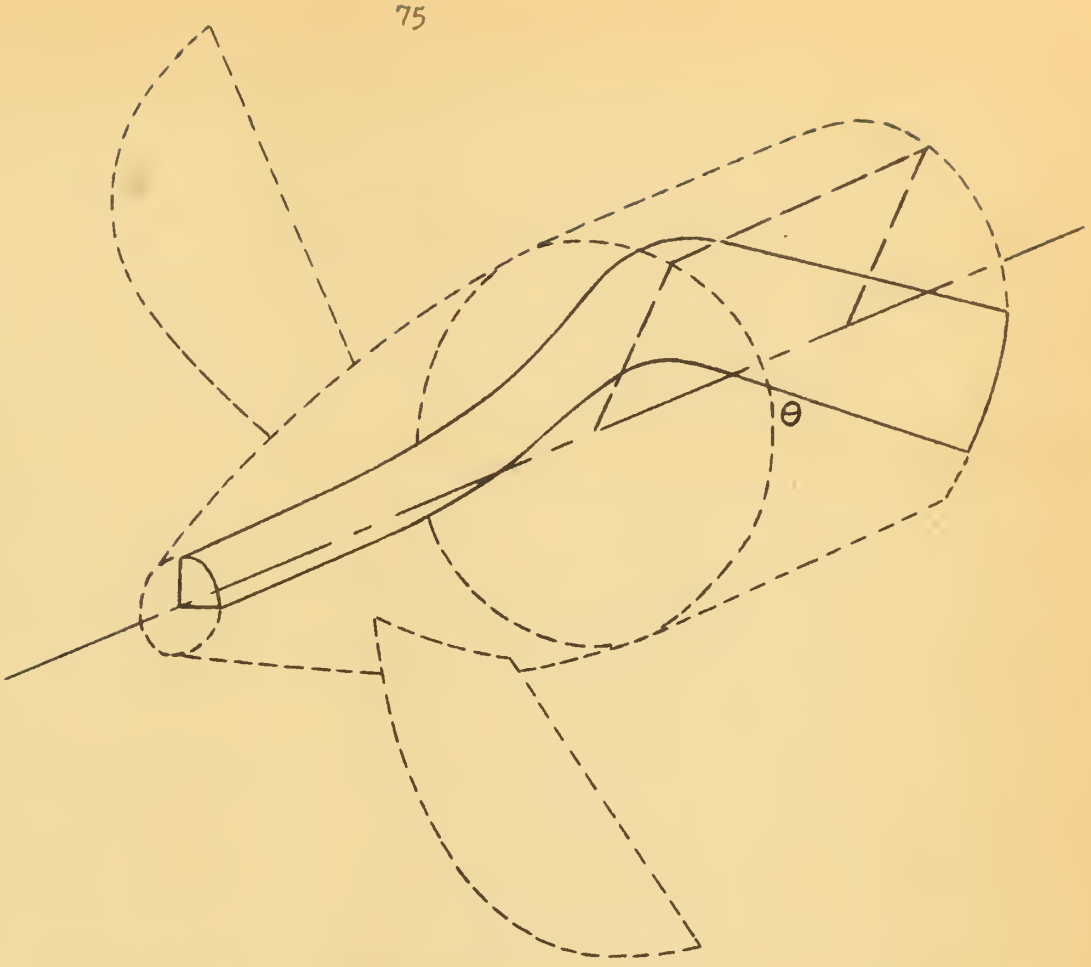
STATIONARY CASING

NOTE: FUEL, IGNITION, AND LUBRICATION SYSTEMS NOT SHOWN



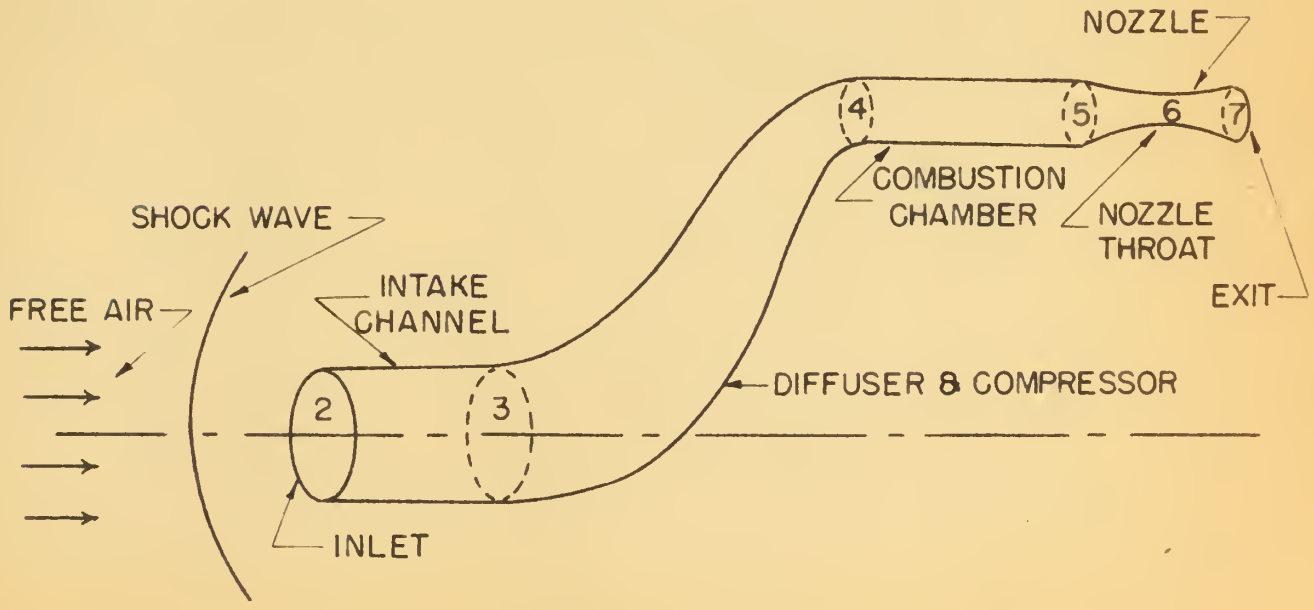
74

FIG. 8



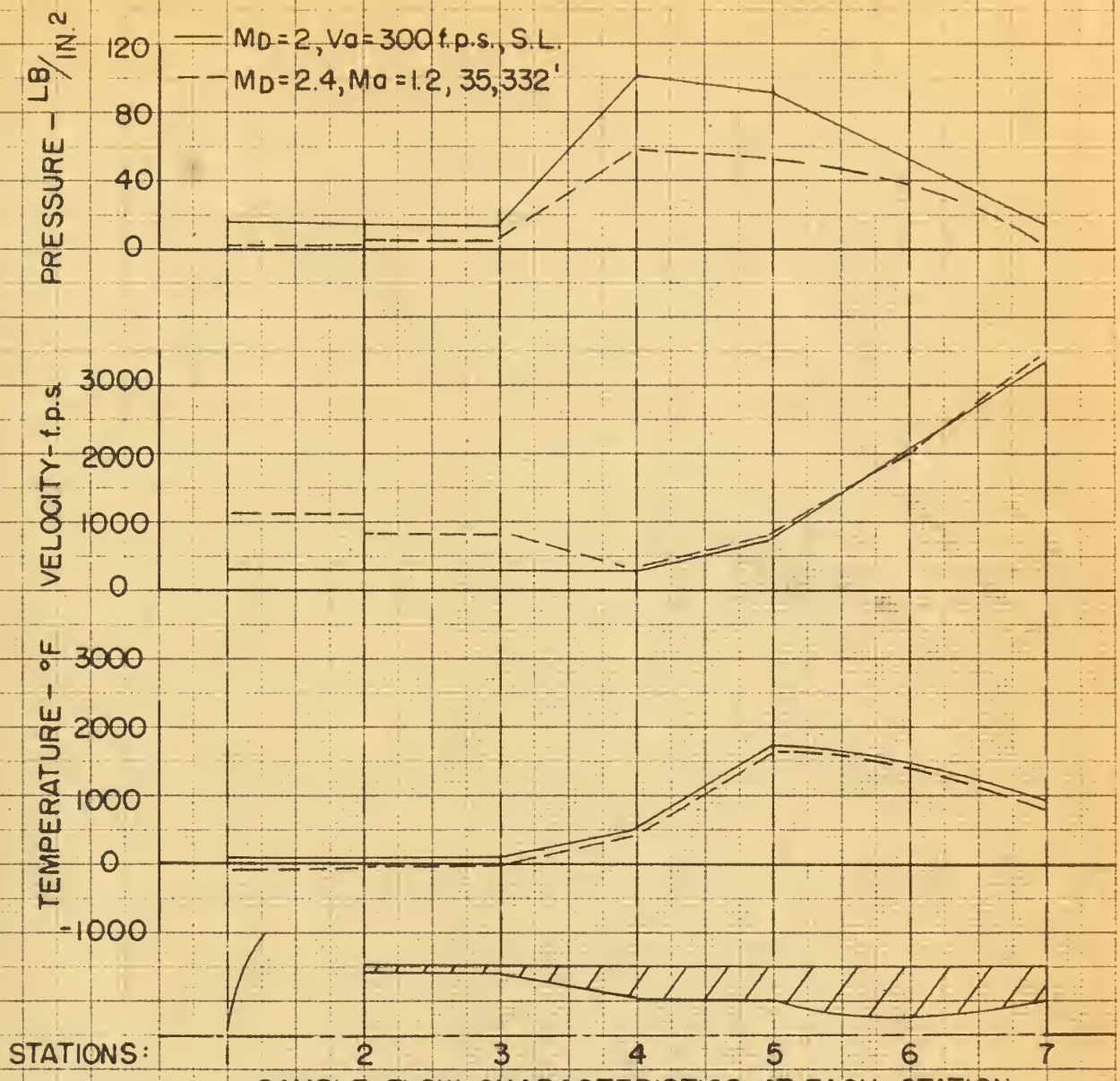
ISOMETRIC FLOW DIAGRAM

FIG.9



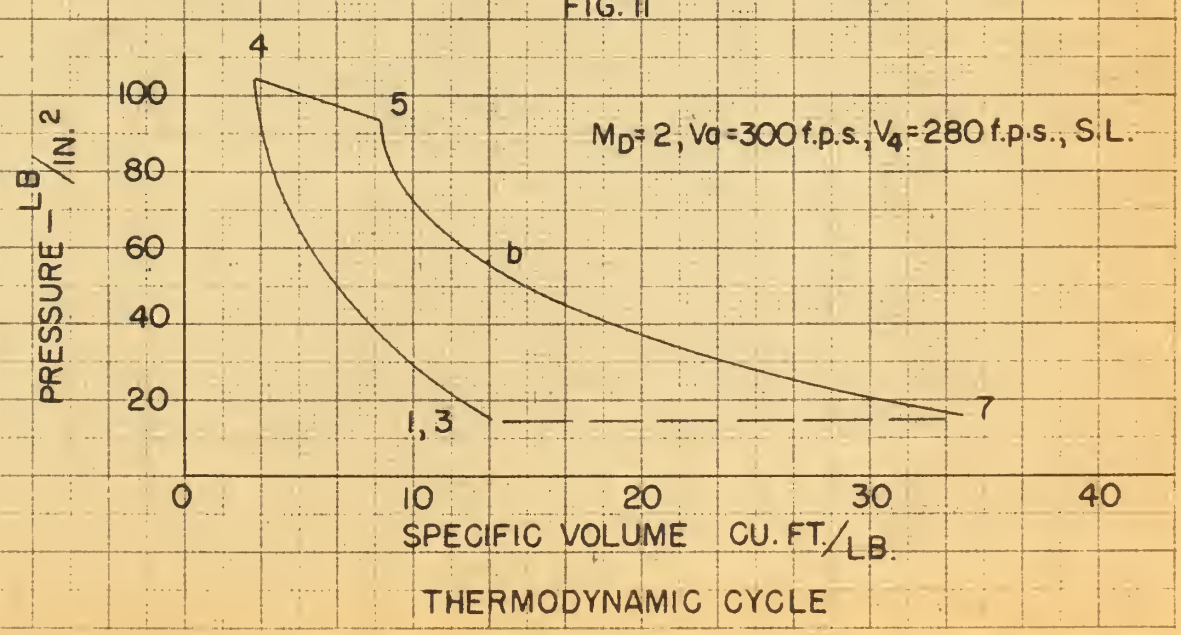
SCHEMATIC STATION DIAGRAM

FIG. 10



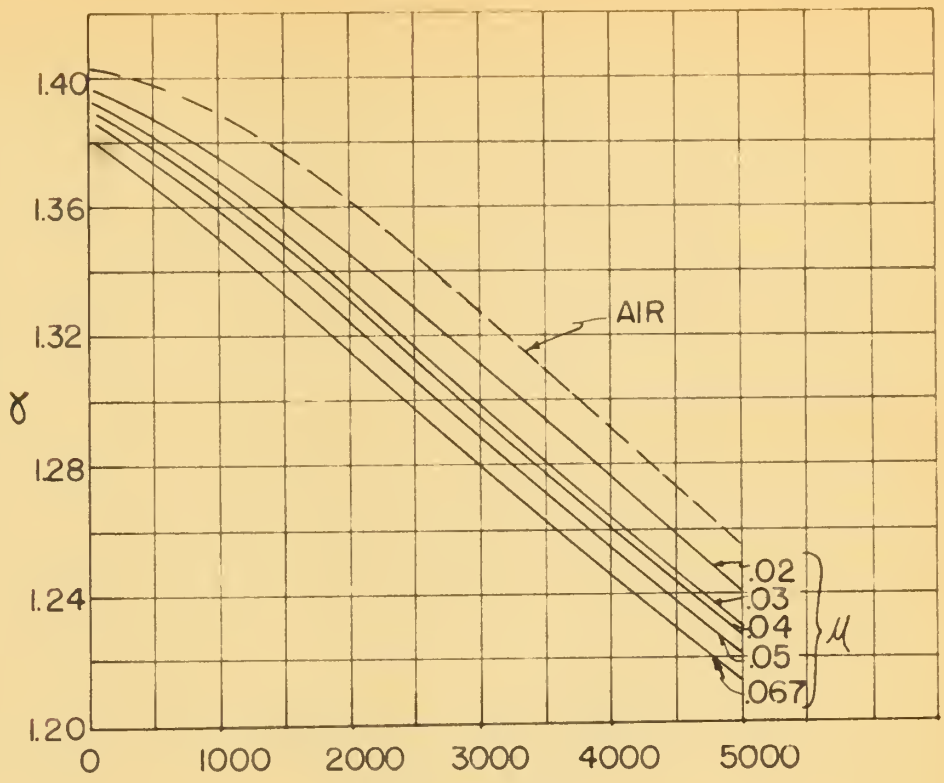
SAMPLE FLOW CHARACTERISTICS AT EACH STATION

FIG. 11



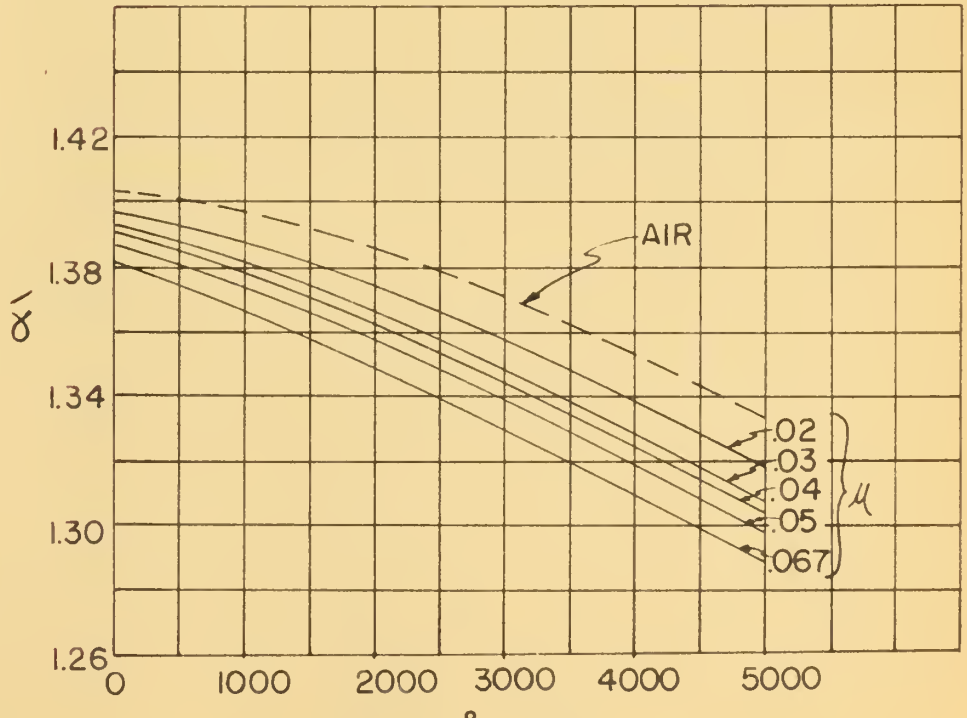
THERMODYNAMIC CYCLE

FIG. 12



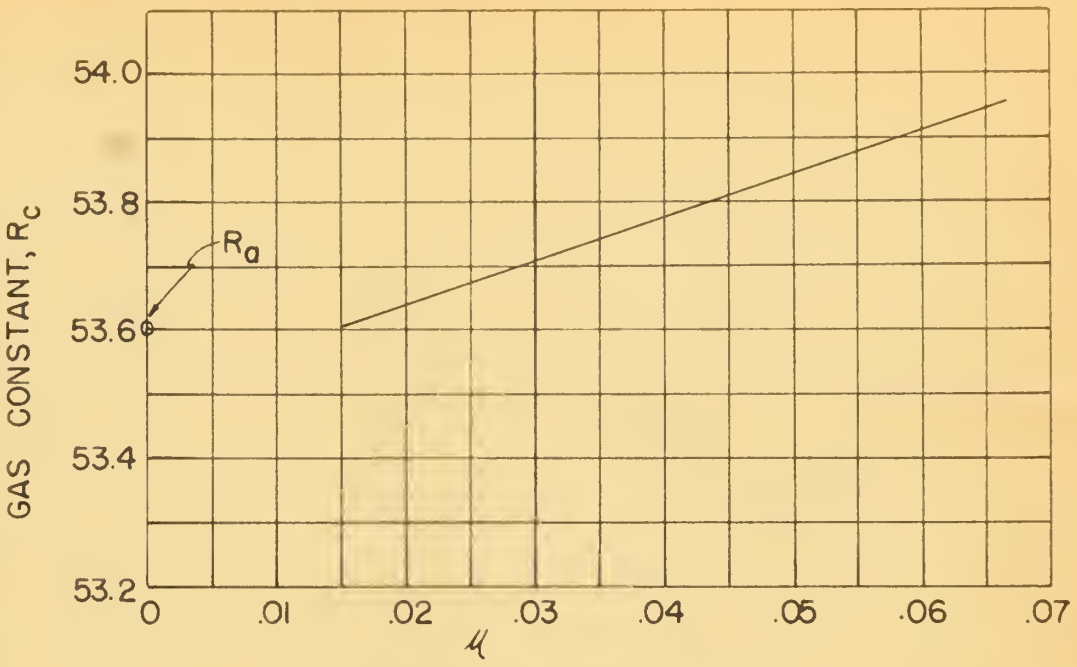
INSTANTANEOUS VALUES OF THE RATIO OF SPECIFIC HEATS

FIG. 13



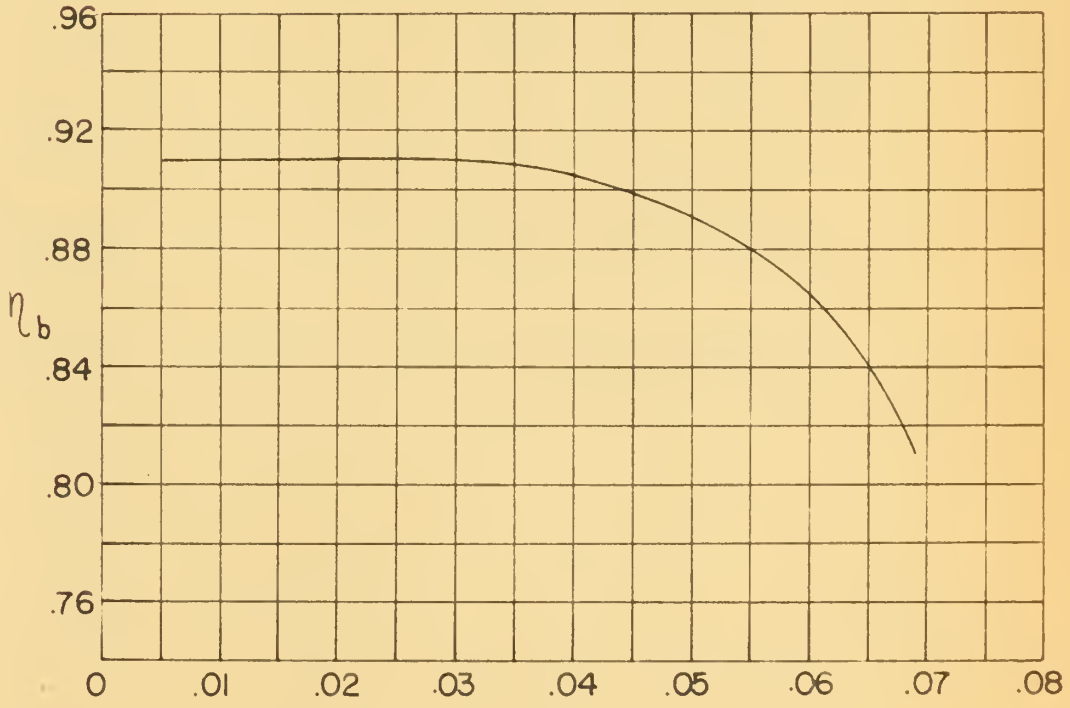
VALUES OF THE RATIO OF SPECIFIC HEATS AVERAGED BETWEEN OAND T

FIG. 14



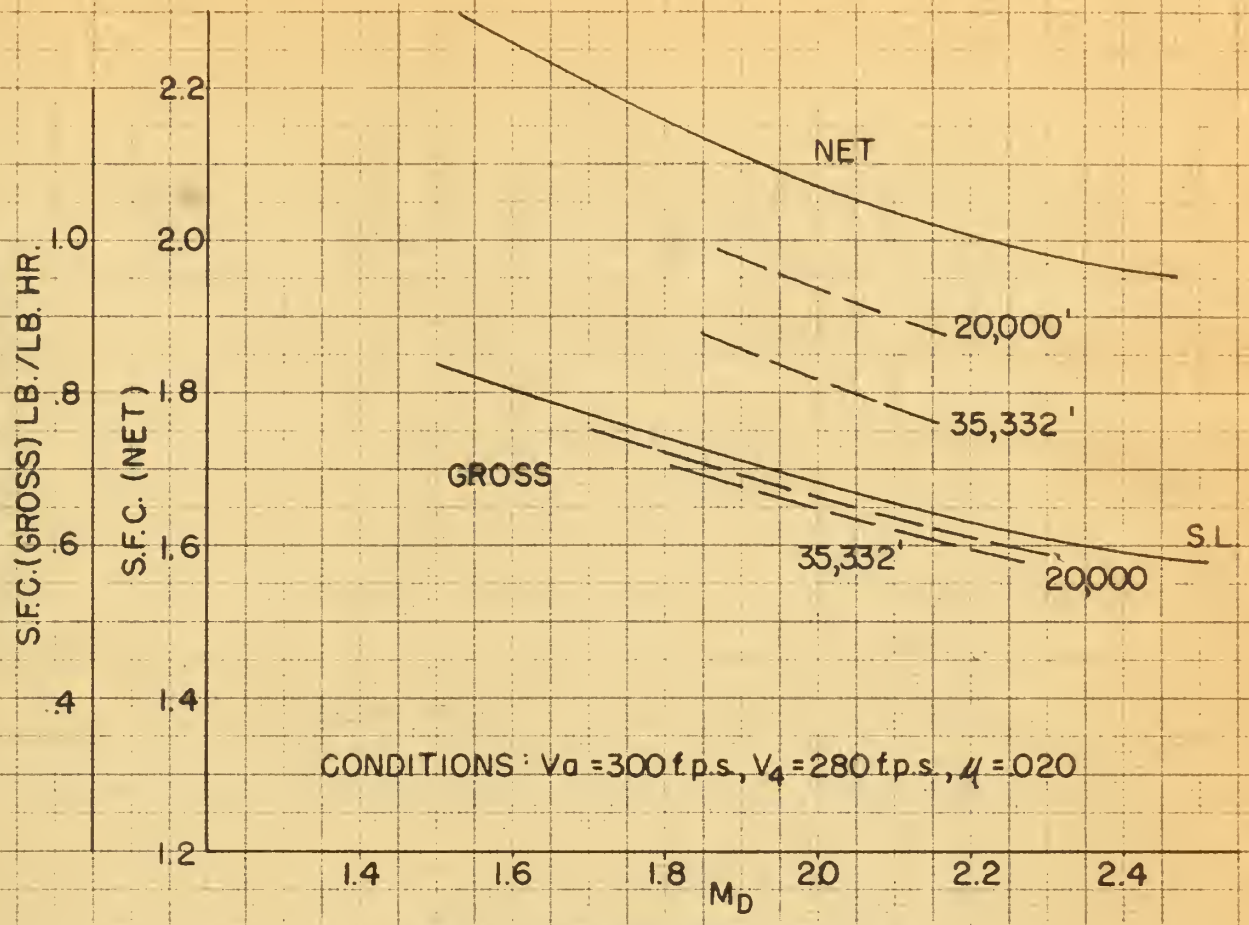
VARIATION OF GAS CONSTANT
WITH FUEL-AIR RATIO

FIG. 15



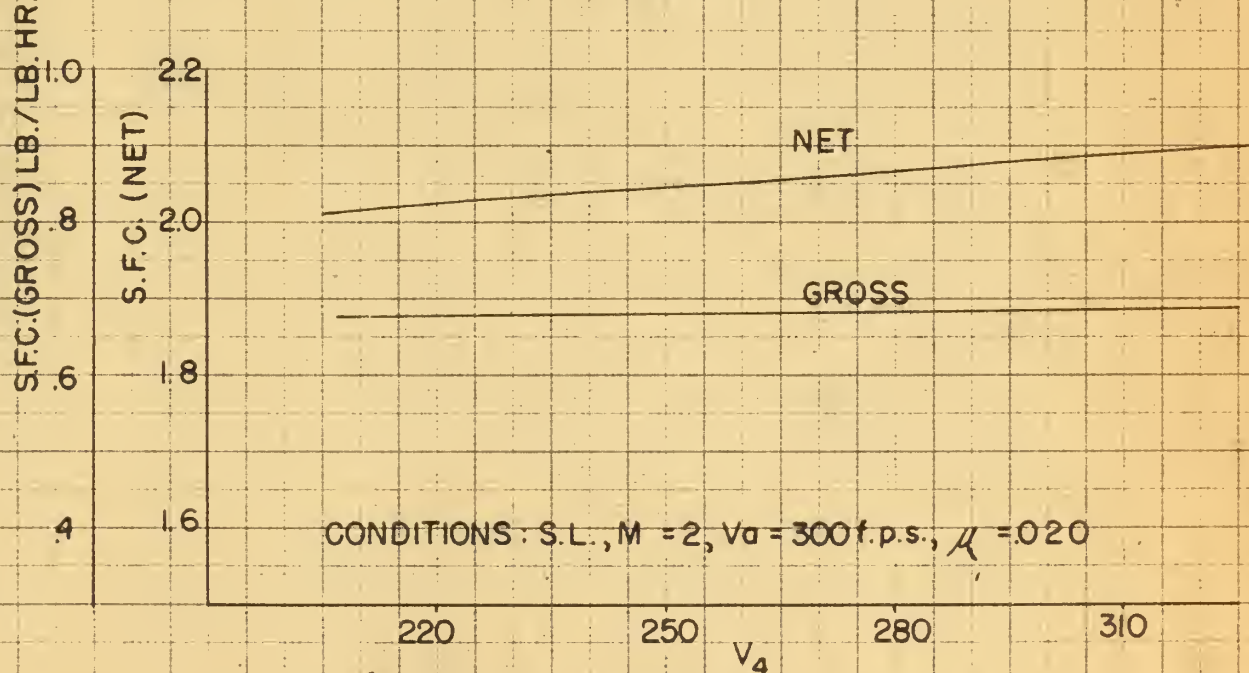
VALUES OF COMBUSTION EFFICIENCY

FIG. 16



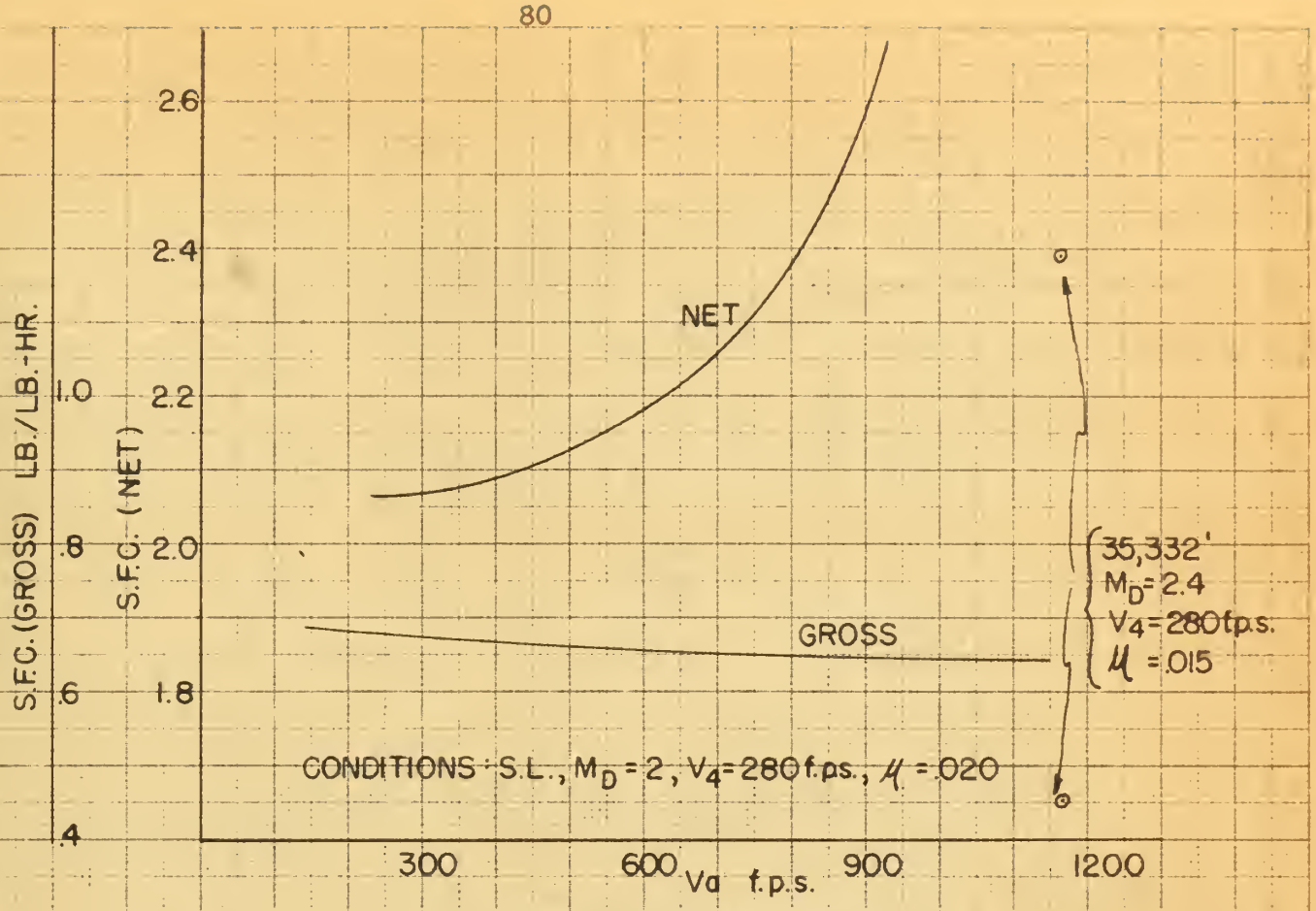
S.F.C. VS. DISC MACH NO. (S.L.)

FIG. 17



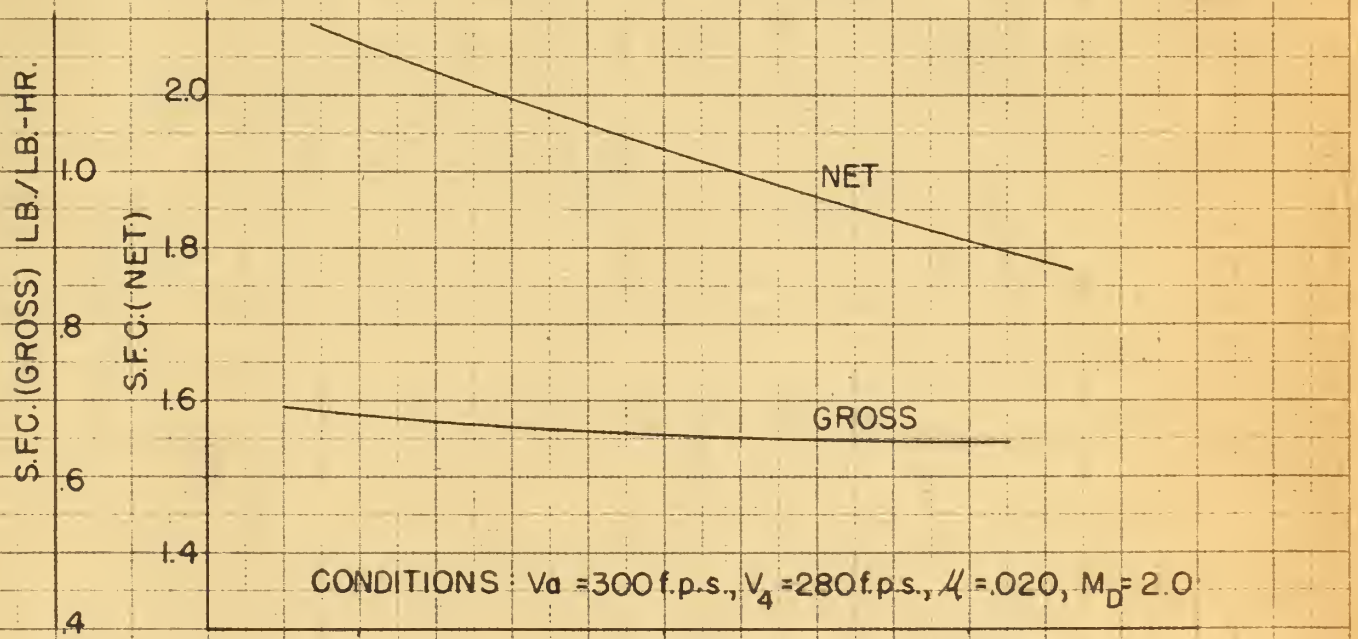
S.F.C. VS. COMBUSTION CHAMBER INLET VELOCITY

FIG. 18



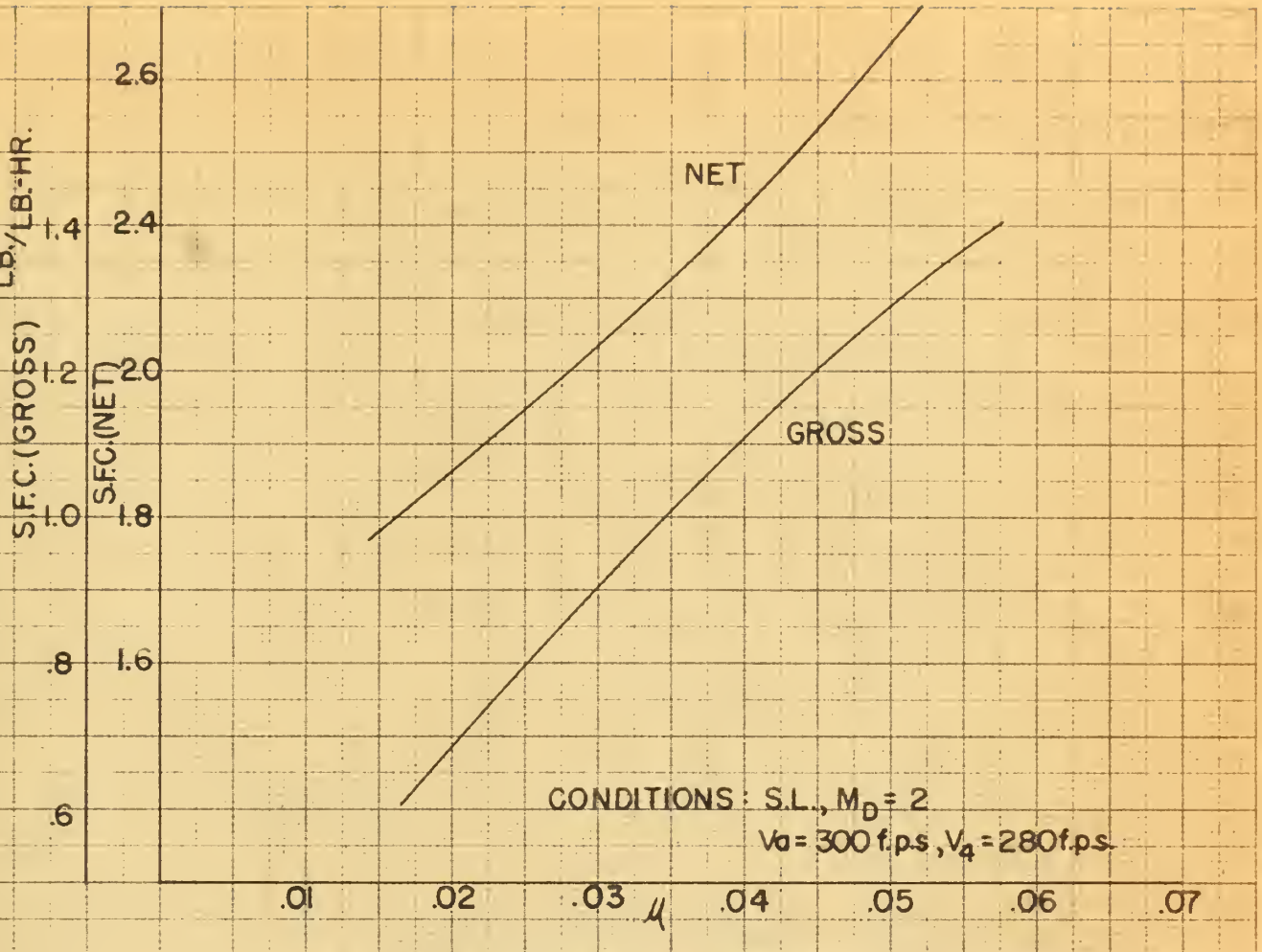
S.F.C. VS. AIRCRAFT SPEED

FIG. 19



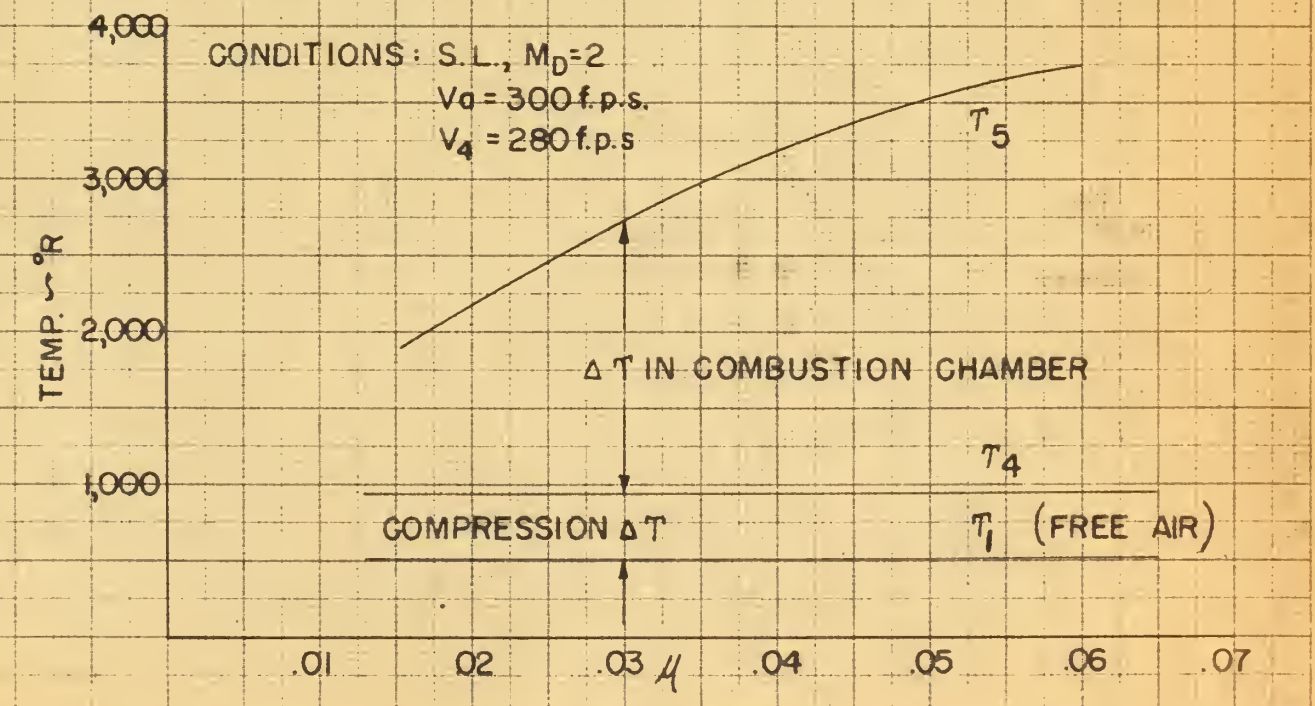
S.F.C. VS. ALTITUDE

FIG. 20



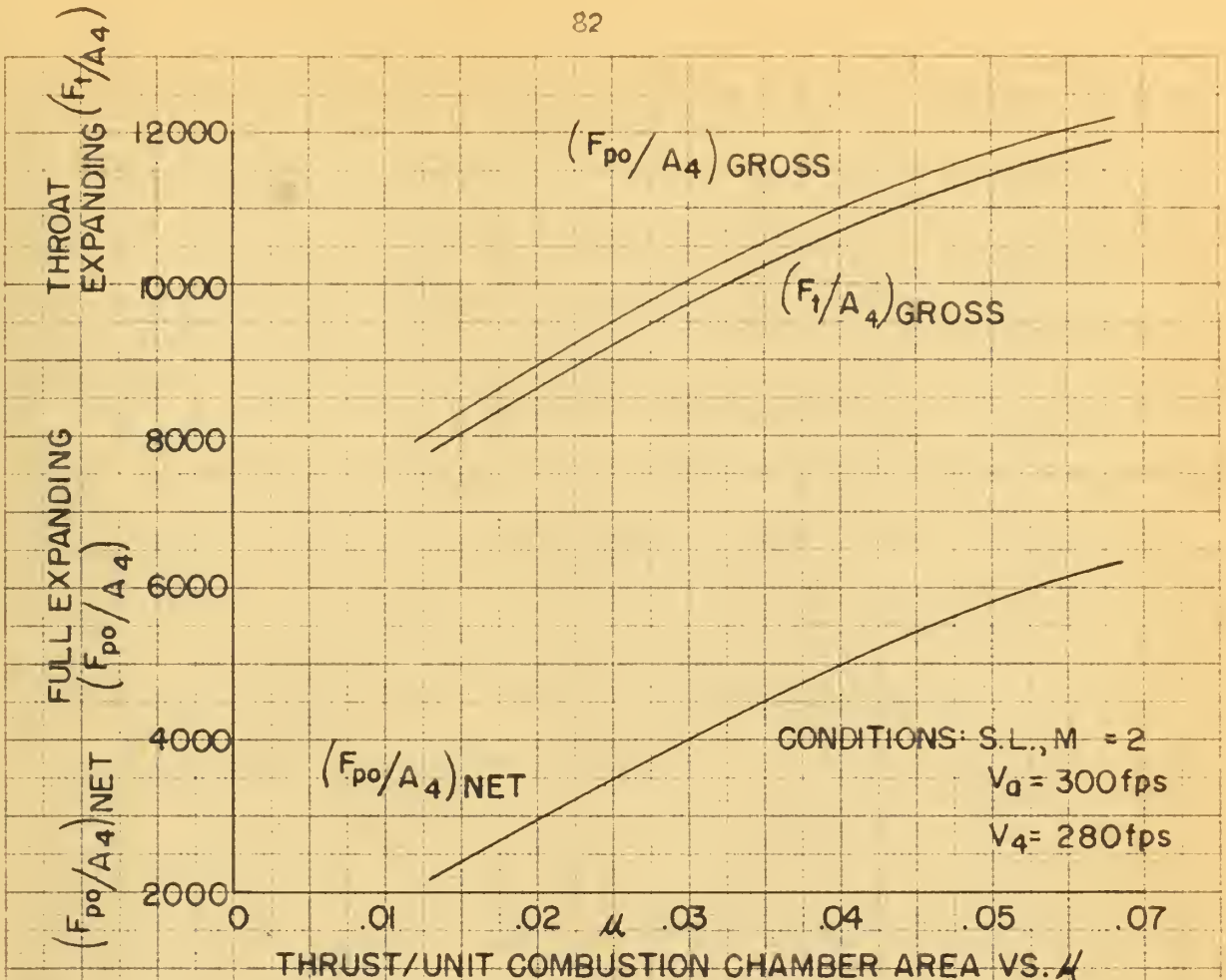
S.F.C. VS. FUEL/AIR RATIO

FIG. 21



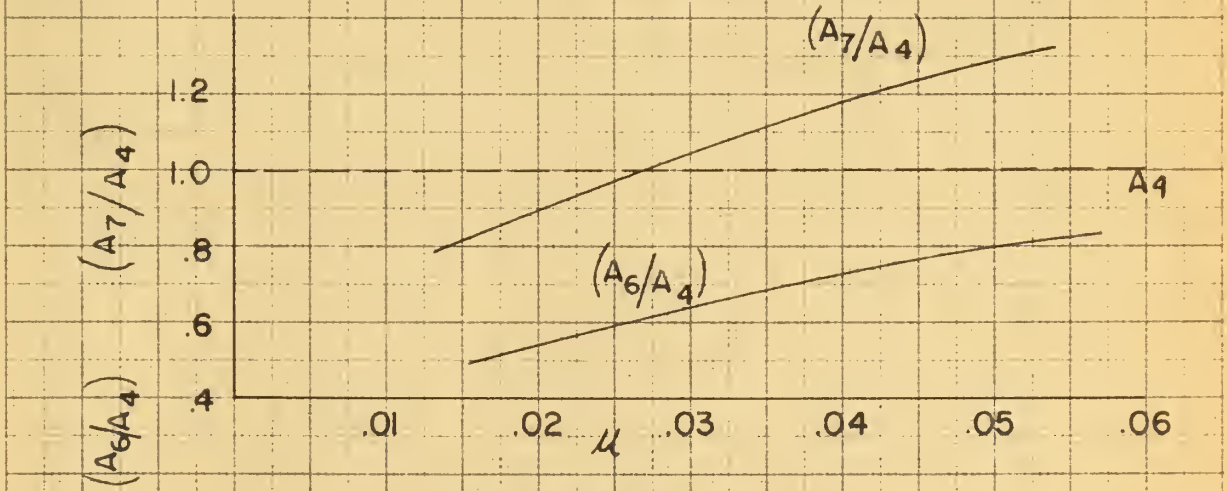
TEMP. VS. FUEL/AIR RATIO

FIG. 22



THRUST/UNIT COMBUSTION CHAMBER AREA VS. μ

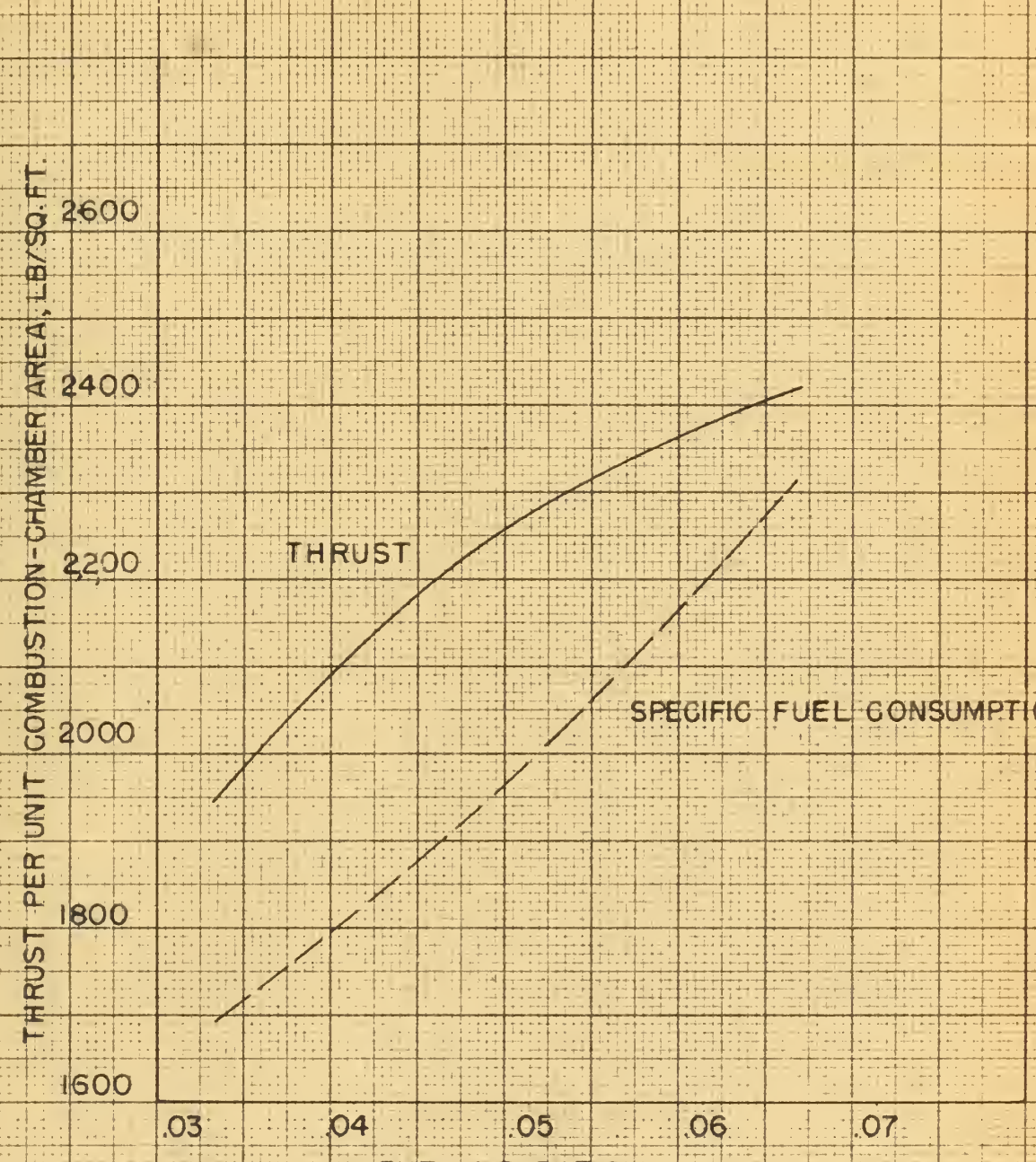
FIG. 23



AREA RATIOS VS. μ

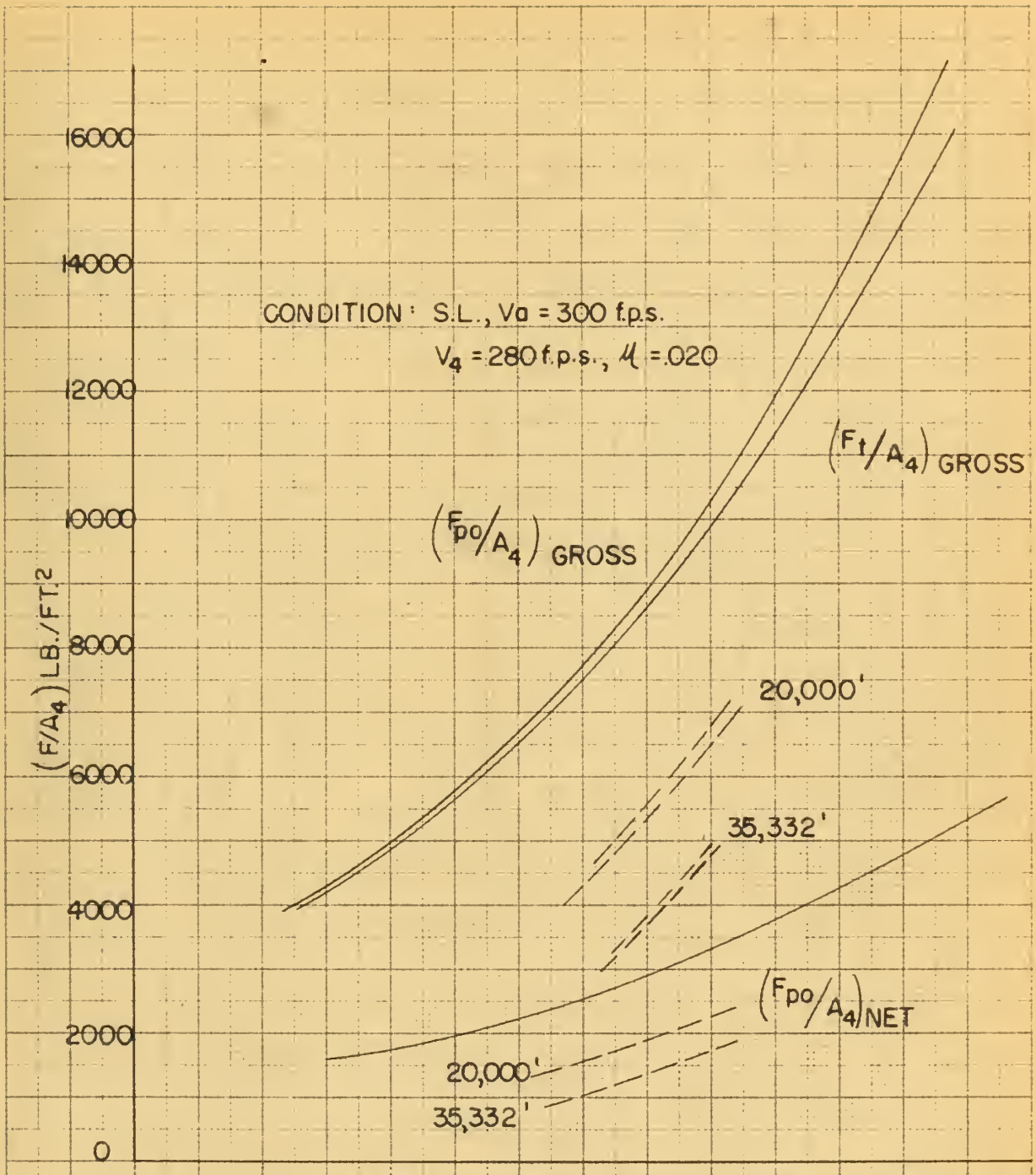
CONDITIONS: S.L., M_D = 2, V_a = 300 fps, V_4 = 280 fps

FIG. 24



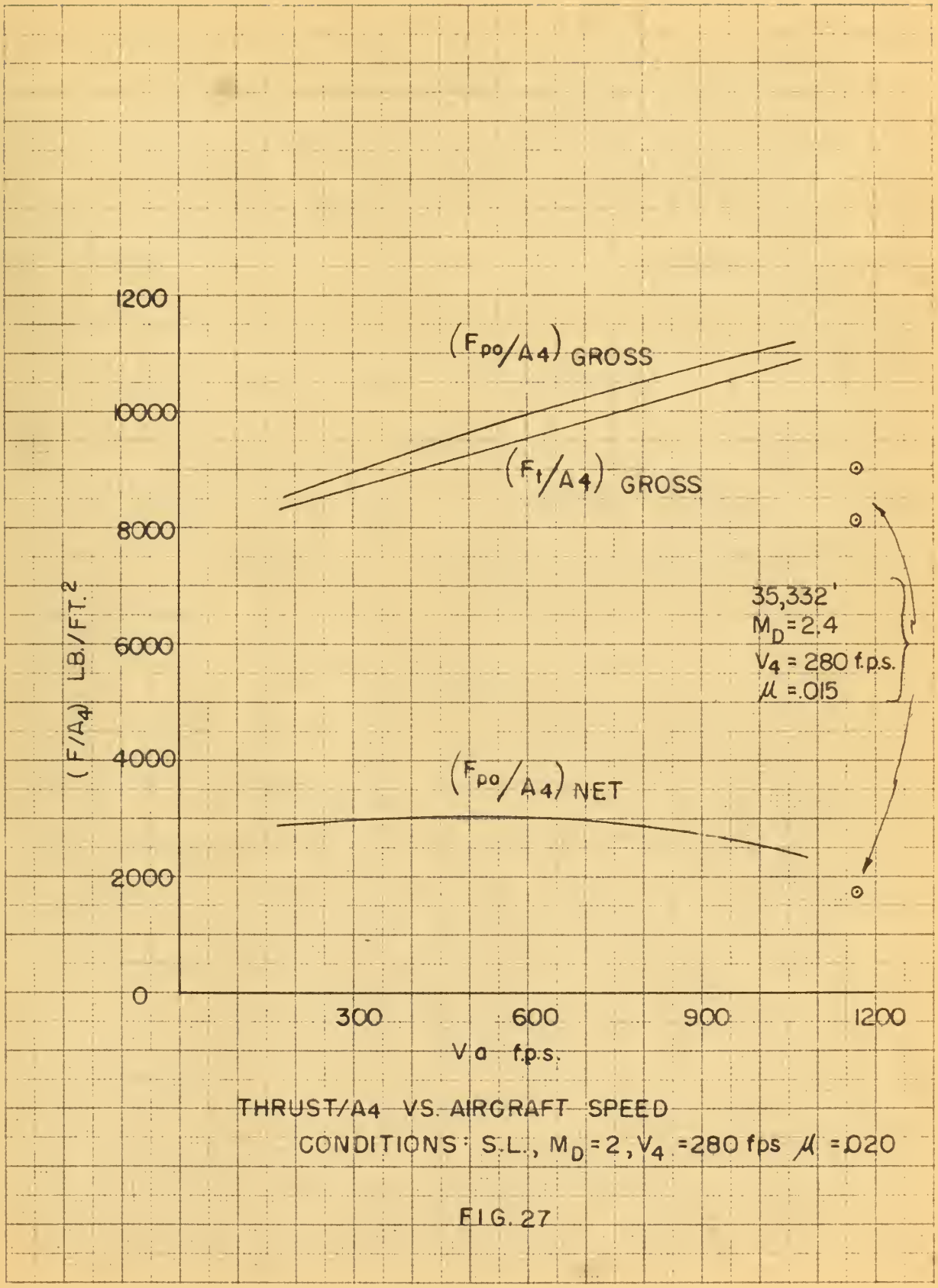
THRUST AND ECONOMY VS. FUEL AIR RATIO FOR A RAM JET OPERATING AT M=1.5 (S.L.)

FIG. 25



THRUST/A_4 VS. DISC MACH NO. (S.L.)

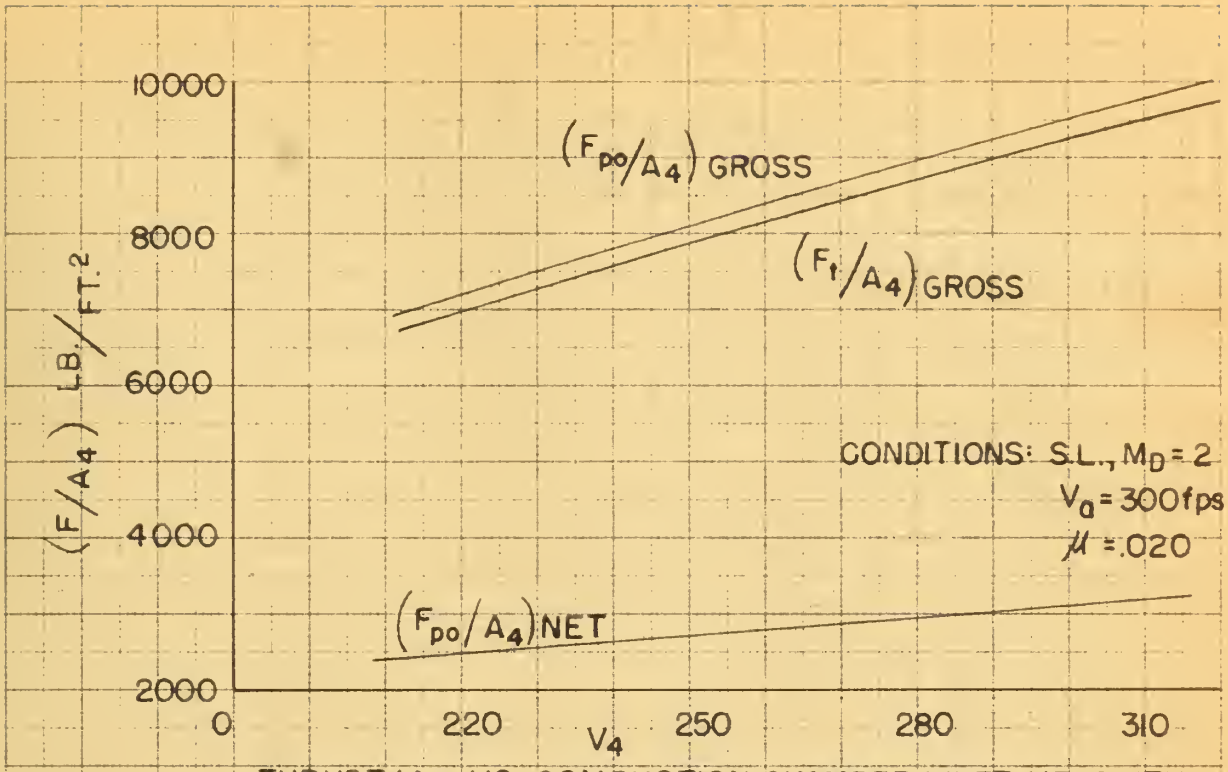
FIG. 26



THRUST/A4 VS. AIRCRAFT SPEED

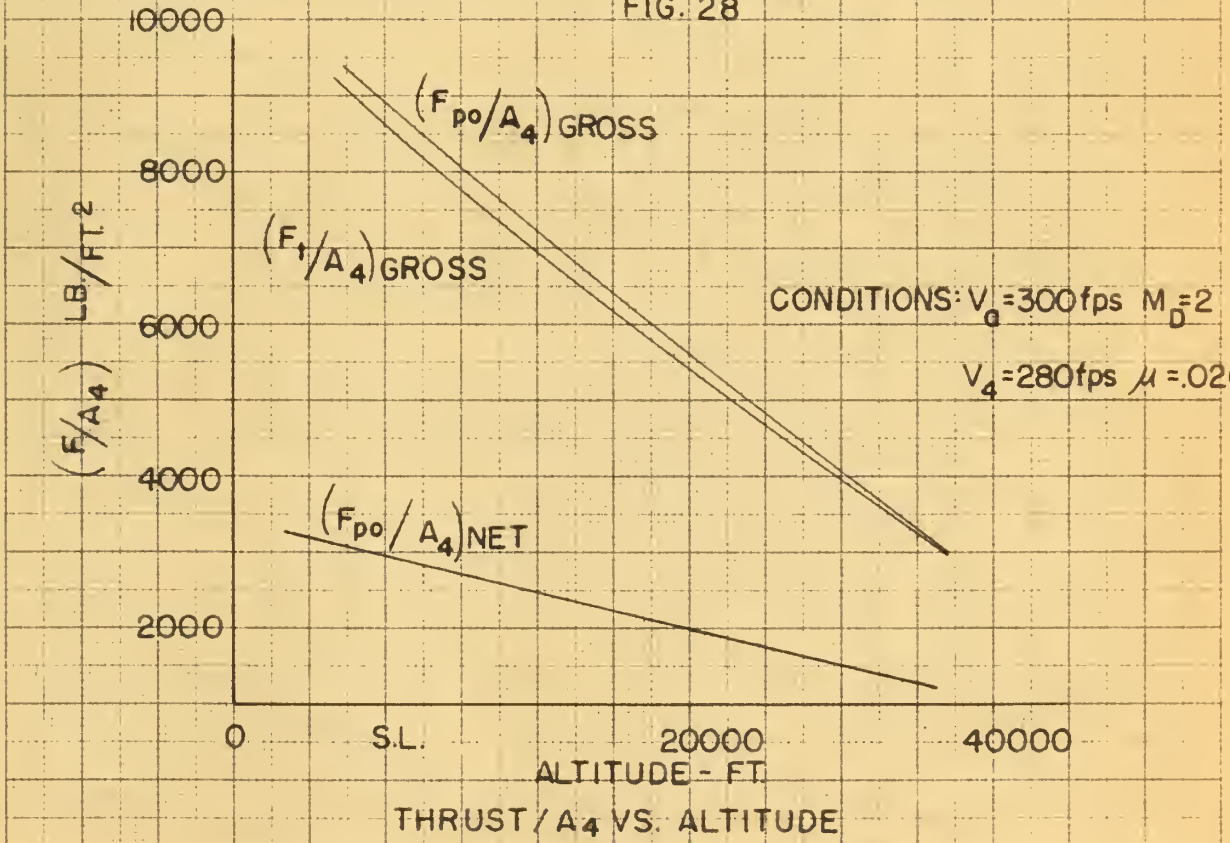
CONDITIONS: S.L., $M_D = 2$, $V_4 = 280$ fps $\mu = .020$

FIG. 27



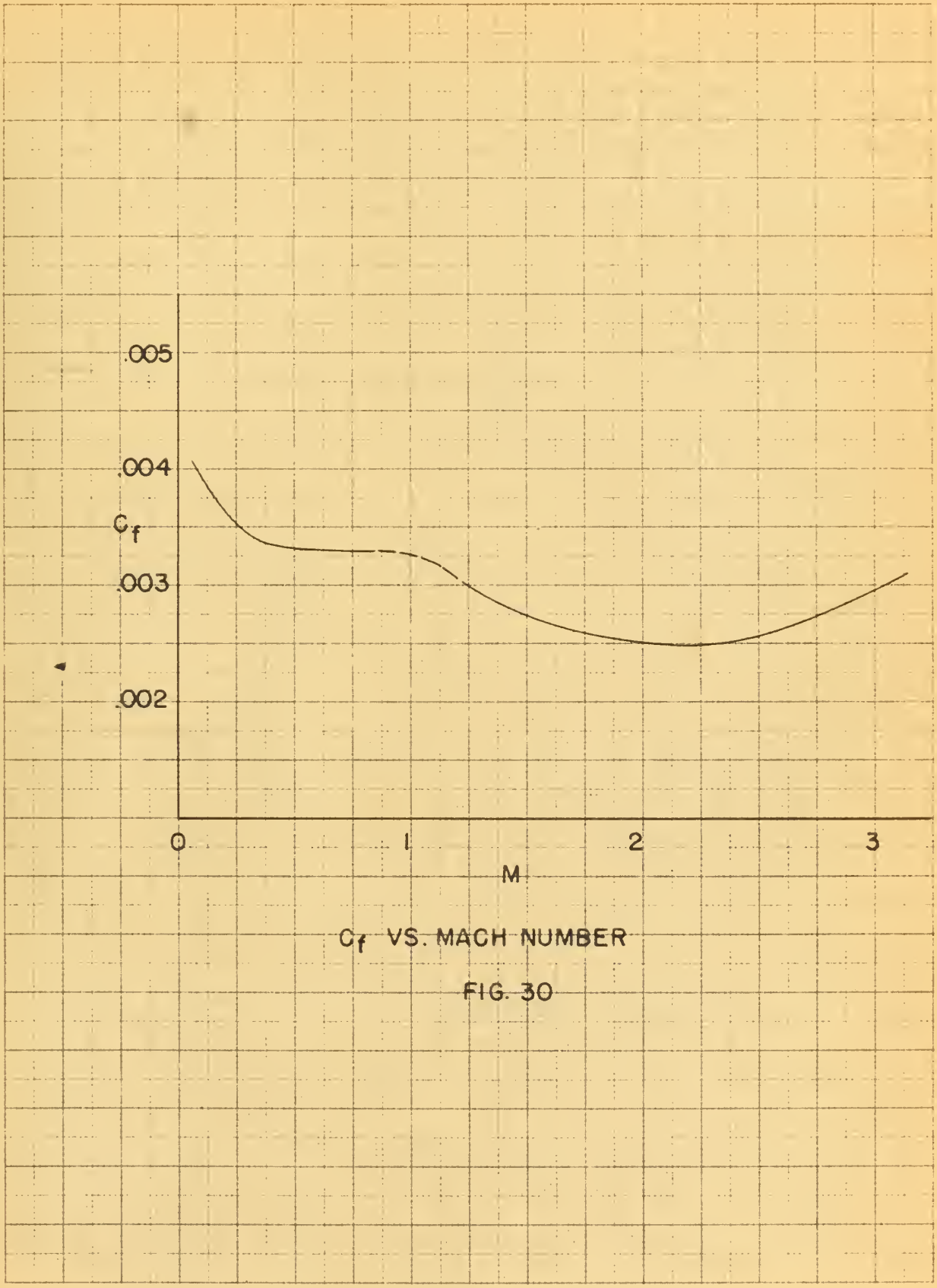
THRUST/A4 VS. COMBUSTION CHAMBER INLET VELOCITY

FIG. 28



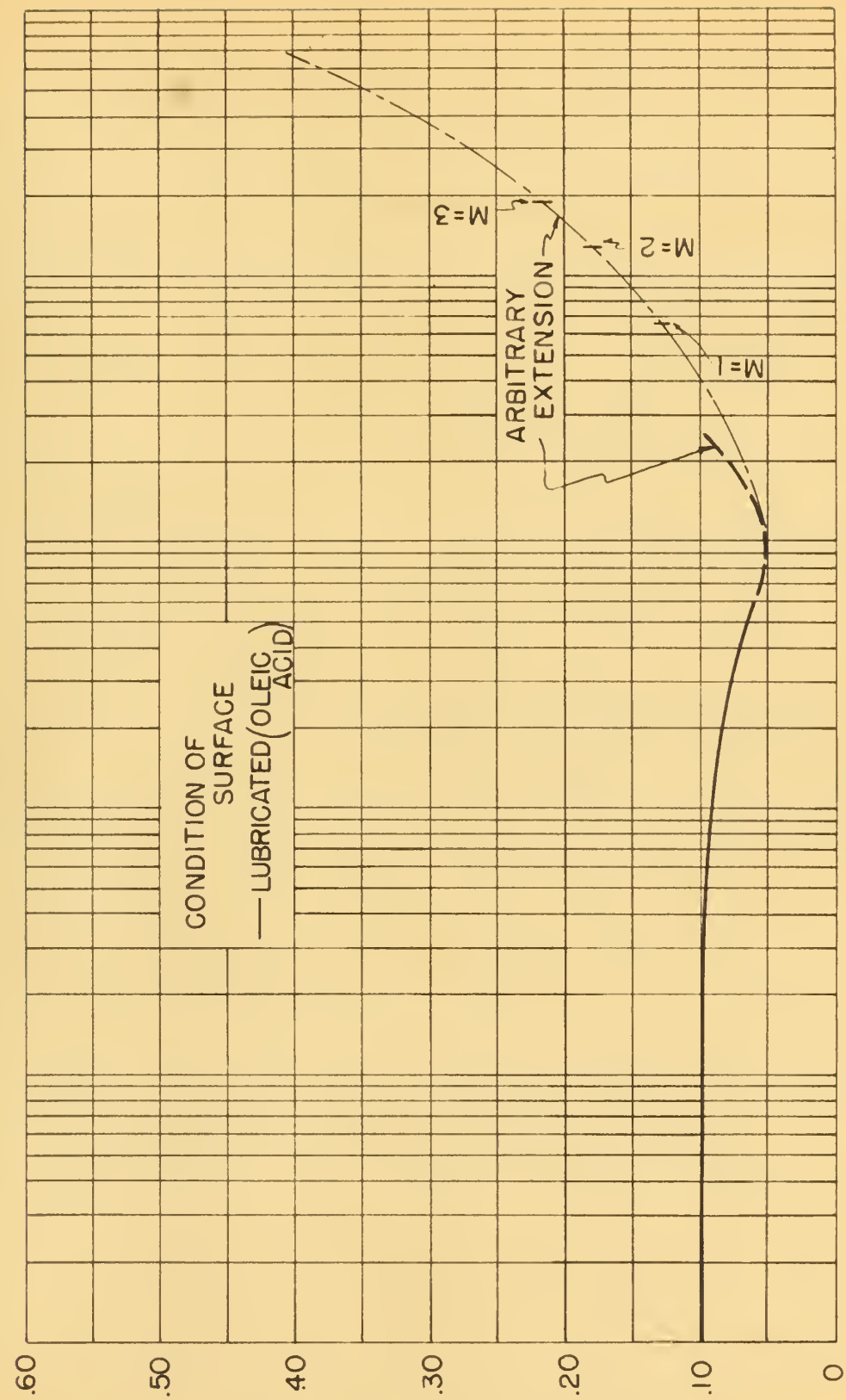
THRUST/A4 VS. ALTITUDE

FIG. 29



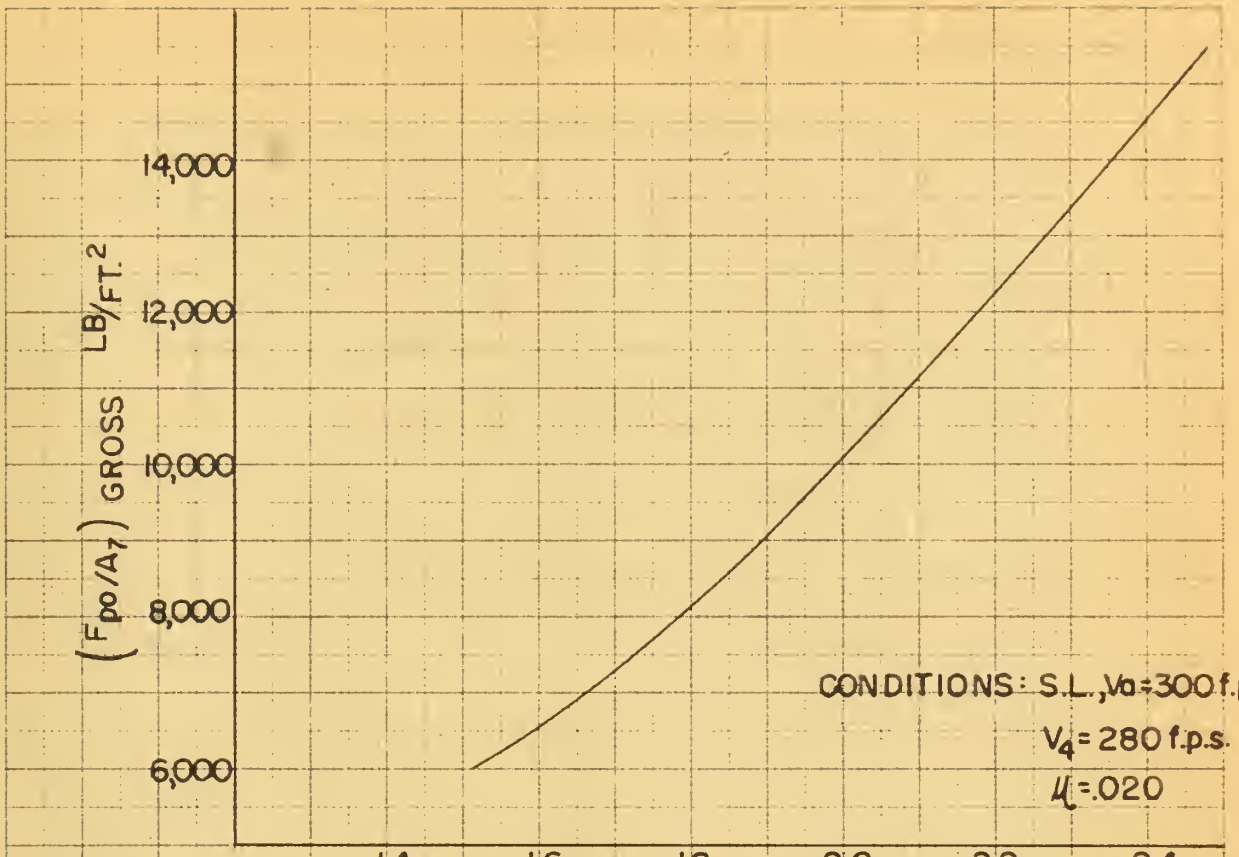
C_f VS. MACH NUMBER

FIG. 30



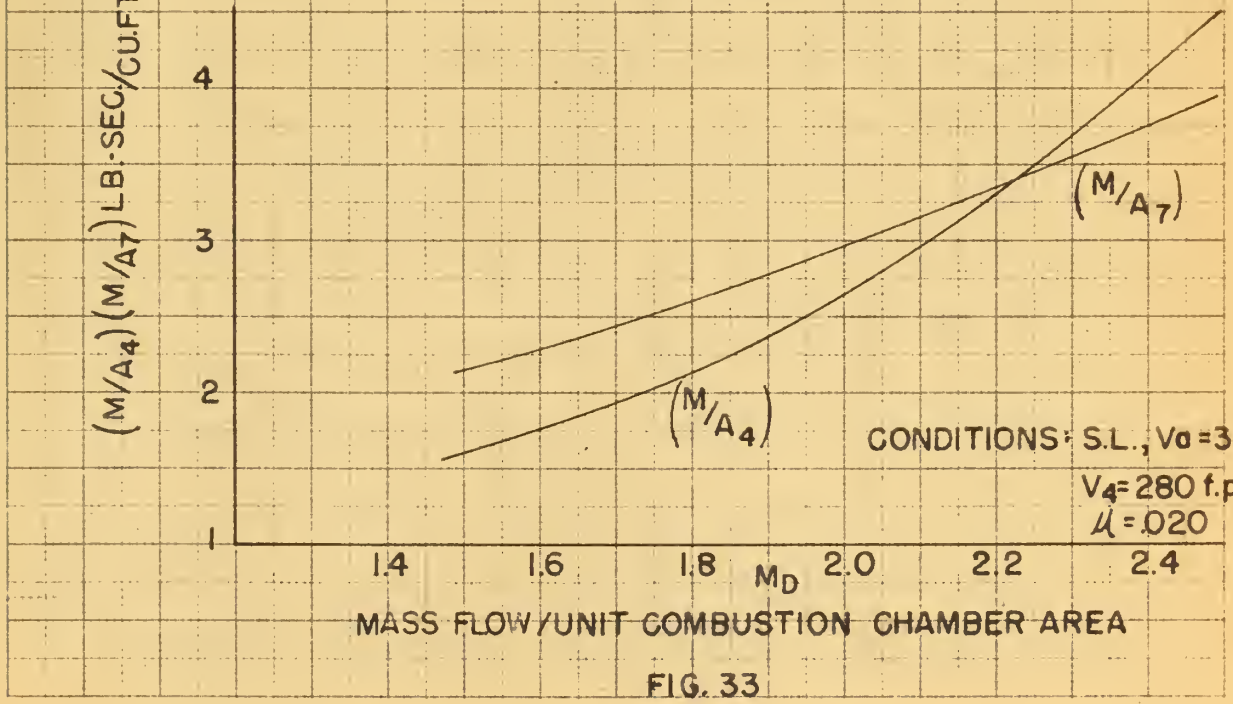
COEFFICIENT OF FRICTION VS. SLIDING VELOCITY

FIG. 31



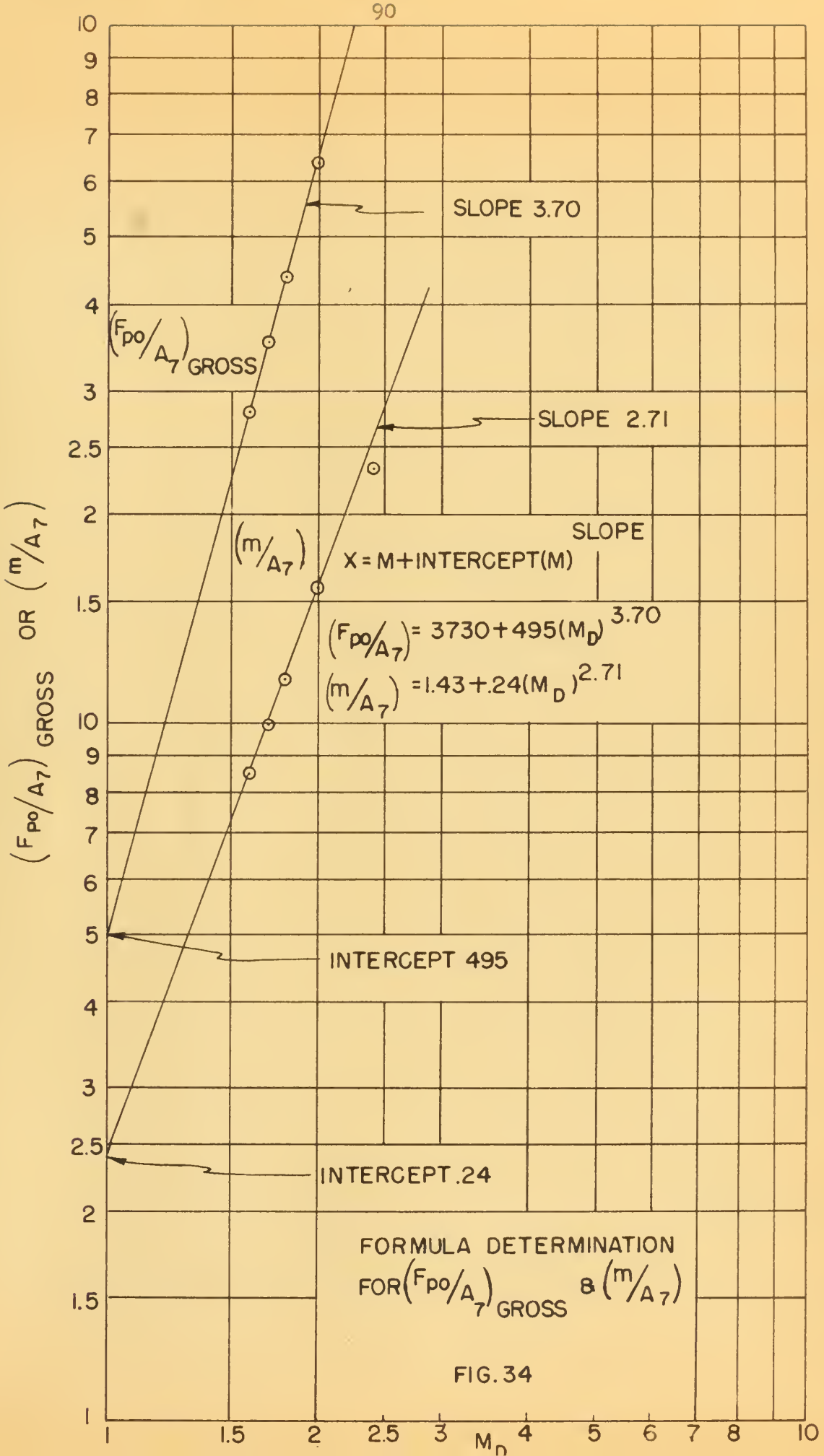
THRUST/UNIT EXIT AREA VS. DISC MACH NO.

FIG. 32



MASS FLOW/UNIT COMBUSTION CHAMBER AREA

FIG. 33



FORMULA DETERMINATION FOR $(F_{po}/A_7)_{GROSS}$ & (m/A_7)

FIG. 34

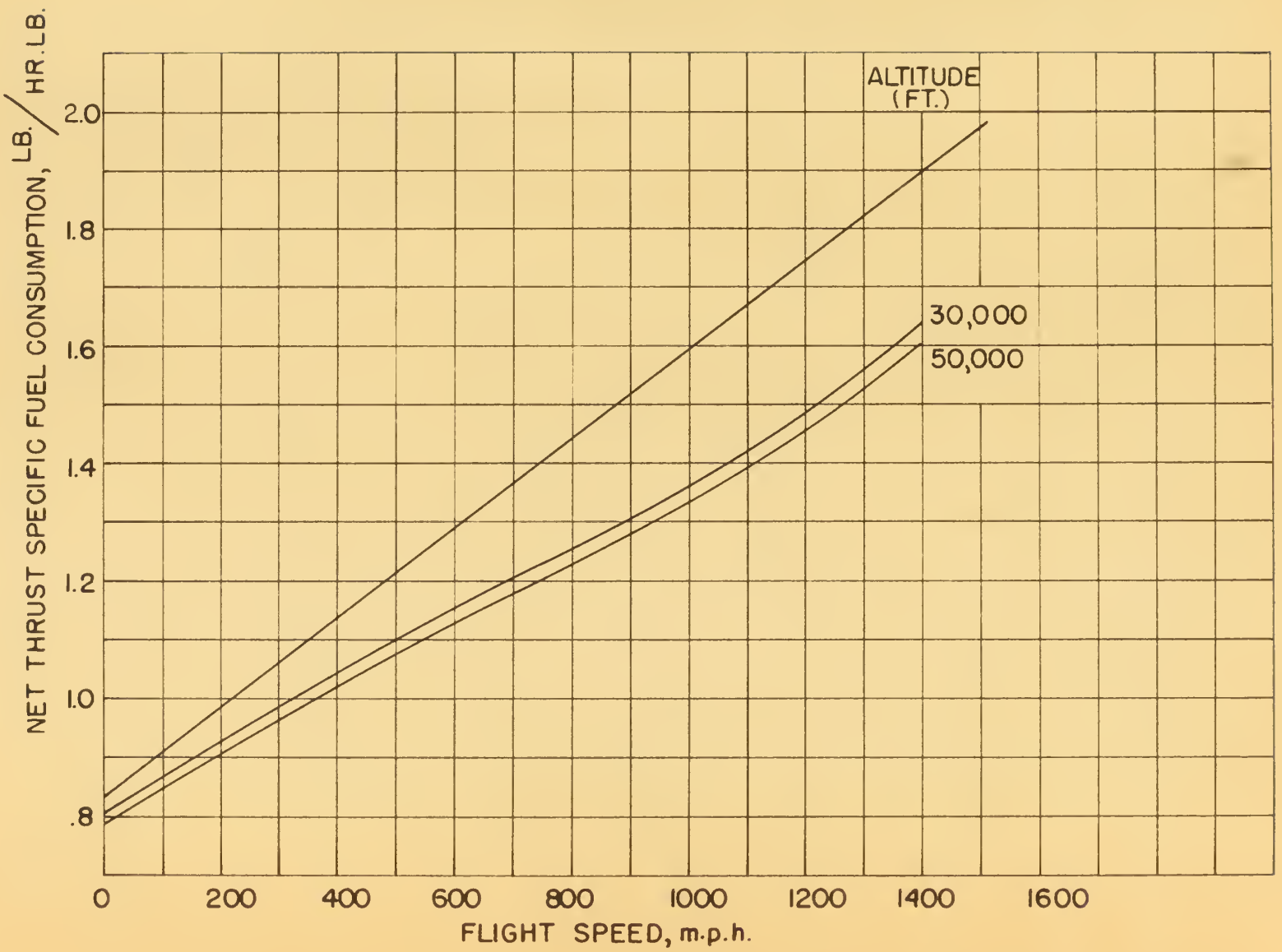
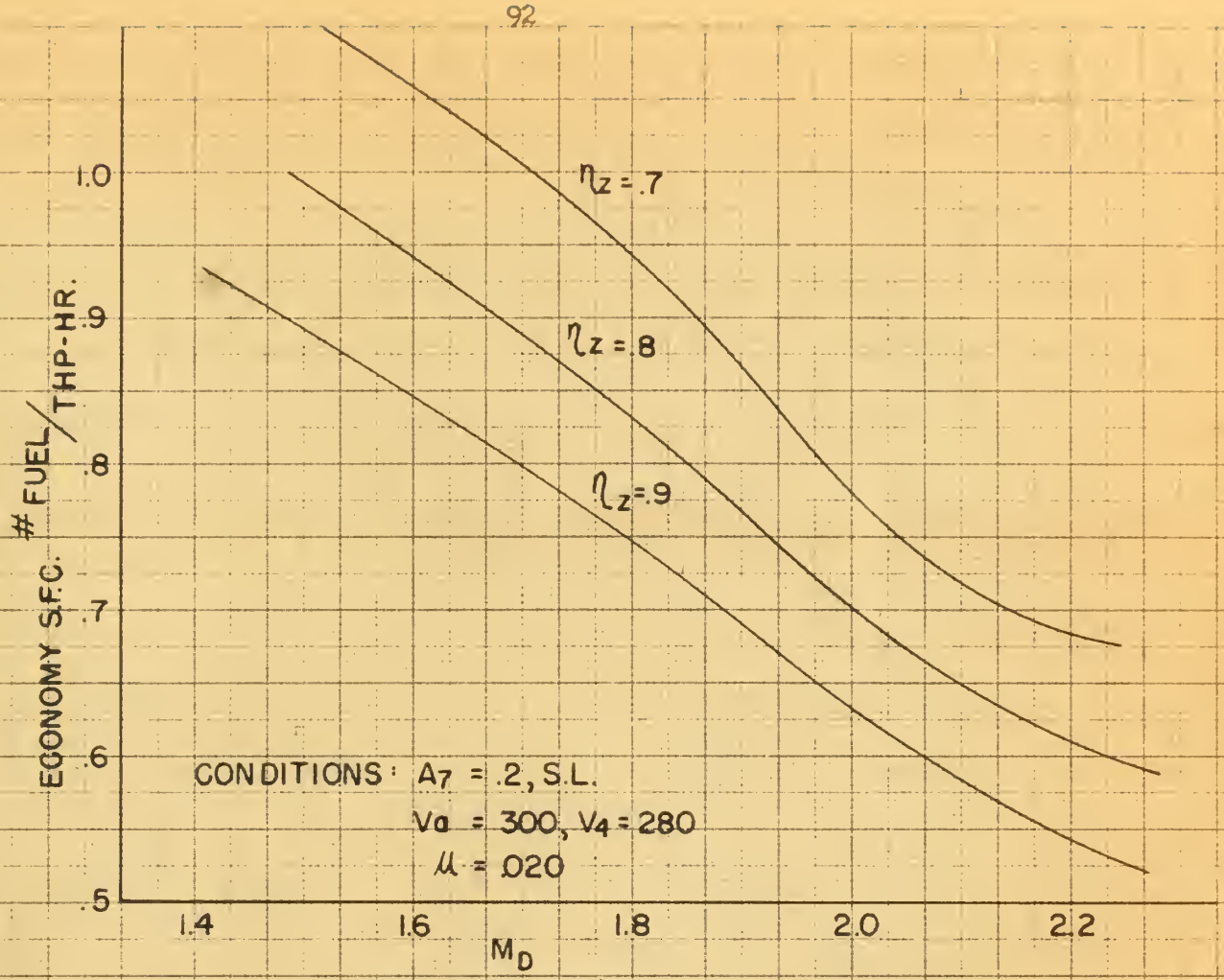
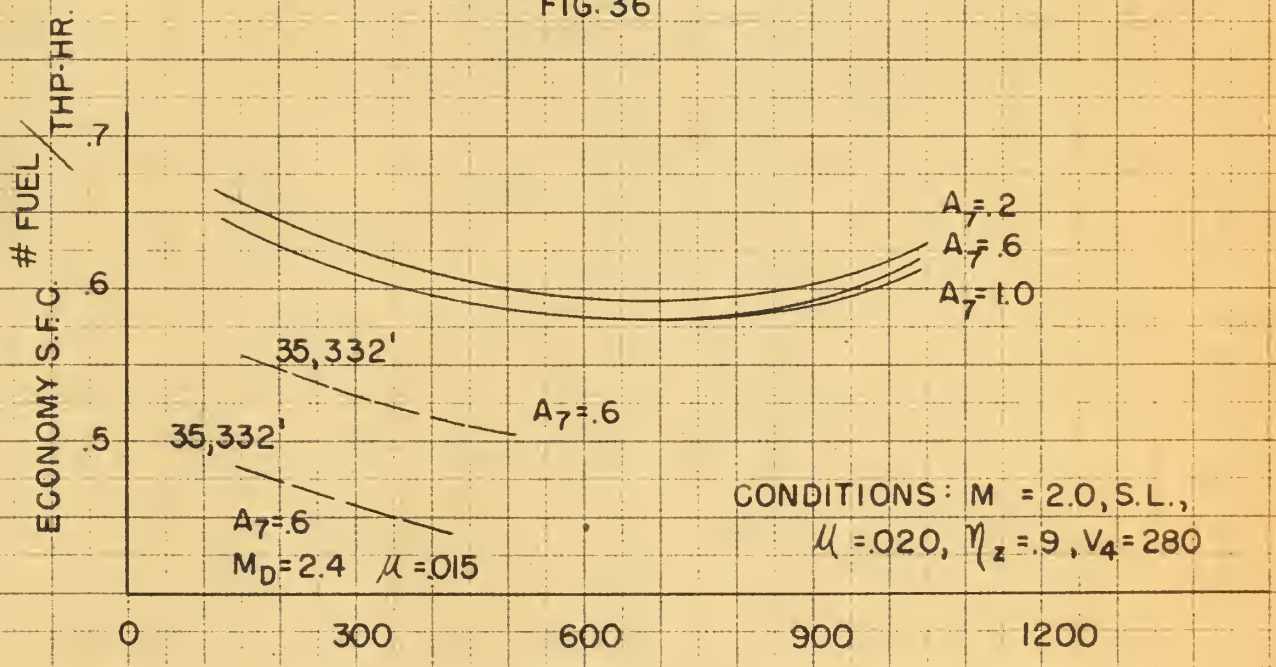


FIG. 35 ~ S.F.C. VS. AIRCRAFT SPEED AND ALTITUDE FOR A TURBO-JET



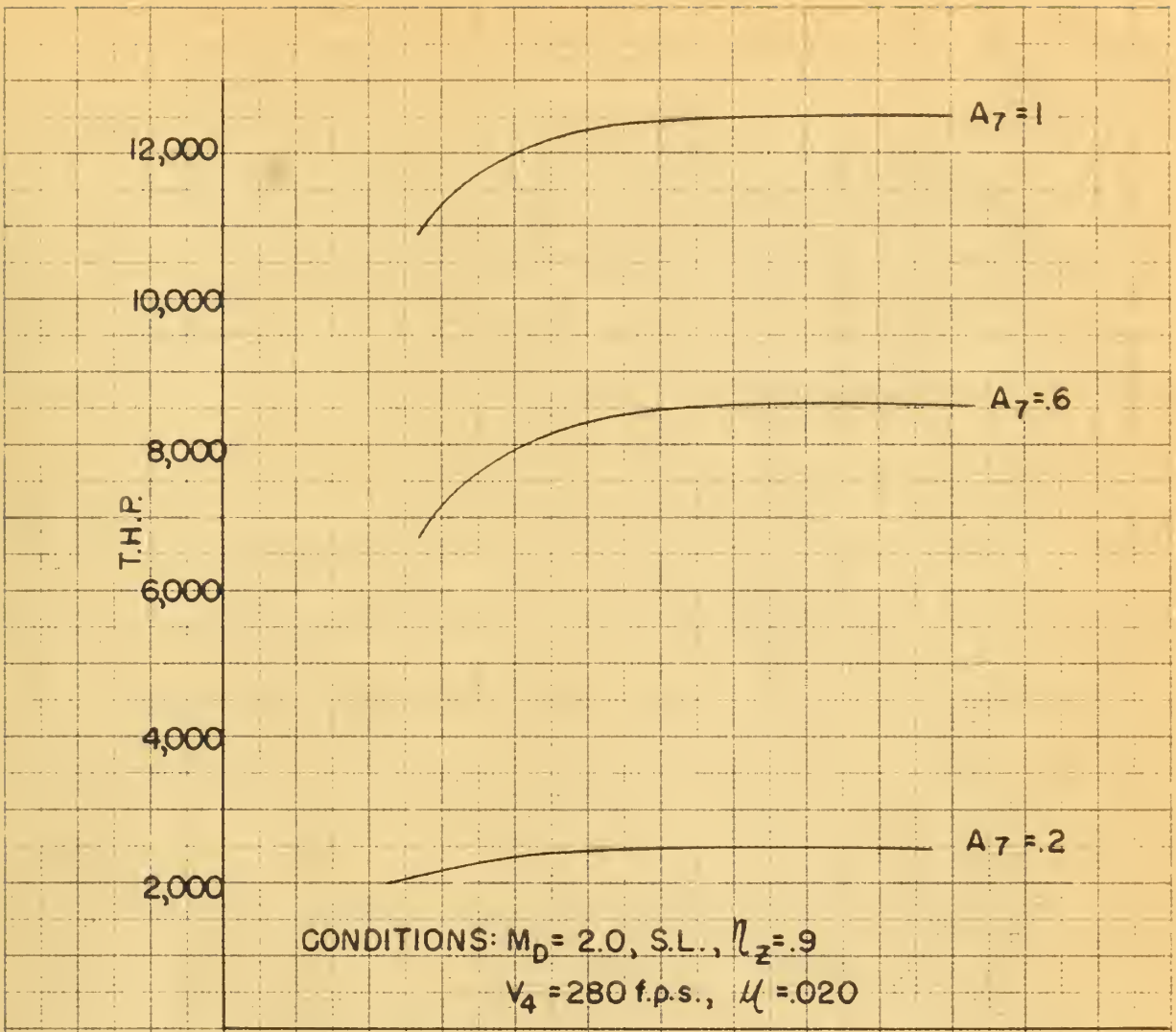
S.F.C. VS. M_D & η_z

FIG. 36



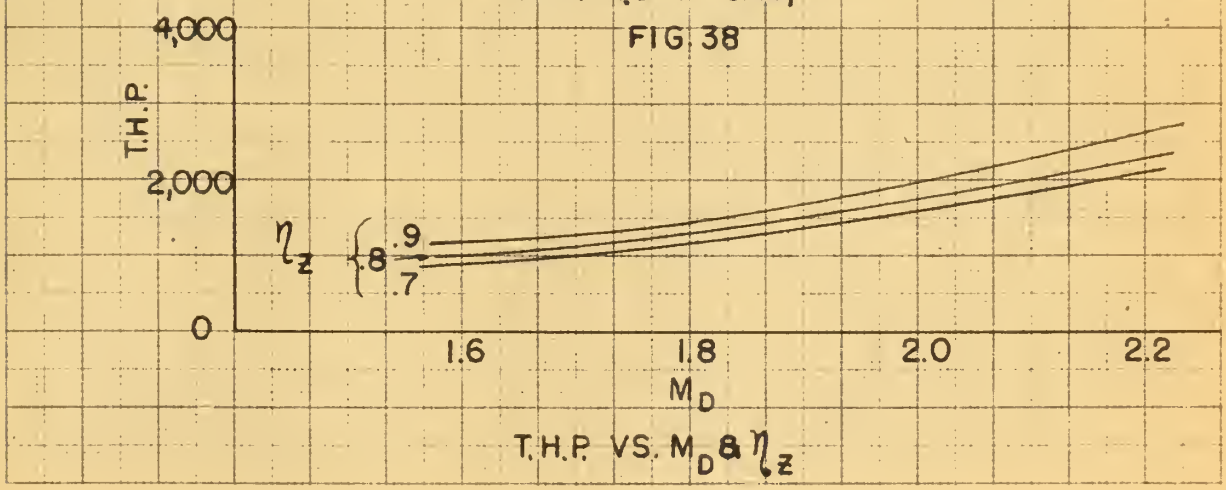
S.F.C. VS. AIRCRAFT SPEED WITH A_7 AS PARAMETER

FIG. 37



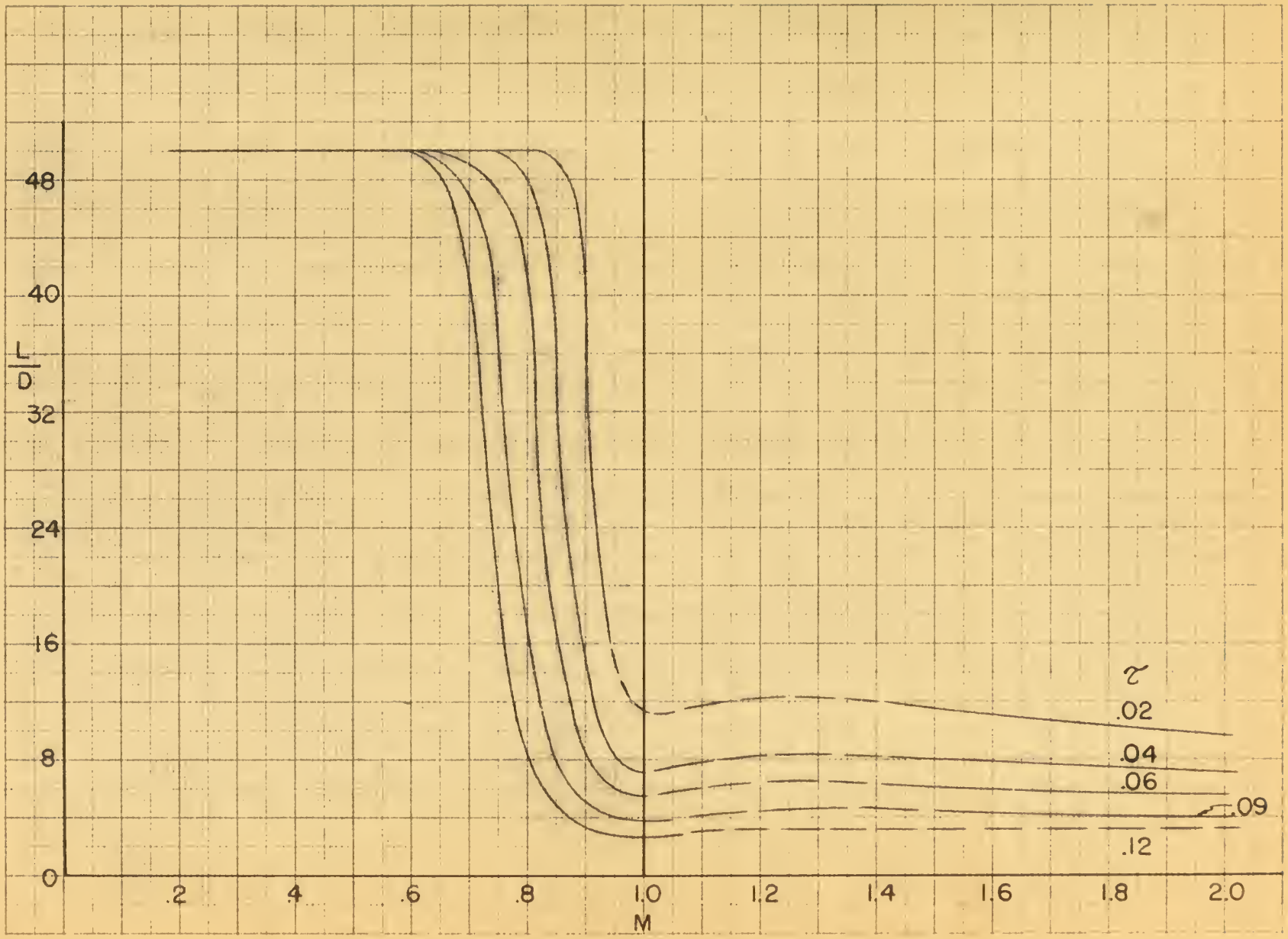
T.H.P. VS. Va & A_7

FIG. 38



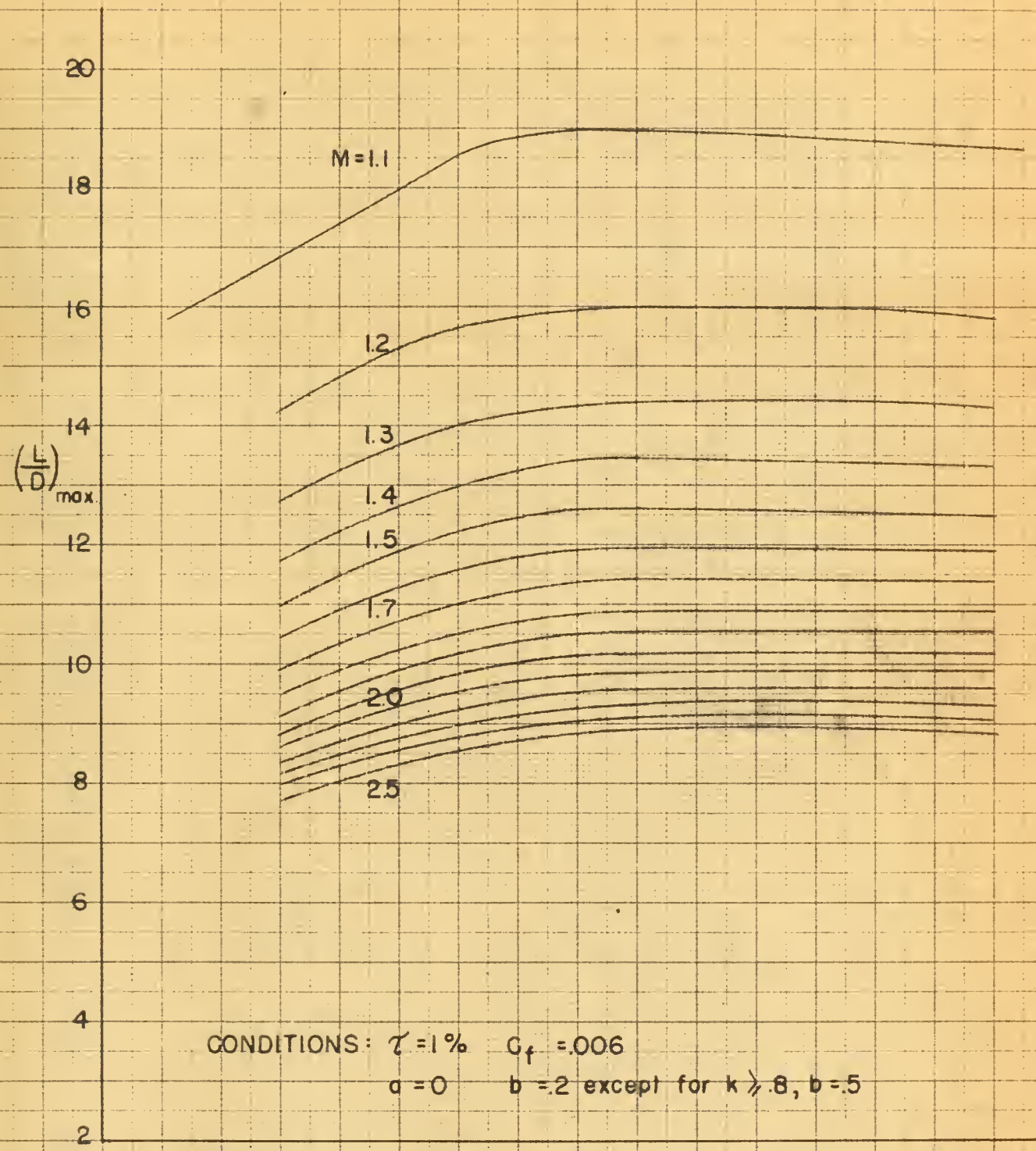
T.H.P. VS. M_D & η_z

FIG. 39



PROFILE LIFT-DRAG RATIOS VS. MACH NO. & τ

FIG. 40

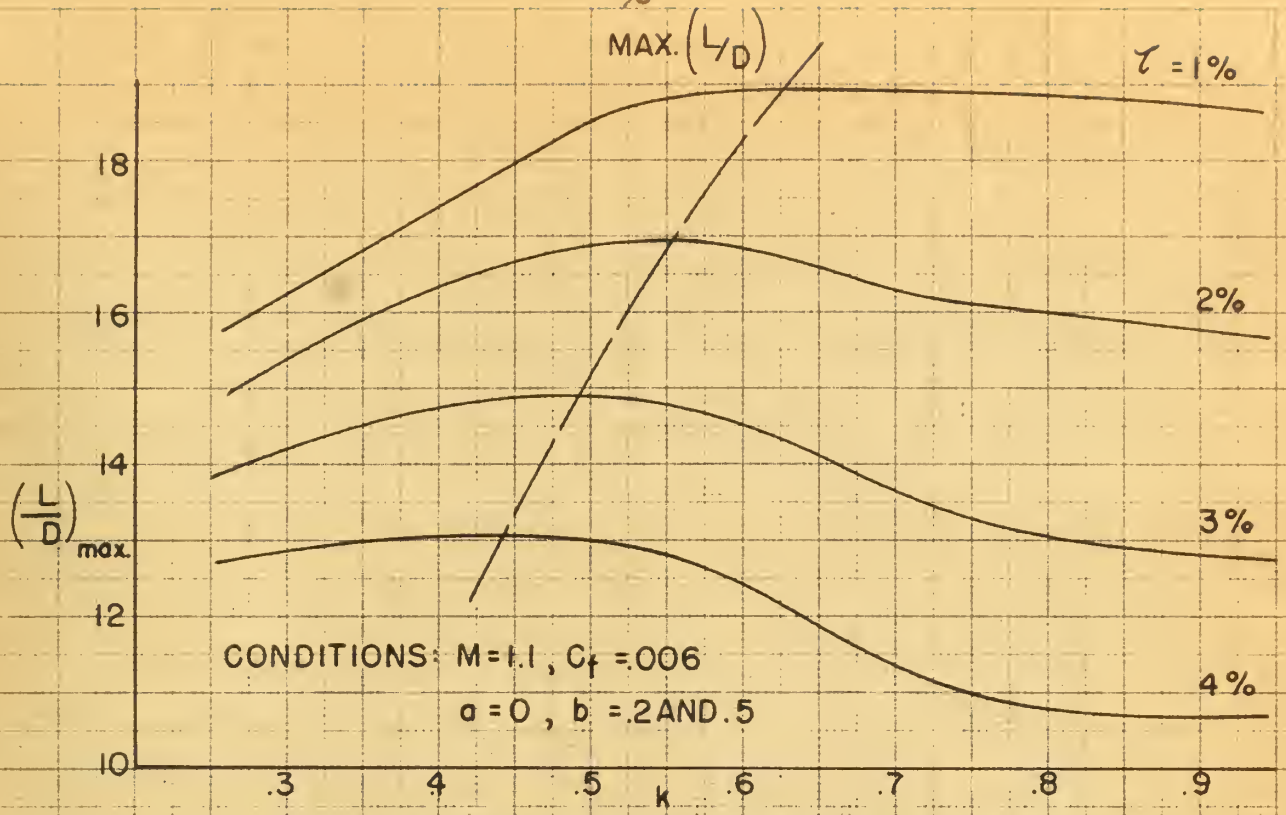


CONDITIONS: $\tau = 1\%$ $C_f = .006$

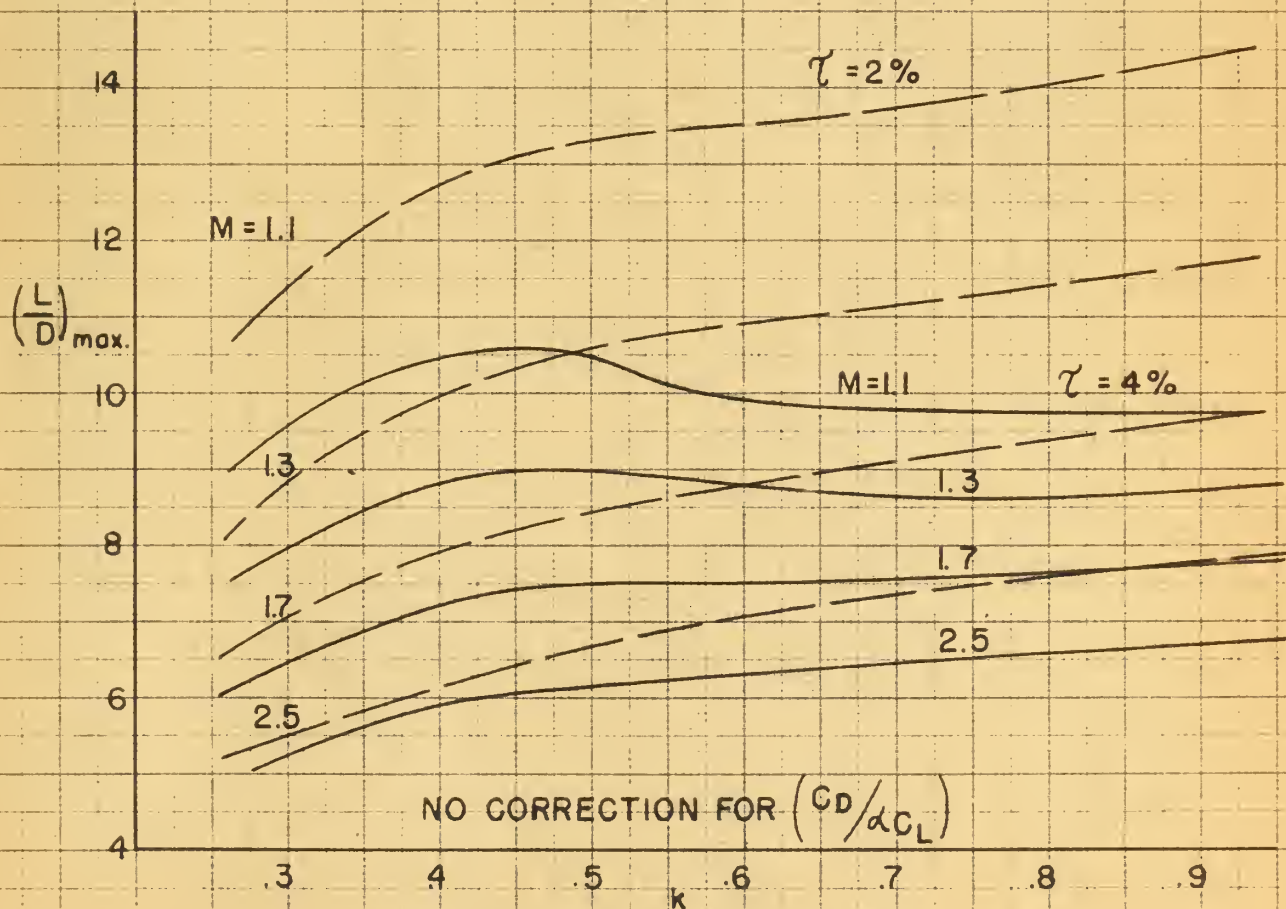
$a = 0$ $b = .2$ except for $k \geq .8$, $b = .5$

LIFT/DRAG RATIOS VS. k & M

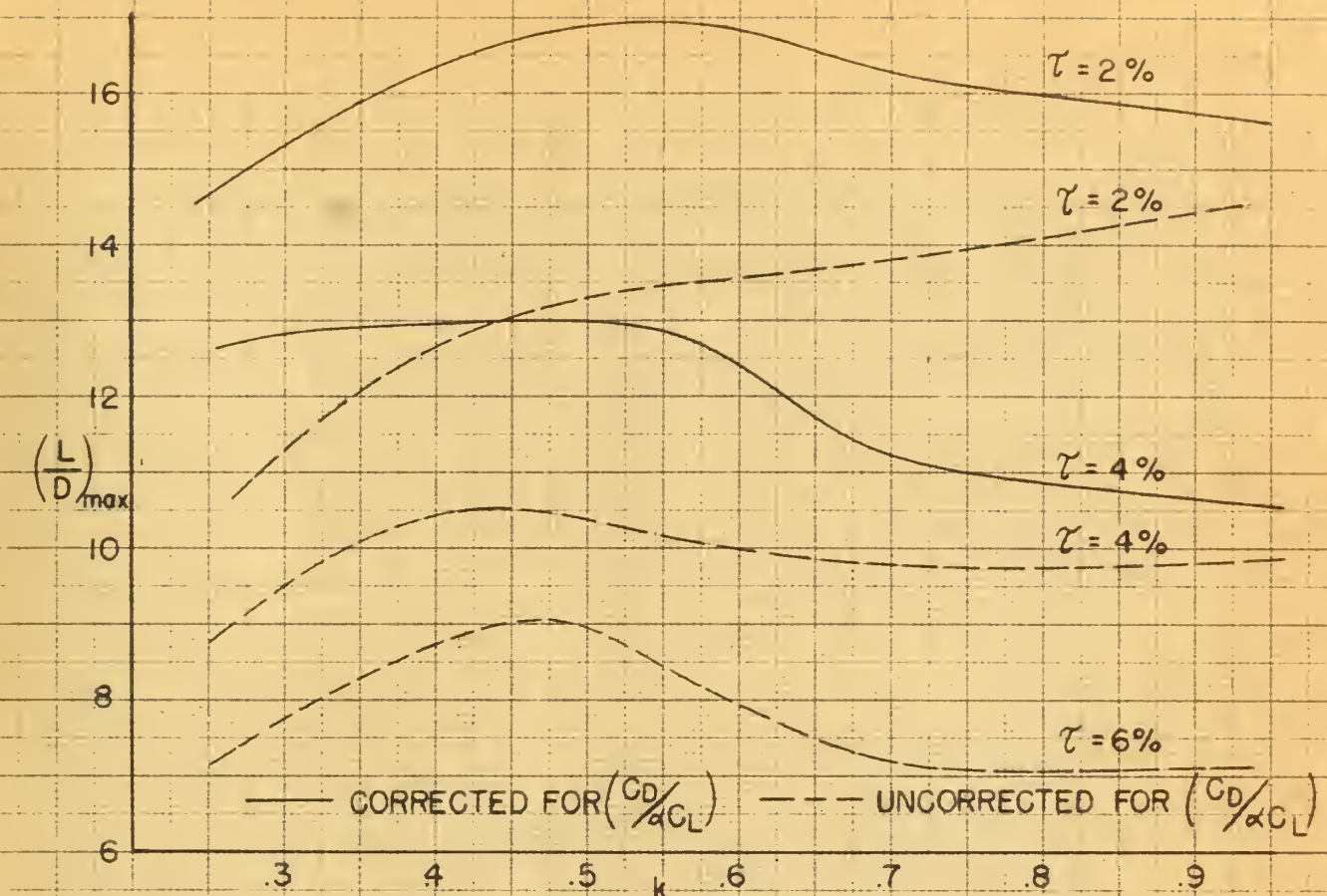
FIG. 41



LIFT/DRAG RATIO VS. k AND THICKNESS RATIO
FIG. 42

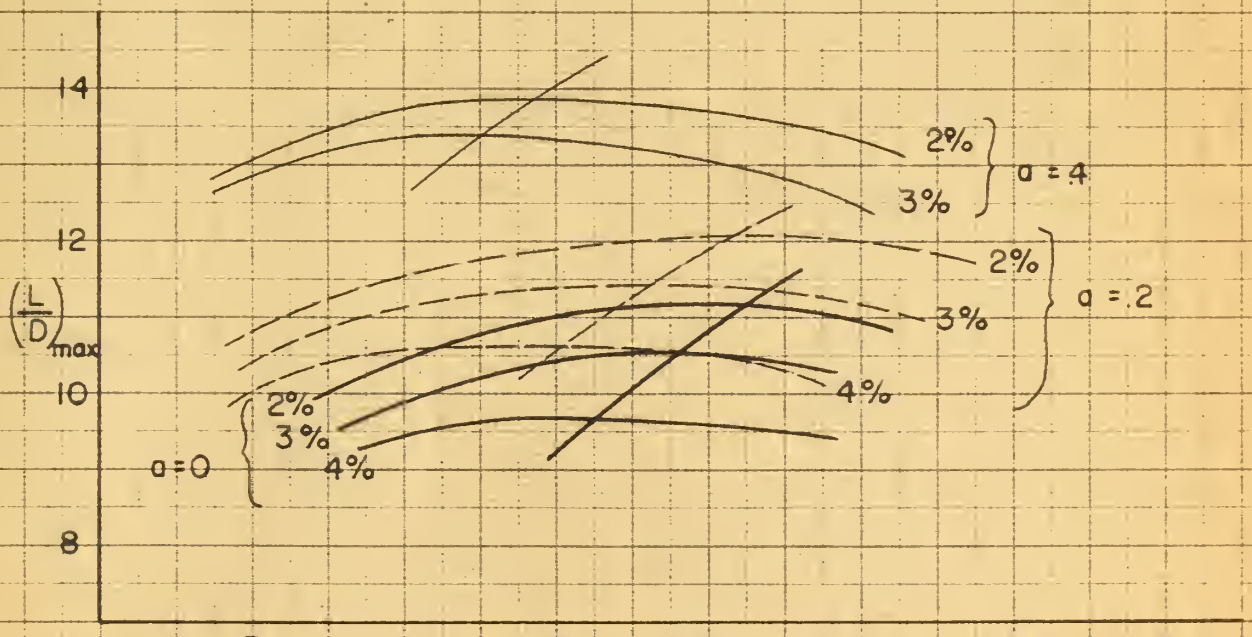


LIFT/DRAG RATIO VS. k AND M
FIG. 43



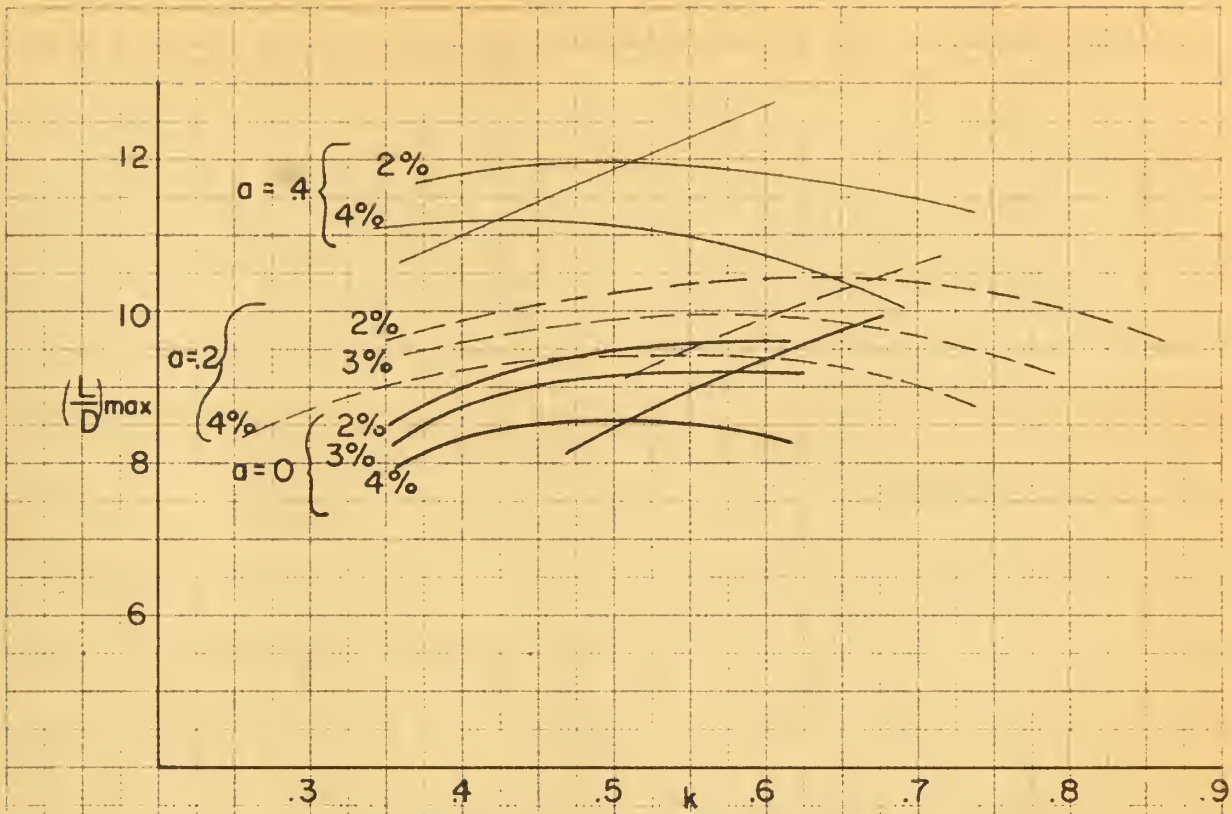
LIFT/DRAG RATIOS VS. k AT M = 1.1

FIG. 44



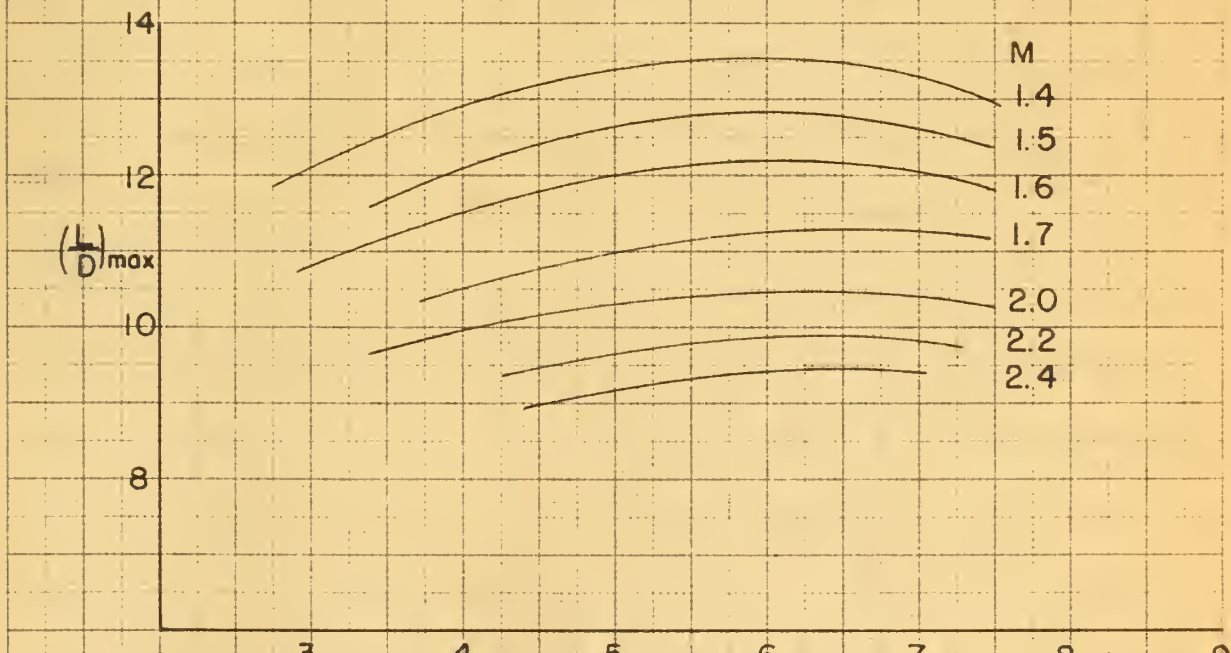
LIFT/DRAG RATIOS VS. k AT M = 1.6

FIG. 45



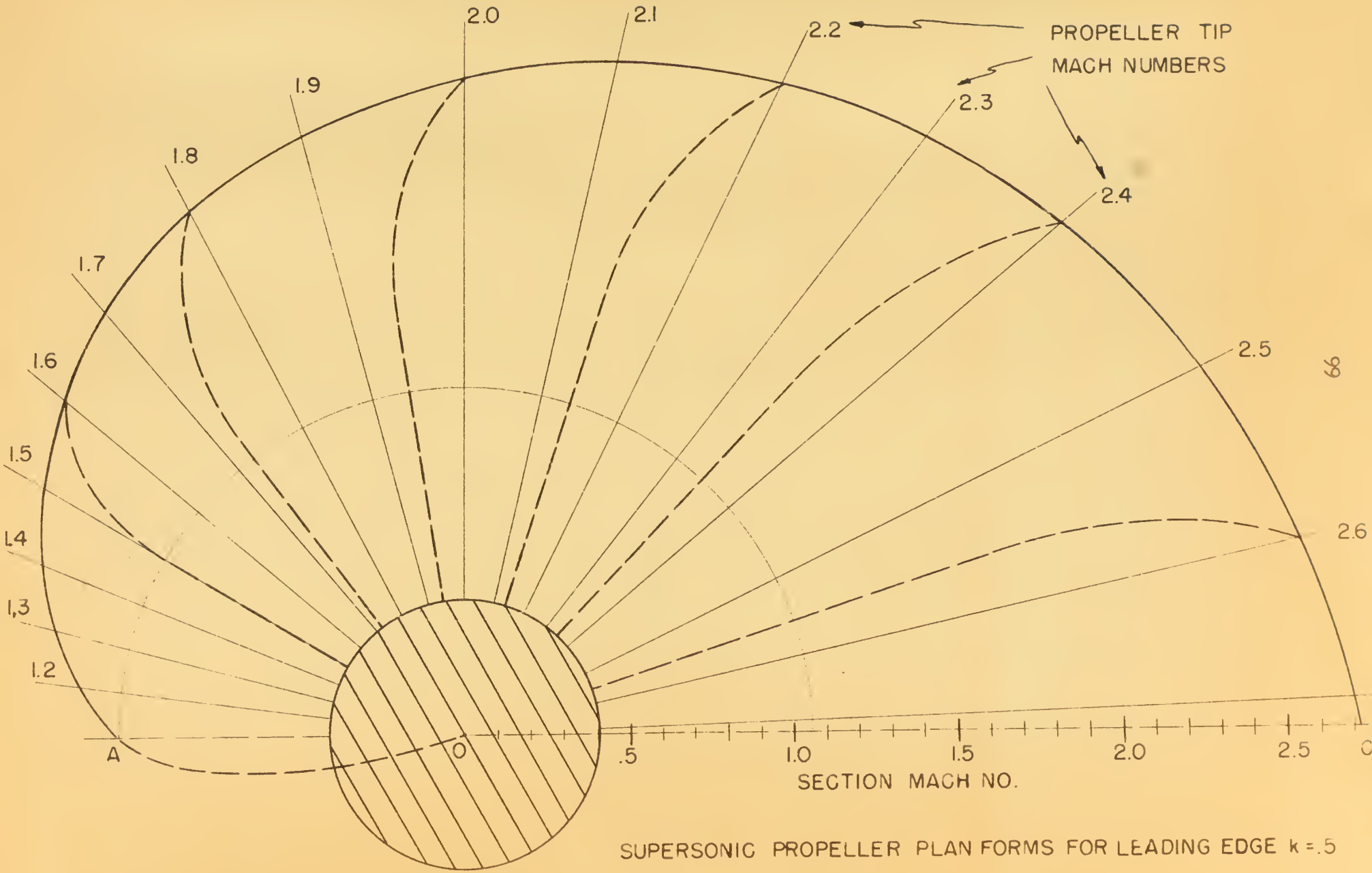
LIFT/DRAG RATIOS VS. k AT M = 2.0

FIG. 46



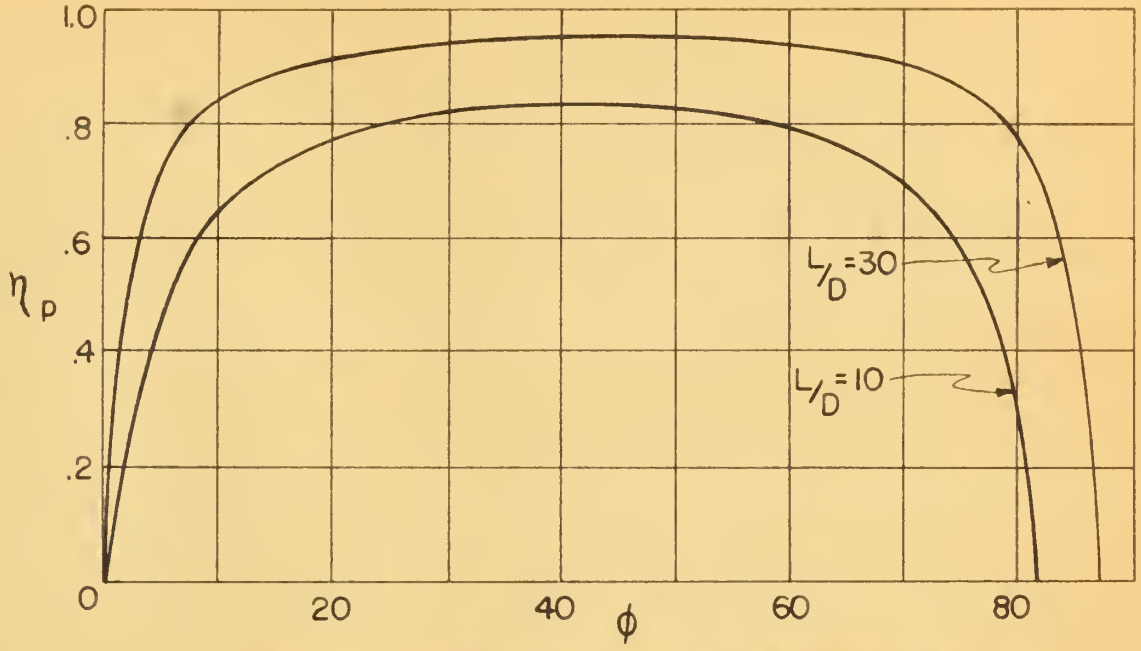
LIFT/DRAG RATIOS VS. k FOR τ = 2% & α = .2

FIG. 47

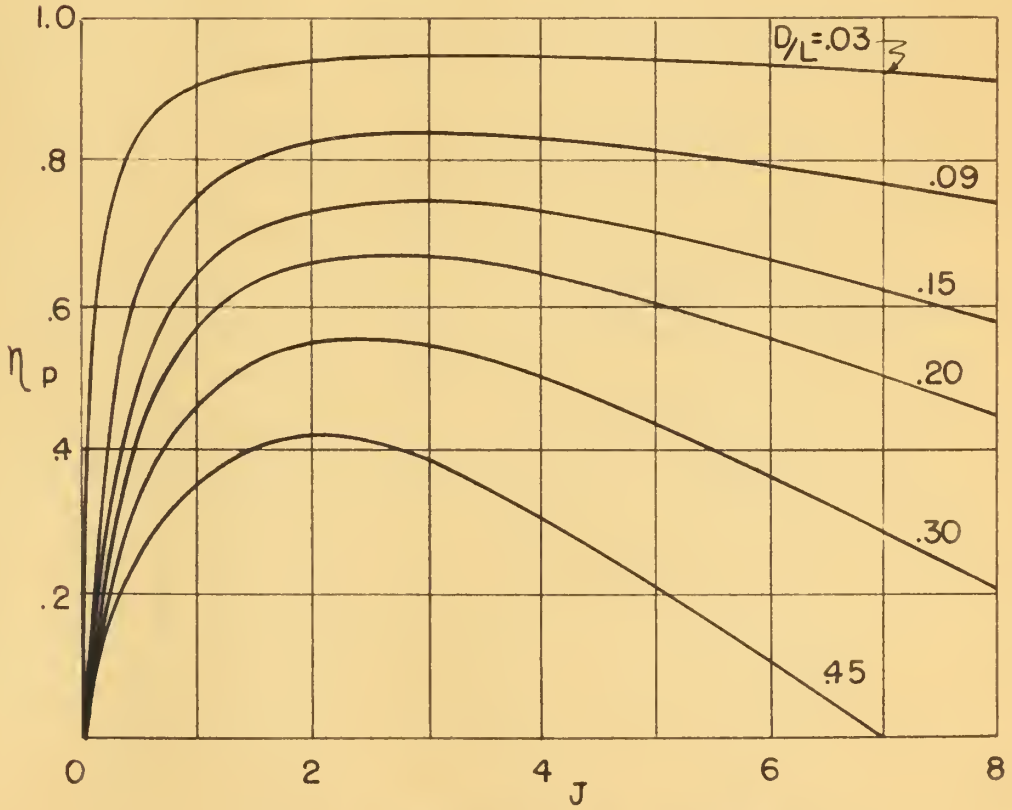


SUPERSONIC PROPELLER PLAN FORMS FOR LEADING EDGE k = .5

FIG. 48

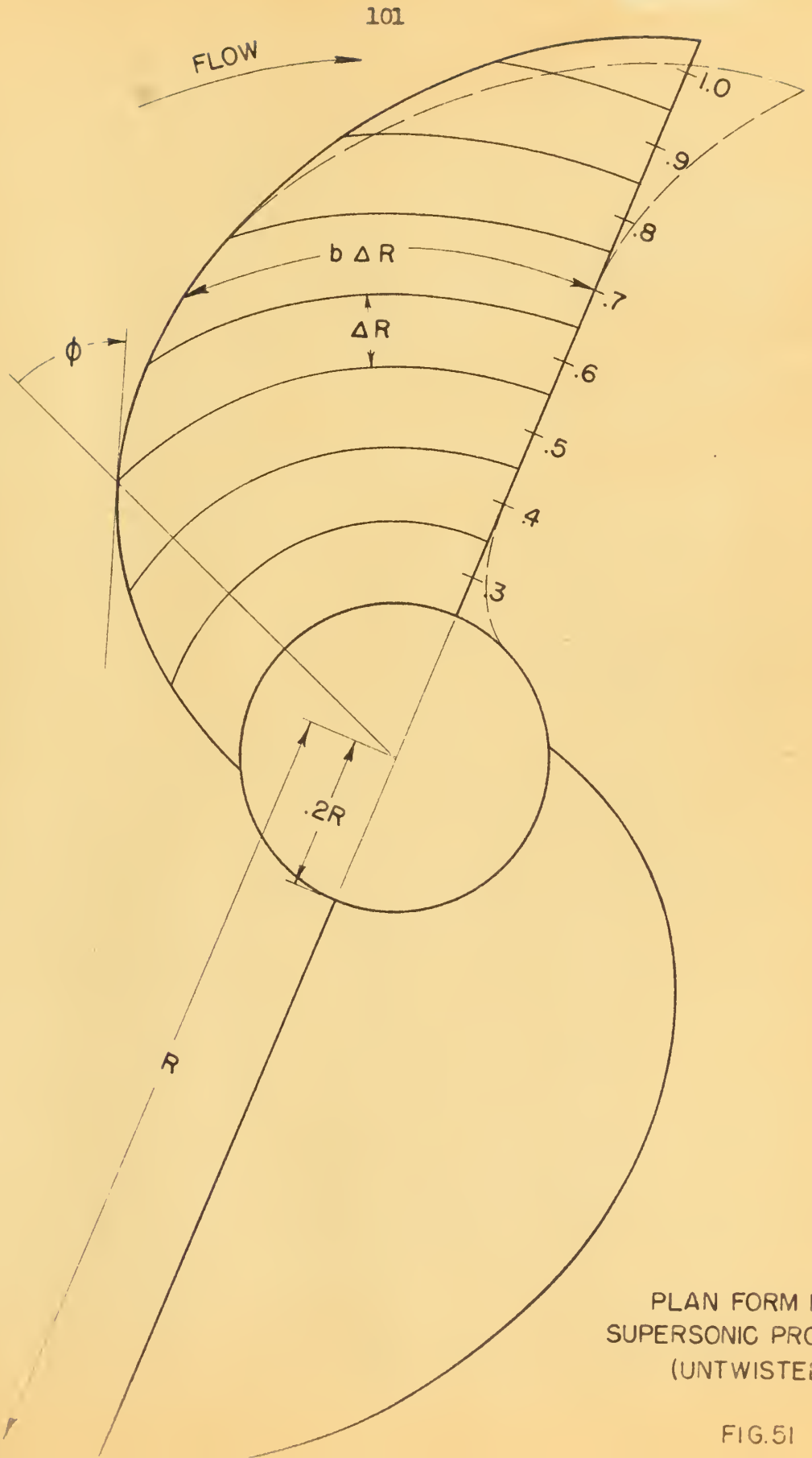


Propeller Efficiency vs. Propeller Advance Angle
FIG. 49



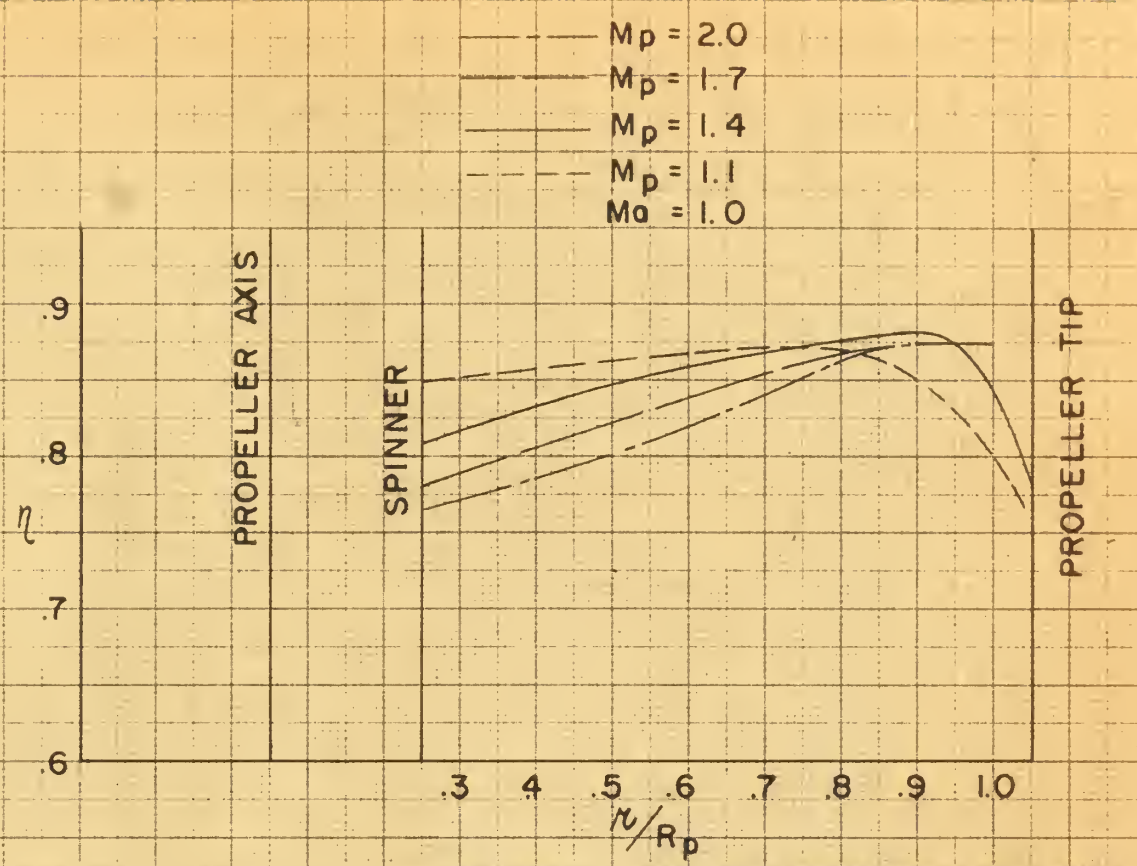
Propeller Efficiency vs. Parameter J

FIG. 50



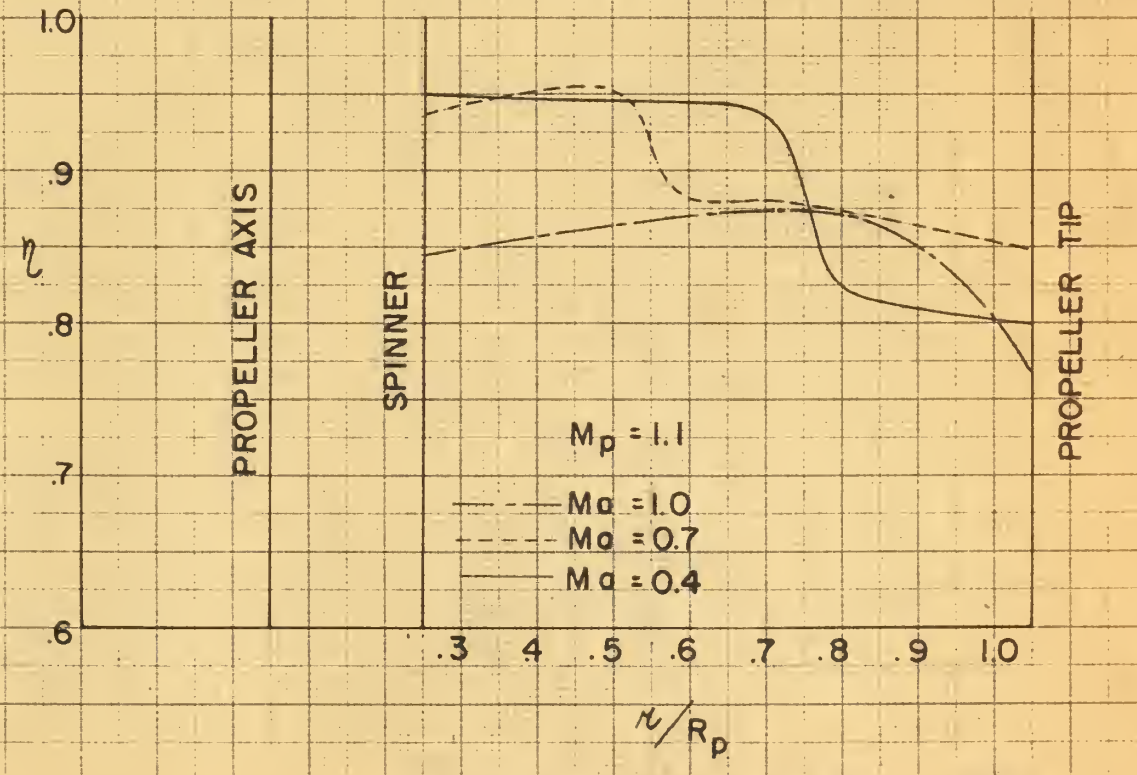
PLAN FORM FOR A
SUPERSONIC PROPELLOR
(UNTWISTED)

FIG. 51



SECTION η VS. RADIUS & PROPELLER SPEED

FIG. 52



SECTION η VS. RADIUS & AIRCRAFT SPEED

FIG. 53

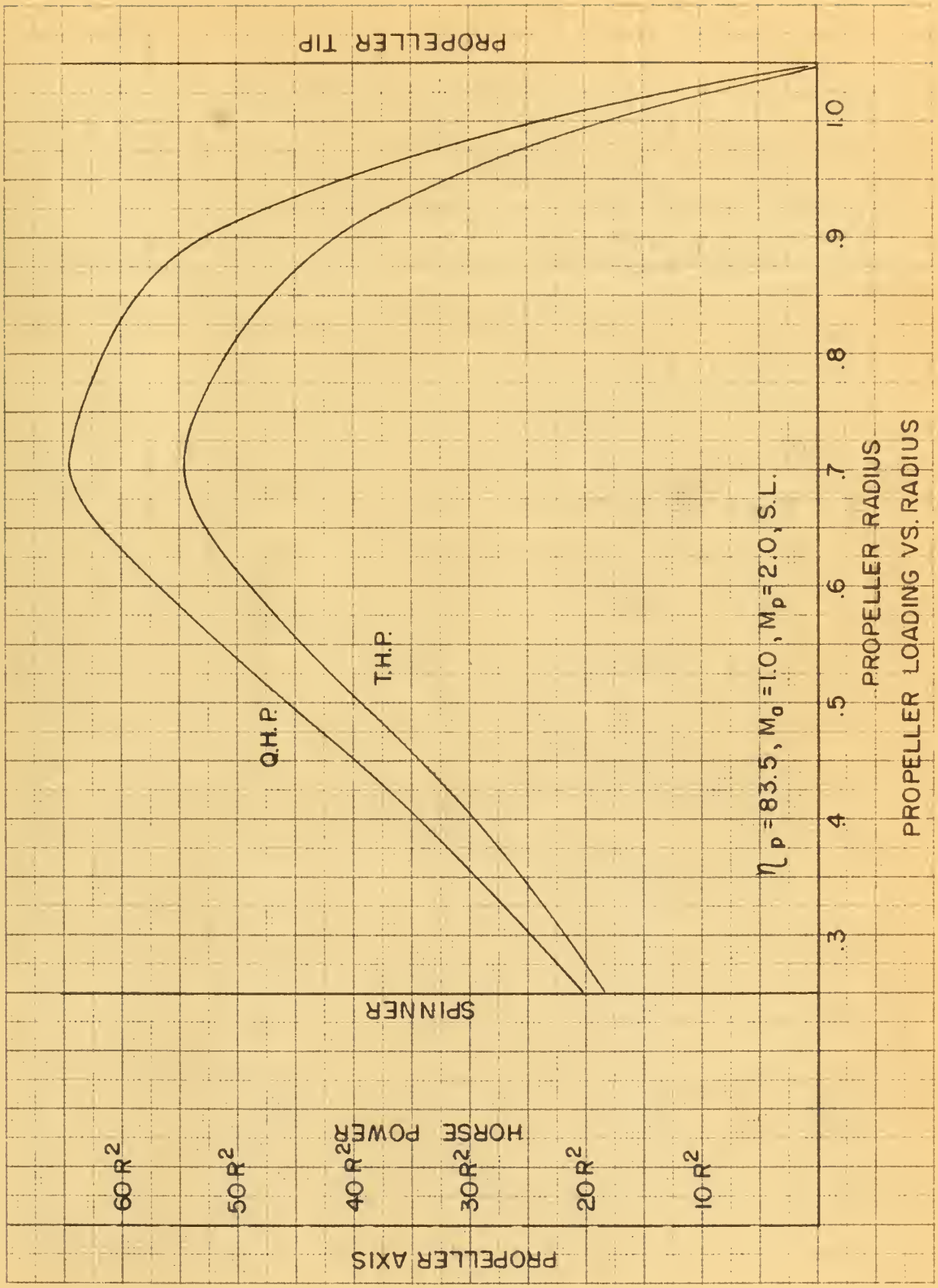
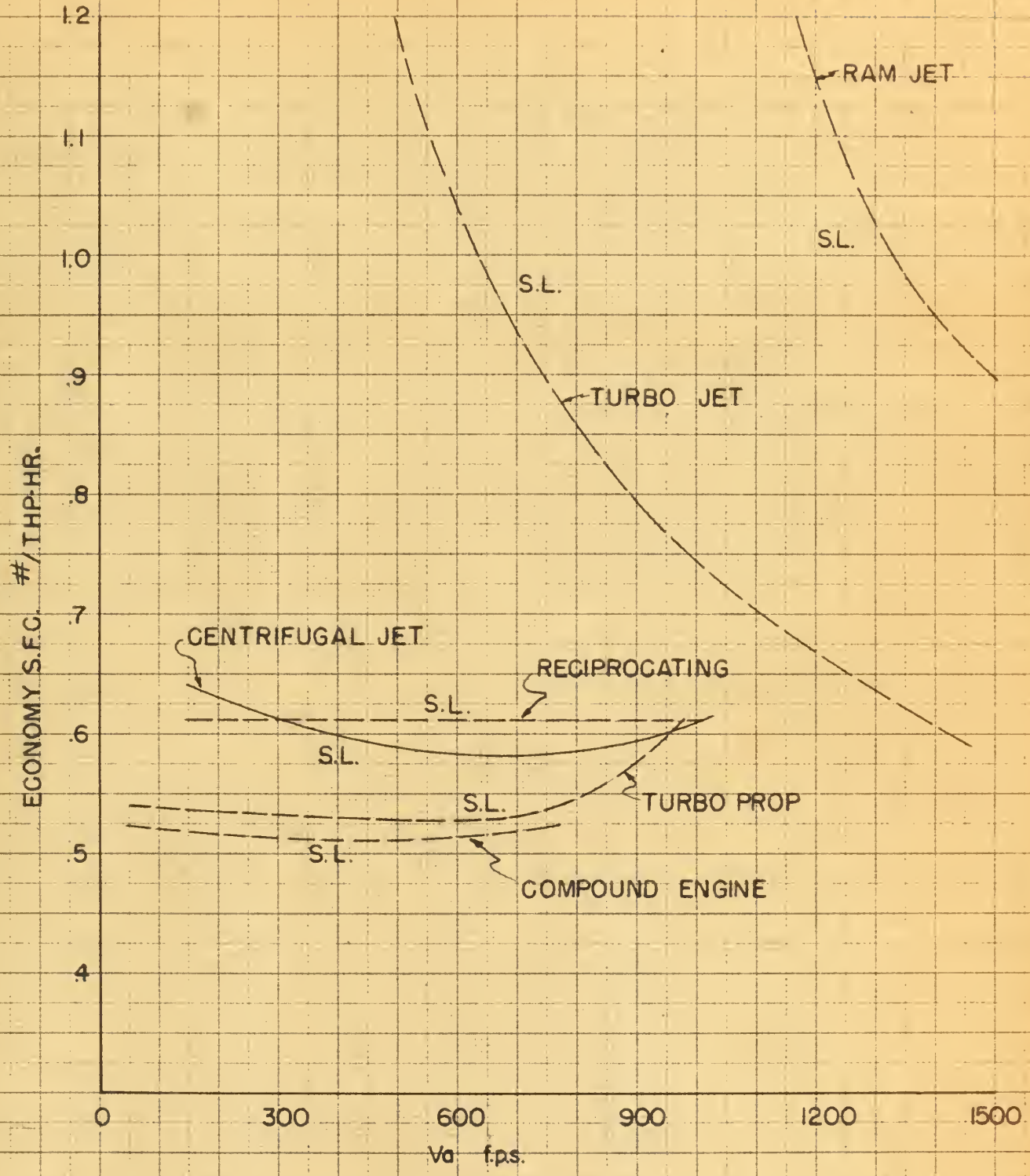
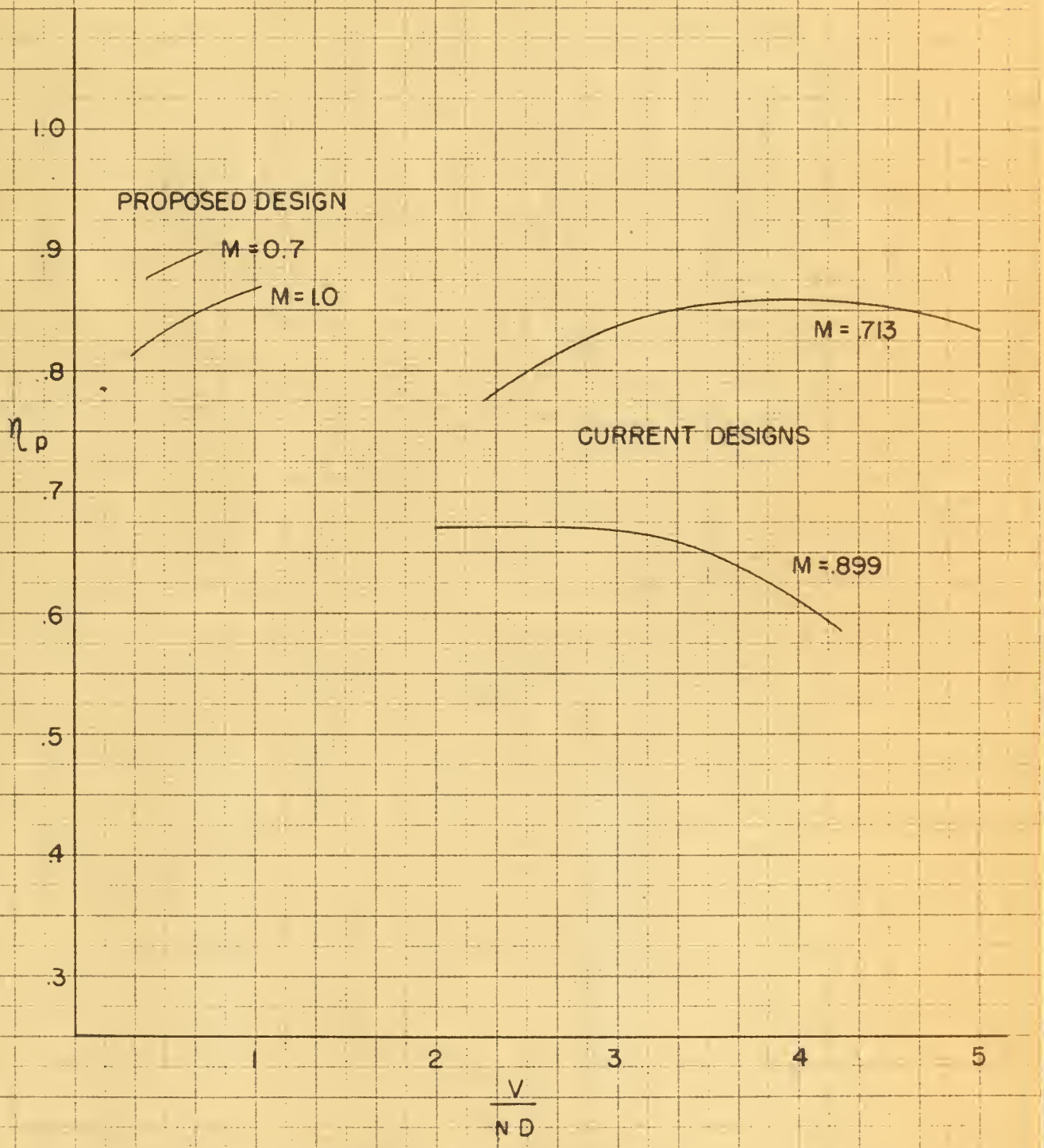

PROPELLER TIP
SPINNER
PROPELLER AXIS
HORSE POWER
60 R²
50 R²
40 R²
30 R²
20 R²
10 R²
Q.H.P.
T.H.P.
η_p = 83.5, M_o = 1.0, M_p = 2.0, S.L.
.3
.4
.5
.6
.7
.8
.9
1.0
PROPELLER RADIUS
PROPELLER LOADING VS. RADIUS

FIG. 54



ECONOMY COMPARISON FOR VARIOUS TYPE ENGINES

FIG. 55



PROPELLER EFFICIENCY VS. V/ND
ENVELOPE EFFICIENCY CURVES FOR VARIOUS FLIGHT SPEEDS

FIG. 56

Thesis
S856 Struble
Preliminary design study of a centrifugal jet engine with a supersonic propeller.
33127

Thesis
S856 Struble
Preliminary design study of a centrifugal jet engine with a supersonic propeller.
33127

thesS856
Preliminary design study of a centrifuga
3 2768 002 02137 0
DUDLEY KNOX LIBRARY